

Electronic Thesis and Dissertation Repository

4-21-2021 2:30 PM

Population and Evolution Dynamics in Predator-prey Systems with Anti-predation Responses

Yang Wang, *The University of Western Ontario*

Supervisor: Zou, Xingfu, *The University of Western Ontario*

A thesis submitted in partial fulfillment of the requirements for the Doctor of Philosophy degree in Applied Mathematics

© Yang Wang 2021

Follow this and additional works at: <https://ir.lib.uwo.ca/etd>



Part of the [Dynamic Systems Commons](#), [Evolution Commons](#), [Non-linear Dynamics Commons](#), [Ordinary Differential Equations and Applied Dynamics Commons](#), and the [Population Biology Commons](#)

Recommended Citation

Wang, Yang, "Population and Evolution Dynamics in Predator-prey Systems with Anti-predation Responses" (2021). *Electronic Thesis and Dissertation Repository*. 7741.
<https://ir.lib.uwo.ca/etd/7741>

This Dissertation/Thesis is brought to you for free and open access by Scholarship@Western. It has been accepted for inclusion in Electronic Thesis and Dissertation Repository by an authorized administrator of Scholarship@Western. For more information, please contact wlsadmin@uwo.ca.

Abstract

This thesis studies the impact of anti-predation strategy on the population dynamics of predator-prey interactions. This work includes three research projects.

In the first project, we study a system of delay differential equations by considering both benefit and cost of anti-predation response, as well as a time delay in the transfer of biomass from the prey to the predator after predation. We reveal some insights on how the anti-predation response level and the biomass transfer delay jointly affect the population dynamics; we also show how the nonlinearity in the predation term mediated by the fear effect affects the long term dynamics of the model system. These results seem to suggest a need to revisit existing predator-prey models in the literature by incorporating the indirect effect and biomass transfer delay.

In the second project, we propose two model systems in the form of ordinary differential equations to mechanistically explore trophic cascade of fear effect. The three species model only considers the cost of the anti-predation response reflected in the decrease of the production, while the four species model also considers the benefit of the response in reducing the predation rate. We perform a thorough analysis on the dynamics of the two models. The results reveal that the 3-D model and 4-D model demonstrate opposite patterns for trophic and such a difference is attributed to whether there is a benefit for the anti-predation response by the meso-carnivore species.

In the last project, to study the evolution of anti-predation strategy, we consider three species predator-prey models in which the two competing prey species have the same population dynamics but different anti-predation strategies. We identify the existence conditions of a singular anti-predation strategy, as well as conditions for it to be a local evolutionarily stable strategy. We use some examples to illustrate our results and compare the results between two different types of predators. Numerical simulations are also carried out to verify our theoretical findings and to demonstrate that three types of outcomes are possible: the mutant fails to invade, or the mutant invades and replaces the resident, or the mutant invades co-persist with the resident. These results help us understand more about the role anti-predation response can play in conveying competitive advantages.

Keywords: Predator-prey, anti-predation response, asymptotic stability, time delay, food chain, adaptive dynamics, evolutionary stability

Summary for Lay Audience

Predator-prey interaction is an important topic in ecology and evolutionary biology. Anti-predation response is a common behavior of prey in predator-prey interaction but it is widely ignored in existing predator-prey models and management of ecosystems because the impact of anti-predation response can not be observed as easily as direct predation. Recent researches showed empirical evidence in both theory and practice that anti-predation strategy can strongly affect the population size of the prey species and therefore, should not be ignored. Preys have many different anti-predation strategies to fight against predators. Some strategies allow individuals to improve their fitness while other strategies could lead to extinction. Therefore, studying the impact of these strategies is of theoretical and practical importance for determining the long-term dynamics of the populations. In this thesis, we use mathematical tools to investigate this problem. We develop models which consider the costs and benefits of anti-predation strategies simultaneously. Secondly, we use mathematical methods and theories to analyze our models. The main objective of this thesis is to reveal some new insights from considering anti-predation strategies and explore the existence of the “best” anti-predation strategy, a strategy which will maximize the long-term survival of the species. Our goal for this thesis is to understand the influence of anti-predation strategies and accordingly suggest ways by which, possible manipulations to the anti-predation response of animals in some area may help preserve the biodiversity of the ecosystem. Some results obtained in this thesis can also be applied to control of some un-wanted biological species in agriculture and forest.

Co-Authorship Statement

This thesis is written by Yang Wang under the supervision of Dr. Xingfu Zou. Chapter 2 has been published in the Journal of Nonlinear Science and was co-authored with Dr. Xingfu Zou. Chapter 3 has been published in Mathematics in Applied Sciences and Engineering and was co-authored with Dr. Xingfu Zou. Chapter 4 is being prepared for submission and is co-authored with Dr. Xingfu Zou.

The drafts of above papers were prepared by Y. Wang. Then they were revised and finalized by Y. Wang and X. Zou.

Acknowledgements

First and foremost, I would like to thank my supervisor, Dr. Xingfu Zou. Without his challenge and support, it is impossible for me to finish this thesis. He has been a model for me and the others. I feel lucky and honor to be one of his graduate students.

Secondly, I would like thank Dr. Pei Yu and everyone in Zou and Yu's group. Thanks everyone for providing me precious discussions to help me understand more and more in mathematical biology and dynamical systems. I also would like to thank Audrey Kager and Cinthia Maclean for their warmhearted helps and assistance since I started my study at University of Western Ontario in 2012.

Last but not the least, I would like to thank my family and my friends, especially Dr. Cody Koykka, Dr. Jianing Huang, Ao Li and my parents. Without your support and love, I will not be able to overcome the difficulties and make it this far. Thank you!

Contents

Abstract	i
Summary for Lay Audience	iii
Co-Authorship Statement	iv
Acknowledgements	v
List of Figures	ix
List of Tables	xiii
1 Introduction	1
1.1 Costs and benefits of anti-predation response	5
1.2 Trophic cascade	6
1.3 Mathematical theories and methodologies	7
1.3.1 Stability analysis of nonlinear systems	8
1.3.2 Adaptive dynamics	9
Bibliography	11
2 On a predator-prey system with digestion delay and anti-predation strategy	16
2.1 Introduction	16
2.2 Well-posedness of the model	19
2.3 Equilibria and their stability	20
2.3.1 Model with linear functional response	21
Local stability and Hopf bifurcation	22
Global stability of the boundary equilibria E_0 and E_u	26

2.3.2	Model with the Holling Type II functional response	27
	Local stability and Hopf bifurcation	29
	Global stability of the boundary equilibria E_0 and E_u	34
2.4	Numerical simulations	35
2.5	Conclusion and discussions	42
	Bibliography	47
3	On mechanisms of trophic cascade caused by anti-predation response in food chain systems	50
3.1	Introduction	50
3.2	Analysis of the model without large carnivores	55
3.2.1	Preliminaries	55
3.2.2	Existence and Stability of the boundary equilibria	56
3.2.3	Existence and stability of a positive equilibrium solution	60
3.2.4	Numerical simulations	63
3.3	Model with restoring large carnivores	66
3.3.1	Well-posedness	68
3.3.2	Existence and Stability of the boundary equilibrium solutions	70
3.3.3	Existence and stability of the positive equilibrium	79
3.3.4	Numerical simulations	82
3.4	Conclusion and discussions	84
	Bibliography	87
4	Evolution of anti-predation response of prey in predator-prey interactions	91
4.1	Introduction	91
4.2	Preliminaries	96
4.2.1	Well-posedness of (4.5)	96
4.2.2	Dynamics of (4.5)	97
4.3	Invasion analysis	102
4.3.1	With specialist predator	105
4.3.2	With generalist predator	110

4.3.3	Difference between specialist and generalist predator	116
4.4	Conclusion and discussions	119
	Bibliography	124
5	Conclusions and discussions	127
	Bibliography	131
	Curriculum Vitae	133

List of Figures

2.1	Population dynamics of (2.53). (a) When $k = 20 > k^* = 15$, the predator free equilibrium E_u is stable, the predator species goes extinct and the prey species eventually goes to its carrying capacity. (b) When $k = 11 < k^* = 15$, E_u is unstable and there is the co-existence equilibrium E^+ which is asymptotically stable for all $\tau \geq 0$ since $p_0 = 0.00075 > q_0 = 0.0005250388635$	37
2.2	Population dynamics of (2.53). (a) When $k = 1 < k^*$, $p_0 = 0.000125 < q_0 = 0.0007484621132$, $\tau = 2 < \tau_0 = 3.678038406$, the co-existence equilibrium is stable. (b) $\tau = 4 > \tau_0 = 3.678038406$, there occurs a periodic solution.	37
2.3	Plot of periodic orbit of (2.53) in $u = v$ plane when $k = 1$ and $\tau = 4 > \tau_0 = 3.678038406$	38
2.4	Bifurcation diagram for (2.53) : (a) fixing $k = 1$ and choosing τ as the bifurcation parameter; (b) fixing $\tau = 2$ and choosing k as the bifurcation parameter. . .	38
2.5	Population dynamics of (2.29). (a) When $k = 20 > k^* = 2.636363636$, the predator free equilibrium E_u is stable. (b) When $k = 2 < k^*$, E_u becomes unstable and there occurs the positive equilibrium E^+ which is asymptotically stable for all $\tau > 0$ because $J_{11} = -0.01184921799 < 0$ and $(2m J_{11} J_{12} K_{21} - J_{12}^2 K_{21}^2) = 1.723290120 \cdot 10^{-7} > 0$	40
2.6	When $k = 1 < k^*$, $J_{11} = -0.003821249991 < 0$, $(2m J_{11} J_{12} K_{21} - J_{12}^2 K_{21}^2) = -2.86322377 \cdot 10^{-8} < 0$. (a) When $\tau = 4 < \tau_0 = 33.27610729$, the co-existence equilibrium E^+ is still stable; (b) When $\tau = 120 > \tau_0 = 33.27610729$, E^+ loses its stability and a periodic solution occurs.	40
2.7	Periodic orbits when $k = 1$ and $\tau = 120$	41
2.8	Bifurcation diagram for (a) fix $k = 1$, choose τ as the bifurcation parameter. (b) fix $\tau = 2$, choose k as the bifurcation parameter.	41

2.9	By setting $k = 3.4$, $J_{11} = 0.00084875902838911633 > 0$. (a) Solutions approach to a periodic solution for $\tau = 0$ (periodic solutions for the ODE). (b) Periodic behaviours are preserved for $\tau > 0$ and are actually magnified by $\tau > 0$.	42
2.10	Critical value of time delay for fixed anti-predation level k for both functional responses	45
3.1	Population dynamics of (3.12) when $d_1 < k$. (a) When $0 < \alpha = 0.4 < 0.5$, the equilibrium E_{13} is stable, (b) $0.5 < \alpha = 2 < 2.954545455$, the coexistence equilibrium E^* is stable, (c) when $2.954545455 < \alpha = 5 < 7.5$, the equilibrium E_{23} is stable, (d) when $\alpha = 10 > 7.5$, the equilibrium E_2 is stable.	65
3.2	(a) Bifurcation diagram of (3.12) when $k > d_1$, (b) In the region when the coexistence equilibrium E^* is stable, we can observe a meso-predator cascade.	66
3.3	Population dynamics of (3.12) when $d_1 > k$. (a) When $0 < \alpha = 2 < 2.5$, the equilibrium E_{13} is stable, (b) $2.5 < \alpha = 6 < 8.409090911$, the coexistence equilibrium E^* is stable, (c) when $8.409090911 < \alpha = 10$, the equilibrium E_{12} is stable.	67
3.4	(a) Bifurcation diagram of (3.12) when $d_1 > k$, (b) In the region when the coexistence equilibrium E^* is stable, we can observe a meso-predator cascade.	68
3.5	Bifurcation diagram of (3.22) when $k < d_1$	83
3.6	Bifurcation diagram of (3.22) when $k > d_1$	84
3.7	(a) Bifurcation diagram of (3.22) when $c_2 = 2$, (b) In the region when the coexistence equilibrium E^* is stable, we can observe a meso-predator cascade with non-monotonically change on top predator.	85
4.1	Pairwise invasibility plot (PIP) for the mutant and for both the resident and the mutant. Left: plot for invasibility of the mutant prey where the two regions carrying “+” (“-”) symbols denote strategy ranges for the mutant prey to be able (unable) to invade the resident prey. Right: plot for mutual invasibility where the two regions with double +’s stand for the strategy ranges for both resident and mutant preys to be able to mildly invade each other leading to co-persistence.	108

4.2	<p>Numerical solutions to (4.25) with parameters given in (4.27) and the initial condition is set to be (u_r^*, ϵ, v^*) where ϵ is small. The strategy pair (α_r, α_m) is chosen respectively from the three types of regions in the right pane in Figure 4.2: (a) when $(\alpha_r, \alpha_m) = (4, 6)$ which is in the $(-, +)$ region, the mutant can grow when rare and eventually replace the resident to become the new resident; (b) when $(\alpha_r, \alpha_m) = (6, 4)$ which is in the $(+, -)$ region, the mutant can not invade when rare, and after a small fluctuation, the solution converge to the equilibrium $(u_r^*, 0, v^*)$; (c) when $(\alpha_r, \alpha_m) = (10, 4)$ which is in it is in the $(+, +)$ region — the mutual invasibility region, the mutant can invade when rare, without replacing the resident, resulting in the co-existence of both the mutant and the resident preys.</p>	109
4.3	<p>With parameter values given in (4.27) except that r_0 is changed to $r_0 = 1.5$, the selection gradient $s(\alpha)$ remains negative.</p>	110
4.4	<p>Numerical simulations of the population dynamics of (4.25). Parameter values are as in (4.27) except that r_0 is changed to $r_0 = 1.5$. The initial condition is set to the form (u_r^*, ϵ, v^*) where ϵ is small. (a) For $\alpha_r = 6$ and $\alpha_m = 4$ (scenario of $\alpha_m < \alpha_r$), the mutant can grow and invade even when it is rare, and it eventually replaces the resident and become the new resident. (b) For $\alpha_r = 6$ and $\alpha_m = 10$ (scenario of $\alpha_m > \alpha_r$), the mutants die out and can not invade when rare; after a small fluctuation, the populations are back to the equilibrium $(u_r^*, 0, v^*)$.</p>	111
4.5	<p>Pairwise invasibility plot(PIP) and mutual invasibility plot. In the PIP, ”+” region denotes where mutants can invade the residents while in ”-” region mutants fail to invade residents. In the mutual invasibility plot, ”++” region notes where mutants and residents are mutually invasive and thus may cause coexistence of both species.</p>	114

4.6	Numerical solutions to (4.29) with parameters given in (4.32) and the initial condition is set to be (u_r^*, ϵ, v^*) where ϵ is small. The strategy pair (α_r, α_m) is chosen respectively from the three types of regions in the right pane in Figure 4.2: (a) when $(\alpha_r, \alpha_m) = (4, 6)$ which is in the $(-, +)$ region, the mutant can grow when rare and eventually replace the resident to become the new resident; (b) when $(\alpha_r, \alpha_m) = (6, 4)$ which is in the $(+, -)$ region, the mutant can not invade when rare, and after a small fluctuation, the solution converge to the equilibrium $(u_r^*, 0, v^*)$; (c) when $(\alpha_r, \alpha_m) = (10, 4)$ which is in it is in the $(+, +)$ region — the mutual invasibility region, the mutant can invade when rare, without replacing the resident, resulting in the co-existence of both the mutant and the resident preys.	115
4.7	With parameter values given in (4.32) except that r_0 is changed to $r_0 = 1.5$, the selection gradient $s(\alpha)$ remains negative.	116
4.8	Numerical simulations of the population dynamics of (4.29). Parameter values are as in (4.32) except that r_0 is changed to $r_0 = 1.5$. The initial condition is set to the form (u_r^*, ϵ, v^*) where ϵ is small. (a) For $\alpha_r = 6$ and $\alpha_m = 4$ (scenario of $\alpha_m < \alpha_r$), the mutant can grow and invade even when it is rare, and it eventually replaces the resident and become the new resident. (b) For $\alpha_r = 6$ and $\alpha_m = 10$ (scenario of $\alpha_m > \alpha_r$), the mutants die out and can not invade when rare; after a small fluctuation, the populations are back to the equilibrium $(u_r^*, 0, v^*)$	117
4.9	$\alpha_r = 2, \alpha_m = 2.4 > 2.2$ is outside of the feasible region. We can find the mutants can still invade and start replace the residents. However, the predator population tends to 0 first and since the absence of predator, the two strains of prey coexist.	120

List of Tables

3.1	Condition of existence and stability of the equilibria in model (3.8)	62
3.2	Condition of existence and stability of the equilibria in model (3.14)	81

Chapter 1

Introduction

Predator-prey interaction is considered one of the most fundamental and important topic in both ecology and mathematical biology[5, 29]. In the real world, predation is most common event in every ecosystem. For every pair of predator and prey, the interaction seems like the same. The predator catches and eats the prey. However, the mechanism behind predator-prey interaction is complicated and species specific, and thus attracts wide research interests. Predators are mainly classified into two different types, specialist and generalist [19]. A generalist predator such as most omnivores can consume a wide range of prey species while a specialist predator's diet is limited to a very small range, sometimes even only to a unique prey species. Different predator types directly affect the ability for adapting to the environment and have effects on survival probability.

The core problem of predator-prey interaction in population ecology is to characterize the population size among different predator and prey species. To this end, ecologists spend massive time and resources on field studies. On the other hand, in order to develop general theory, mathematicians use mathematical modeling to study the dynamics of predator-prey interactions. The early pioneering and probably most well-known predator-prey model [23, 24, 44, 45] was proposed by Lotka-Volterra about a century ago. There has been a large number of literature on the models for predator-prey interactions since then. Considering spatial invariance and ignoring the maturation, a general predator-prey model can be described by a system of

ordinary differential equations of the form

$$\begin{cases} \frac{du}{dt} = f_1(u(t)) - p(u(t), v(t))v(t), \\ \frac{dv}{dt} = f_2(v(t)) + cp(u(t), v(t))v(t), \end{cases} \quad (1.1)$$

where $u(t)$ and $v(t)$ are the population densities of the prey and predator respectively. $f_1(u)$ and $f_2(v)$ represent the demographics of the prey and predator in the absence of other species. $p(u, v)$ is known as the functional response which models the encounter between predator and prey. The constant c is the conversion rate in biomass transfer from predation. In the classic Lotka-Volterra model, $p(u, v)$ is chosen to be proportional to u with a constant capture rate and is recognized as Holling Type I functional response [17]. Later literature argued that this kind of constant capture rate is only valid for a narrow range of predations such as for passive feeders. Therefore, Holling Type II functional response is introduced as $p(u, v) = \frac{au}{1+ahu}$ where a is the capture rate and h accounts for handling time. In this functional response, per capita capture rate of prey from predation decreases when its population size increases and predator consumption saturates when the prey's population reaches high level. Holling Type III functional response in the form $p(u, v) = \frac{au^2}{1+ahu^2}$ has similar saturation mechanism to Holling Type II when prey's density is high. But different from Holling Type II, it suggests a low per capita capture rate for prey when it is rare and this rate reaches maximum value at an intermediate level of the prey's density. All these types of functional responses have been studied in vast and rich literature. While the functional responses mentioned above are all driven by the density of the prey, some further modifications suggest that the functional response can also be predator-density-dependent [3, 36, 1, 18, 39]. In general, the encounter mechanism between predator and prey in direct predation is complex and heterogeneous among different pairs of species. Each of the aforementioned types works for a range of predations but fails for the others.

However, unlike the rich understanding and investigation of direct predation, classic predator-prey models and studies on ecosystem management usually ignored the indirect effect between predator and prey[8], such as reductions in prey reproduction due to the perceived risk of predation and energy cost of prey in induced defense. This is mainly because these indirect

effects cannot be easily observed, in contrast to direct predation which can be easily observed, measured and incorporated into the change of population density. Lacking awareness of these anti-predation responses, their impact on population dynamics was traditionally thought to be small when compared to direct predation. Recently, empirical studies have shown that indirect effects like anti-predation responses can be large, sometimes even larger than the effects from direct predation. Pangle et al[32] examined the indirect effect of predatory spiny water fleas (*Bythotrephes longimanus*) on zooplankton. The result showed that the indirect effects on prey growth rate were more than seven times larger than direct predation. Zanette et al [49] studied the fear effect of song sparrows by eliminating direct predation and manipulating fear of predator by its playback. They observed a 40% reduction in offspring of song sparrow by only perceiving predation risk. More evidence can be found in [37, 30, 34]. These field study results suggest the anti-predation response alone is powerful enough to regulating the population dynamics in a predator-prey interaction and therefore, motivate us to revisit the classic mathematical modeling on predator-prey system by incorporating anti-predation response to reveal new insight into complex dynamical behaviors in predator-prey interactions.

Mathematical modeling on biological problems is a powerful tool for understanding main features of the field work and predicting the phenomenon which have not been examined in experiments. Wang et al[46] proposed a predator-prey system to consider some indirect effect motivated by the field study in [49]. The model is formulated as follow:

$$\begin{cases} \frac{du}{dt} = f(k, v(t)) r_0 u(t) - d u(t) - a u^2(t) - g(u(t)) v(t), \\ \frac{dv}{dt} = c g(u(t)) v(t) - m v(t), \end{cases} \quad (1.2)$$

where u and v denote the population density of prey and predator respectively. r_0 is the intrinsic growth rate of prey. d and m are natural mortality rate of prey and predator respectively. au is the density dependent mortality rate of prey due to intra-species' competition. $g(u)$ is the functional response accounting for the encounter mechanism of the predator and prey. The indirect fear effect is incorporated in the model in terms of function $f(k, v)$ where k is the positive parameter denoting the level of anti-predation response. This model assumes a cost in reproduction because of the fear of predator. So naturally, $f(k, v)$ is a decreasing function

with respect to both k and v . According to the analysis, high level of anti-predation response in the model with Holling Type II functional response can forbid the occurrence of periodic solution and stabilize the system. Furthermore, when anti-predation response is low, it is possible to have limit cycles because of Hopf bifurcation. The Hopf bifurcation in model (1.2) can be either supercritical or subcritical while the models without fear effect can only have supercritical Hopf bifurcation. The subcritical Hopf bifurcation can lead to an unstable limit cycle and as a result, a bistability scenario arises from such kind of bifurcation. These differences between (1.2) and classic predator-prey system show that incorporating indirect effect into modeling is essential, and can cause substantial differences.

Following their pioneering work, there have been more predator-prey models taking indirect effect into account. Wang and Zou [47] considered an age-structured model incorporating fear effect. They used delay differential equation model to study avoidance mechanism of adult prey. The result suggested either strong adaption of adult prey or huge cost of anti-predation response can destabilize the system and therefore introduce periodic behavior. Wang and Zou [48] also considered spatial heterogeneity of the environment and proposed a partial differential equation model to study the pattern formation induced by anti-predation response.

This thesis is deeply motivated by the important findings in field study on anti-predation response as well as previous mathematical modeling and analysis by Wang [46]. But one central question about the model (1.2) is that they only considered the cost of anti-predation response. In the real world, anti-predation strategies are applied mostly because of its protective benefits. Purely considering costs of anti-predation response may miss some key features about the response itself and also under or over estimate the change in population dynamics. Another direction to extend the study of anti-predation response is to consider more than two species interactions. In real ecosystems, the structure of food web is more complex and can have interesting biological phenomenon. For example, Suraci et al [41] found that anti-predation response can not only affect the prey but also have great impact on the species in lower trophic level, which leads to a trophic cascade[42]. So we examine the food chain models to find out the existence and direction of trophic cascade induced by anti-predation response.

Thus, the main questions in this thesis have been raised to explore how the costs and benefits

of anti-predation response affect population dynamics of predator and prey? Will anti-predation strategies stabilize or destabilize a predator-prey system? What role does anti-predation strategy play in more complex food chain ecosystems? When should a prey adopt anti-predation response and when it should not? Is there an optimal anti-predation strategy? How anti-predation strategies evolve in the predator-prey interaction?

In this thesis, we address these problems by qualitatively analyzing the models with anti-predation response and numerically exhibiting the population dynamics of the species involving in the interaction. In Chapter 2, we start from a two species predator-prey system and demonstrate the integrated impact of anti-predation strategies and digestion delay. We show both the anti-predation strategy and the time delay in biomass transfer can play important roles in determining the long term population size of both predator and prey species. In Chapter 3, we examine the food chain models with anti-predation response. The occurrence of trophic cascade illustrates that the response not only affects the single species but also changes the dynamics of whole ecosystem. In Chapter 4, we study how the anti-predation strategies evolves and compare two predation types to show that possible endpoints of evolution are different depending on the type of predator. In Chapter 5, we briefly summarize the main results of this thesis and discuss some future directions of studying anti-predation response.

The rest of introduction exhibits basic ecological aspects mentioned in this thesis: costs and benefits of anti-predation response (Chapters 2, 3 and 4) and trophic cascade (Chapter 3), along with the main mathematical tools used in this thesis: stability analysis of nonlinear system (Chapters 2,3 and 4) and adaptive dynamics (Chapter 4).

1.1 Costs and benefits of anti-predation response

The impact of anti-predation response on population dynamics can not be understood without understanding of its trade-off mechanism. Direct protective benefits such as avoiding detection [6, 7], escaping from direct predation [7, 28] and development of beneficial behaviors can be considered as reducing the predation risk, which are intuitive, and therefore are reflected in the predation term in our model [8, 43].

Compared to the benefits, the costs of anti-predation response are much more complicated and widely ignored in study of wildlife management. This is mainly due to lack of general theory to measure the costs in comparison with benefits and direct effect. The costs of anti-predation response include classical allocation costs which are resulted from the use of energy and material to form and maintain the anti-predation behaviors [4, 20, 43]. For example, most escape strategies need higher energy requirement and form energetic consequences on reproduction. A possible type of costs induced by aforementioned allocation cost is called opportunity costs [11]. For example, a species may leave a habitat with abundant resource to avoid detection by predator and therefore lose a potential growth opportunity because of the anti-predation response. This kind of costs is almost impossible to measure. Also there are self damage costs [15, 31, 38] like when honeybee use its sting and sacrifice to defense colony. Among these different types of costs, the mechanism is really complicated and species specific. In order to capture the main feature and also make it mathematically tractable, in this thesis, we assume all the costs affect only the intrinsic growth rate of the prey species.

1.2 Trophic cascade

In real world ecosystems, the predator-prey interactions most likely involve more than just two species. Most organisms play the roles of both predator and prey simultaneously. So it is natural to extend our interest of anti-predation response into food chain environment. In a complex food web, apex predators has a very important position to regulate the food web below them [42]. This is understood as a top-down process which counters the bottom-up flow from productivity. In 1960, the famous “green world” hypothesis was proposed by Hairston, Smith and Slobodkin [12]. In short, the hypothesis claims the effect that carnivores’ proper consumption of herbivores can enrich plant and keep our world green. This hypothesis has motivated ecologist to consider trophic cascade. But because top-down processes are difficult to study (need large space, long timescale and are expensive to implement), the understanding of these effects is far behind the understanding of bottom-up phenomenon. So the acceptance of “green world” hypothesis has been delayed. Recently, empirical evidences have shown severe effects that break the balance of ecosystems due to the loss of top predator [2, 27, 35]. The

importance of these top-down effects to sustain the ecosystem and preserve the biodiversity has widely captured research interests in both field experiments and theory development.

For example, a tri-trophic mesopredator cascade was examined by Suraci et al [41] by manipulating the fear of large carnivore to cause the behavior change of mesocarnivore. As a result, the prey of the mesocarnivore gained benefits reflected in population growth and further affected lower trophic level species. This leaves an avenue for us to consider applying manipulated anti-predation response as a control tool to shift the balance of ecosystem and conserve the biodiversity.

1.3 Mathematical theories and methodologies

Mathematical modeling in biology are characterized by rate of changes in biological meaningful variables [5, 29]. In this thesis, we use differential equations to continuously track the changes in population sizes. These differential equations use time as independent variable and populations as state variables to demonstrate the development of species with time varying. To connect these mathematical models with real world problems, we first use dynamical system theory to check the well-posedness of each model [33, 40, 13]. In more details, we show the global existence of the unique solution and verify that the biological meaningful state variables (such as populations) are non-negative and bounded. Most modern differential equation models for population dynamics are nonlinear systems and therefore, it is hard and impossible in most of the times to find the solution explicitly. So it is essential to use some mathematical tools and numerical simulations to examine the qualitative behavior of the systems. In particular, for population dynamics, we use standard stability analysis for nonlinear systems to reveal the long term behavior of the systems. For phenotypic evolution problems, we use the method of adaptive dynamics to study the evolutionary stability of the traits. Next, I briefly outline the main ideas of these core mathematical analysis techniques.

1.3.1 Stability analysis of nonlinear systems

By dynamical system theory, in deterministic differential equation models, the whole dynamics is determined by the flow defined by the differential equations. We mainly seek for the asymptotic behavior of the models since it predicts the final scenario of our interested biological phenomena. This dynamical terminology often refers to the so-called α -limit set and ω -limit set depending on time going forward and backward respectively.

To study these limit sets, a common start point is to analyze the time independent solutions, called equilibria. They are also called steady states of the systems. Stability of equilibria can provide rich information of the whole dynamical system. Here, stability refers to the classic Lyapunov stability. That is, an equilibrium solution is called locally stable if trajectories starting close to the equilibrium will remain close to it forever. It is called locally asymptotically stable if any trajectories start close will eventually converge to this equilibrium solution. It is called globally asymptotically stable if trajectories start everywhere will eventually approach to the equilibrium solution. By Hartman-Grobman Theorem [33], near a hyperbolic equilibrium solution, the dynamics of a nonlinear systems is equivalent to that of its corresponding linearization. Therefore, local stability of an equilibrium solution can be obtained by the linearization around the equilibrium solution, which is determined by the eigenvalues of the Jacobian matrix of the linear system. If all eigenvalues of the Jacobian matrix at an equilibrium solution have negative real part, then the equilibrium solution is locally asymptotically stable. If at least one eigenvalue has positive real part, then it is unstable. However, with the changing of the parameters, the local stability of an equilibrium solution may change, such a phenomenon is called local bifurcation. Some well-known bifurcations such as saddle-node bifurcation, transcritical bifurcation and pitch-fork bifurcation [33] account for changes of stability of equilibrium solutions respectively such that the dynamical behavior of the system dramatically vary with the parameters passing some threshold values.

This linearization strategy is always applicable unless the equilibrium solution is non-hyperbolic, in another words, some eigenvalues of the corresponding Jacobian matrix have zero real part. In this case, the local behavior of the original nonlinear system can not be full characterized by its corresponding linear system and more complicated dynamical structure

like periodic orbits may occur. This kind of bifurcation by which limit cycle is created when the stability of the equilibrium solution changes, is called Hopf bifurcation. To confirm the existence of Hopf bifurcation, we also need to check the transversal condition that ensures the pure imaginary eigenvalue crosses the imaginary axis in complex plane with the change of parameter. The stability of these limit cycles induced by Hopf bifurcation can be determined by center manifold theory which is often related to the normal form theory [33].

On the other hand, global stability is more difficult to determine because of its nonlinearity. There are no generally applicable tools for this problem. But for some special cases, Lyapunov function method is available to decide the global stability [33]. A strict Lyapunov function is a non-negative function of state variables. It is zero at the equilibrium solution and strictly positive at anywhere else. If the derivative of this Lyapunov function with respect to the time variable along the model system is negative at everywhere in the feasible region, then the equilibrium is globally asymptotically stable. The construction of Lyapunov functions, often referred as Lyapunov direct method, can be found in some standard models. But one should notice at present, there is no general way to construct a Lyapunov function for a general system.

1.3.2 Adaptive dynamics

Different from the basic mathematical theory in studying population dynamics, adaptive dynamics is introduced about thirty years ago to solve the problems involving phenotypic evolution [9, 26]. In adaptive dynamics, the goal is to examine the evolution of a continuous trait, a phenotype for a species. The trait can be represented as a real number. Imagine there is a resident strain which has reached a steady state by its trait. Now consider a rare mutant who plays a different strategy. The question is whether it can invade or not. To answer this question, invasion analysis is applicable to check the growth rate of the mutant at current environment. To this end, we can define a fitness function of the rare mutant says, $h(r, m)$, depending on both the resident strategy, r and the mutant strategy, m . The fitness function is directly related to a condition that determines whether the mutant can have a growing population or not. That is, when $h > 0$, the mutant can invade and when $h < 0$, the mutant will be wiped out. Notice that $h(r, r) = 0$ when the mutant plays same strategy as the resident.

Next, we can define the selection gradient $s(r) = \left[\frac{\partial}{\partial m} h(r, m) \right]_{m=r}$. This shows the evolution direction of the trait. When $s(r) > 0$ (< 0), a slightly stronger (weaker) strategy is favored. The strategy r^* that satisfies $s(r^*) = 0$ is called an evolutionary singular strategy. A central concept in evolutionary biology is called *evolutionarily stable strategy (ESS)*[25, 14]. That is, a strategy once played by the resident, any mutant can never invade it by applying a different strategy. As we can see, the singular strategy is a candidate for an evolutionary stable strategy. Since we have $h(r^*, r^*) = 0$ and $s(r^*) = 0$, we only need $C_{22} = \left[\frac{\partial^2}{\partial m^2} h(r, m) \right]_{m=r=r^*} < 0$ such that $h(r^*, m)$ has a local maximum value zero when $m = r^*$ along the direction of varying m only, that is, for any other nearby strategies, the fitness is negative and the invasion is impossible. Another related concept is called *convergence stable strategy*. A singular strategy r^* is called a convergence stable strategy if a resident play a nearby strategy r will always be invaded by a mutant with strategy m lying in between r and r^* . To this end, we need the selection gradient $s(r)$ be a decreasing function around r^* , that is, $\left. \frac{ds(r)}{dr} \right|_{r=r^*} = \left[\frac{\partial^2 h(r, m)}{\partial r \partial m} + \frac{\partial^2 h(r, m)}{\partial m^2} \right]_{m=r=r^*} < 0$. Remember we have $h(r, r) = 0$, so $\left[\frac{\partial^2 h(r, m)}{\partial r^2} + \frac{2\partial^2 h(r, m)}{\partial r \partial m} + \frac{\partial^2 h(r, m)}{\partial m^2} \right]_{m=r} = 0$. We can define $C_{11} = \left[\frac{\partial^2}{\partial r^2} h(r, m) \right]_{m=r=r^*}$ and therefore, the criterion of convergence stable can be rewritten as $C_{11} > C_{22}$. For mutual invasibility, we need both $h(r, m) > 0$ and $h(m, r) > 0$, the generic condition can be concluded as $C_{11} > -C_{22}$.

One should be careful about the evolutionarily stability and convergence stability. In general, they are not related. A singular strategy that is both evolutionarily stable and convergence stable is called a *continuously stable strategy (CSS)*, which is a possible endpoint of the evolution. To avoid confusion between continuously stable strategy and convergence stable strategy (which is also called CSS in some literatures [22]), we follow [9] and use the term *evolutionarily attraction strategy (EAS)* to denote a convergence stable strategy.

After determining the local evolutionary stability, a further question is whether the successfully invaded strain replaces the resident to become a new resident or coexists with the resident to form a dimorphic resident. However, this requires nonlinear analysis and there is no general method to solve the problem. Only in some special models, these properties can be determined by relating to the global stability of dynamical systems [10, 16, 21].

Bibliography

- [1] Abrams, P. A., Ginzburg, L. R., *The nature of predation: prey dependent, ratio dependent or neither ?*, Trends in Ecology and Evolution **15**(2000), 337-341.
- [2] Alverson, W.S., Waller, D.M., Solheim, S.L., *Forests too deer: edge effects in northern Wisconsin.*, Conserv. Biol. **2**(1988), 348–358.
- [3] Arditi, R., Ginzburg, L. R., *Coupling in predator-prey dynamics: ratio dependence*, Journal of Theoretical Biology **139**(1989), 311-326.
- [4] Berenbaum, M. R., Zangerl, A. R., *Costs of inducible defense: protein limitation, growth, and detoxification in parsnip webworms.* Ecology **75**(1994), 2311–2317.
- [5] Britton, N. F., *Essential Mathematical Biology* Springer, Berlin (2003).
- [6] Caro, T., *Antipredator Defenses in Birds and Mammals.*, University of Chicago Press (2005).
- [7] Cott, H. B., *Adaptive Coloration in Animals.*, Methuen (1940).
- [8] Creel, S., Christianson, D., *Relationships between direct predation and risk effects*, Trends Ecol Evolut **23**(2008), 194-201.
- [9] Diekmann, O., *Beginner's Guide to Adaptive Dynamics*, Banach Center Publications, **63** (2004), 47-86.
- [10] Dockery, J., Hutson, V., Mischaikow, K. and Pernarowski, M., *The evolution of slow dispersal rates: A reaction diffusion model.*, J. Math. Biol., **37**(1998), 61-83.

- [11] Gulmon, S. L., Mooney, H. A., *Costs of defense on plant productivity*. In: Givnish, T. J. (ed) *On the economy of plant form and function*. Cambridge University Press, Cambridge, (1986), 681–698.
- [12] Hairston, N. G., Smith, F. E. and Slobodkin, L. B., *Community structure, population control, and competition*. *American Naturalist* **94**(1960), 421–425.
- [13] Hale, J. K., Verduyn Lunel, S. M., *Introduction to Functional Differential Equations*, Springer-Verlag New York, 1993.
- [14] Hamilton, W. D., *Extraordinary sex ratios*, *Science* **156**(1967), 477–488.
- [15] Harvell, C. D., West, J. M. and Griggs, C., *Chemical defense of embryos and larvae of a West Indian gorgonian coral*, *Briareum asbestinus*. *Inven. Reprod. Dev.* **30**(1996), 239–246.
- [16] Hastings, A., *Can spatial variation alone lead to selection for dispersal?*, *Theor. Popul. Biol.*, **24**(1983), 244–251.
- [17] Holling, C. S., *The functional response of predator to prey density and its role in mimicry and population regulation*, *Mem. Ent. Sec. Can.* **45**(1965), 1–60.
- [18] Jeschke, J. M., Kopp, M., Tollrian, R., *Predator function responses: discriminating between handling and digesting prey*, *Ecological Monographs* **72**(1) (2002), 95–112.
- [19] Krebs, J. R., Davies, N. B., *An Introduction to Behavioural Ecology*, Wiley-Blackwell(1993).
- [20] Kusch, J., Kuhlmann, H. W., *Cost of *Stenostomum*-induced morphological defense in the ciliate *Euplotes octocarinatus**. *Arch Hydrobiol* **130**(1994), 257–267.
- [21] Lam, K. Y., Lou, Y., *Evolution of conditional dispersal: evolutionarily stable strategies in spatial models*, *J. Math. Biol.* **68**(4) (2013), 851–877.
- [22] Lam, K. Y., Lou, Y., *Evolutionarily stable and convergent stable strategies in reaction-diffusion models for conditional dispersal*, *Bull Math Biol* **76**(2) (2014), 261–291.

- [23] Lotka, A. J., *Analytical Note on Certain Rhythmic Relations in Organic Systems*, Proc. Natl. Acad. Sci. U.S.A. **6**(1920), 410-415 .
- [24] Lotka, A. J., *Elements of Physical Biology*, Williams and Wilkins (1925).
- [25] Maynard Smith, J., Price, G., *The logic of animal conflict*, Nature, **246**(1973), 15–18.
- [26] McGill, B.J., Brown, J.S, *Evolutionary game theory and adaptive dynamics of continuous traits*. Annu. Rev. Ecol. Evol. Syst. **38**(2007), 403–435.
- [27] McShea, W. J., Underwood, H. B., Rappole, J. H., *The Science of Overabundance: Deer Ecology and Population Management*. Washington, DC: Smithsonian Inst. Press (1997).
- [28] Merilaita, S. et al, *Number of eyespots and their intimidating effect on naïve predators in the peacock butterfly.*, Behavioral Ecology, **22**(6) (2011), 1326–1331.
- [29] Murray, J. D., *Mathematical Biology*, Springer-Verlag, Berlin, (1989).
- [30] Nelson, E.H. et al., *Predators reduce prey population growth by inducing changes in prey behavior*. Ecology **85**(2004), 1853–1858.
- [31] Orians, G. H., Janzen, D. H., *Why are embryos so tasty?* Am. Nat. **108**(1974), 581-592.
- [32] Pangle, K.L. et al., *Large nonlethal effects of an invasive invertebrate predator on zooplankton population growth rate.*, Ecology **88**(2007), 402–412.
- [33] Perko, L., *Differential equations and dynamical systems*, Springer, New York(1996).
- [34] Preisser, E.L. et al., *Scared to death? The effects of intimidation and consumption in predator–prey interactions*. Ecology **86**(2005), 501–509.
- [35] Rooney, T. P., Waller D. M., *Direct and indirect effects of deer in forest ecosystems*. For.Ecol. Manag. **181**(2003), 165–176.
- [36] Rosenzweig, M. L., MacArthur, R. H., *Graphical representation and stability conditions of predator-prey interactions*, American Naturalist **97** (1963), 209-223.

- [37] Schmitz, O. J., A. P. Beckerman, and K. M. O'Brien. *Behaviorally mediated trophic cascades: effects of predation risk on food web interactions*. *Ecology* **78**(1997), 1388–1399.
- [38] Simms, E.L., *Costs of plant resistance to herbivory.*, In: Fritz, R. S. and Simms, E.L. (ed) *Plant Resistance to Herbivores and Pathogens: Ecology, Evolution, and Genetics*. University of Chicago Press, Chicago, (1992), 392–425.
- [39] Skalski, G. T., Gilliam, J. F., *Functional responses with predator interference: viable alternatives to the Holling Type II model*, *Ecology* **82**(2001), 3083-3092.
- [40] Smith, H., *An Introduction to Delay Differential Equations with Applications to the Life Sciences*, Springer-Verlag New York, 2010.
- [41] Suraci, J. P., Clinchy, M., Dill, L. M., Roberts, D., Zanette, L. Y., *Fear of large carnivores causes a trophic cascade*, *Nat Commun.* **7**(2016), 10698.
- [42] Terborgh, J., Estes, J. A., *Trophic Cascades: Predators, Prey, and the Changing Dynamics of Nature.*, Island Press (2010).
- [43] Tollrian, R., Harvell, C. D., *The Ecology and Evolution of Inducible Defenses.*, Princeton University Press (1999).
- [44] Volterra, V., *Variazioni e fluttuazioni del numero d'individui in specie animali conviventi*, *Mem. Acad. Lincei Roma.* **2**(1926), 31-113.
- [45] Volterra, V., *Variations and fluctuations of the number of individuals in animal species living together*, In Chapman, R. N. *Animal Ecology*. McGraw-Hill, 1931.
- [46] Wang, X., Zanette, L. Y., Zou, X., *Modelling the fear effect in predator-prey interactions*, *J Math Biol.* **73**(2016), 1179-1204.
- [47] Wang, X., Zou, X., *Modeling the Fear Effect in Predator-Prey Interactions with Adaptive Avoidance of Predators*, *Bull Math Biol* **79**(2017), 1325-1359.
- [48] Wang, X., Zou, X., *Pattern formation of a predator-prey model with the cost of anti-predator behaviours*, *Mathematical Biosciences and Engineering*, **15**(2018), 775-805.

- [49] Zanette, L. Y., White, A. F., Allen, M. C., Clinchy, M., *Perceived predation risk reduces the number of offspring songbirds produce per year*, *Science* **334** (6061)(2011), 1398-1401.

Chapter 2

On a predator-prey system with digestion delay and anti-predation strategy

2.1 Introduction

Predator-prey system is one of the most important topics in mathematical biology. Since the early pioneering model by Lotka-Volterra [15, 16, 22, 23], there has been a vast and rich literature on the models for predator-prey interactions. Without considering spatial and age structure, a predator-prey model can be generally described by a system of ordinary differential equations of the form

$$\begin{cases} \frac{du}{dt} = f_1(u(t)) - p(u(t), v(t))v(t), \\ \frac{dv}{dt} = f_2(v(t)) + cp(u(t), v(t))v(t), \end{cases} \quad (2.1)$$

where $u(t)$ and $v(t)$ are the population densities of the prey and predator respectively under consideration. Here, $f_1(u)$ is the growth rate of the prey population in the absence of the predator, and $f_2(v)$ is the growth rate of the predator population in the absence of the prey; $p(u, v)$ is referred to as the functional response which accounts for the predation rate and biomass transfer after predation, from the prey to the predator; and the constant c explains the efficiency in biomass transfer. For some frequently used forms of the functional response $p(u, v)$, see, e.g., [2, 8, 18] for some earlier works and [1, 11, 19] for some more recent works.

Predator-prey ODE models of the form (2.1) only consider the direct effect between the

predator and prey, reflected by the predation term. In the real world however, presence of predators also has indirect effects on prey population, in various ways. For example according to a recent field experimental study on song sparrow population by Zanette et al [29], the perception of predation risk can reduce the number of prey's offspring by as much as 40%, even without any direct predation. This evidence showed that the indirect effect can be as significant as direct predation for some species, sometimes even more significant. This phenomenon has attracted some biologists, both theoretical and experimental, and there have been some biological hypotheses proposed on such effects and some field experiments reported confirming such effects. See, e.g., [4, 5, 13, 14, 29] and the references therein.

The aforementioned preliminary biological studies strongly suggest that the neglect of indirect effect due to fear in the traditional predator-prey models, such as models of the form of (2.1), may not be reasonable for many species. This means that the existing mathematical models for predator-prey interactions need to be modified to include the fear effect that is indirect. Recently, Wang et. al. [24, 25, 26] made some initial efforts along this direction by an ordinary differential equation (ODE) model, a delay differential equation (DDE) model, and a partial differential equation (PDE) model respectively to address different aspects of the anti-predation responses of the prey caused by the fear. This work is mainly motivated by Wang et. al. [24] which proposed the following ODE model

$$\begin{cases} \frac{du}{dt} = f(k, v(t)) r_0 u(t) - d u(t) - a u^2(t) - g(u(t)) v(t), \\ \frac{dv}{dt} = c g(u(t)) v(t) - m v(t), \end{cases} \quad (2.2)$$

where u is the population density of prey species, v is the population density of predator species, r_0 is the reproduction rate of prey in the absence of predator, d is the natural (density independent) death rate and the term $au^2 = (au)u$ reflects the crowing effect with au accounting for density dependent death rate, c is the biomass transform efficiency constant. The function $g(u)$ is the functional response which is assumed to depend on the prey population only. Here the function $f(k, v)$ is incorporated into the model to account for the prey's anti-predation response with the positive parameter k measuring the response level due to the prey's perceived fear, and hence, $f(k, v)$ is decreasing in k and v . By analyzing this model, Wang et al [24]

obtained some interesting results on how the anti-predation response affects the population dynamics of this predator-prey model.

Obviously, in (2.2) *only the cost* of the anti-predation response in prey's reproduction is considered, but the benefits of such responses are ignored. However, there should be some *benefits*, as the prey's anti-predation response will obviously decrease the chance of the prey being caught by predators. This suggests a replacement of $g(u)$ in (2.2) by $g(k, u)$ which is decreasing in the response level parameter k . Moreover, in (2.2) it is assumed that the biomass transfer from prey to predator after predation is instantaneous. But in reality, such transfer takes time (see, e.g., [6, 27, 12, 28] and the references therein). With the above observations of the mentioned two drawbacks in (2.2), we propose, in this chapter, the following modification:

$$\begin{cases} \frac{du}{dt} = f(k, v(t)) r_0 u(t) - d u(t) - a u^2(t) - g(k, u(t)) v(t), \\ \frac{dv}{dt} = c g(k, u(t - \tau)) v(t - \tau) - m v(t). \end{cases} \quad (2.3)$$

where $\tau \geq 0$ is the average time needed for biomass transfer after predation from prey to predator. Here, by the meanings of the parameter k , and the non-negative functions $f(k, v)$ and $g(k, u)$, it is reasonable to pose the following assumptions:

$$\begin{cases} f(0, v) = 1, f(k, 0) = 1, \frac{\partial f}{\partial k} < 0, \frac{\partial f}{\partial v} < 0, \\ \lim_{k \rightarrow \infty} f(k, v) = 0, \lim_{v \rightarrow \infty} f(k, v) = 0, \\ g(k, 0) = 0, \frac{\partial g}{\partial k} < 0, \\ \lim_{k \rightarrow \infty} g(k, u) = 0. \end{cases} \quad (2.4)$$

This model is a system of delay differential equations and hence is of infinite dimension. In the rest of this chapter, we will analyze this infinite dimensional dynamical system. To make the analysis more explicit and for convenience of comparison, we will follow Wang et al [24] to consider two particular forms for the functional response g : (i) Holling Type I (linear) and (ii) Holling Type II. The main concern is the long time dynamics and thus, we will perform stability analysis by employing the stability theory and methods for delay differential equations. For the linear functional response mediated by the prey's anti-predation response, we find that

there are two thresholds for the anti-predation strategy k : when k is large, the prey species can always survive from the predation and predator species will die out; an intermediate value of k will lead to a stable co-existence equilibrium; when k is further decreased to a very small level, the co-existence equilibrium becomes unstable and a Hopf bifurcation occurs, leading to the occurrence of a stable periodic solution. This is in strong contrast to the results for (2.2) in [24], where there is no Hopf bifurcation when the functional response is linear. For the Holling Type II functional response mediated by the prey's anti-predation response, we do similar analysis and the analytic results reveal how the cost and benefit of the prey's anti-predation response interplay to affect the population dynamics. We also perform some numerical simulations to confirm our analytic results, and to explore, more visually, how the anti-predation strategies and the biomass transfer delay will impact the population dynamics.

The remainder of this chapter is organized as follows. In Section 2, we will address the well-posedness of the model system (2.3) including the existence and uniqueness of solution to (2.3) with biologically meaningful initial conditions, the positivity and boundedness of the solution. In Section 3, we investigate the existence and stability of equilibria. To this end, we consider two particular forms for the functional response g , with Subsection 3.1 dealing with the linear functional response mediated by the prey's anti-predation response, and Subsection 3.2 covering the case of Holling Type II functional response. In Section 4, we present some numeric results to confirm and demonstrate our analytic results. In Section 5, we summarize our main results and discuss their biological implications. We also discuss some possible future projects along this direction of fear effect in predator-prey interactions.

2.2 Well-posedness of the model

The model (2.3) is a system of delay differential equations for which an initial condition needs to be specified on the interval $[-\tau, 0]$. Considering the biological meanings of the variables u and v , non-negativity is required, motivating the following initial condition

$$\begin{cases} u(\theta) = u_0(\theta), \\ v(\theta) = v_0(\theta), \end{cases} \quad (2.5)$$

where $(u_0(\theta), v_0(\theta)) \in C([- \tau, 0], \mathcal{R}_+^2)$.

By the fundamental theory of functional differential equations (see, e.g., Hale and Verduyn Lunel [9]), the system (2.3)-(2.5) has a unique solution $(u(t), v(t)) = (u(t, u_0, v_0), v(t, u_0, v_0))$ which exists in a maximal interval $[0, T_m)$. We now prove the well-posedness of (2.3) in the sense that $u(t) \geq 0$ and $v(t) \geq 0$ for all $t \in [0, T_m)$, and $T_m = \infty$ meaning that the solution exists globally. Indeed, the non-negativity of $u(t)$ and $v(t)$ is a direct result of Theorem 2.1 in Smith [20]. To prove that $T_m = \infty$, by the extension theory for delay differential equations (see, e.g., Hale and Verduyn Lunel [9]), we just need to establish *a priori* boundedness for the solution. To this end, we consider $W(t, \tau) = u(t - \tau) + v(t)/c$. Simple calculations lead to

$$\begin{aligned} W'(t) &= r_0 u(t - \tau) f(k, v(t - \tau)) - d(u(t - \tau)) - a u^2(t - \tau) - \frac{m}{c} v(t) \\ &\leq (r_0 - d) u(t - \tau) - \frac{m}{c} v(t) - a u^2(t - \tau) \\ &\leq r_0 u(t - \tau) - a u^2(t - \tau) - \min(d, m) W \\ &\leq \frac{r_0^2}{4a} - \min(d, m) W =: \frac{r_0^2}{4a} - \mu W, \end{aligned}$$

where $\mu = \min(d, m/c)$. This implies that $\limsup_{t \rightarrow \infty} W(t) \leq r_0^2/(4a\mu)$, concluding the boundedness of $u(t - \tau) + v(t)/c$. Since we have already shown that $u(t)$ and $v(t)$ are non-negative, $u(t)$ and $v(t)$ are also bounded.

Combining the above, we have proved the well-posedness of (2.3)-(2.5) as stated in the following theorem.

Theorem 2.2.1 *Initial value problem (2.3)-(2.5) has a unique solution which exists for all $t \geq 0$ and is bounded in $[0, \infty)$.*

2.3 Equilibria and their stability

In this section, we investigate the long time behaviour of solutions to (2.3)-(2.5). To be more concrete, we will consider two particular forms for the functional response $g(k, u)$: (i) linear; (ii) Holling Type II.

2.3.1 Model with linear functional response

In this subsection, we consider $g(k, u)$ being linear in u , that is, $g(k, u) = \rho(k)u$. With this choice, (2.3) becomes

$$\begin{aligned}\frac{du}{dt} &= r_0 u(t) f(k, v(t)) - d u(t) - a u^2(t) - \rho(k) u(t) v(t), \\ \frac{dv}{dt} &= c \rho(k) u(t - \tau) v(t - \tau) - m v(t),\end{aligned}\tag{2.6}$$

The dependence of $g(k, u)$ on k assumed in (2.4) naturally poses the following condition on $\rho(k)$:

$$\begin{cases} \rho(k) \text{ is a decreasing function with respect to } k, \\ \lim_{k \rightarrow \infty} \rho(k) = 0. \end{cases}\tag{2.7}$$

System (2.6) has three possible equilibrium solutions. The trivial equilibrium $E_0 = (0, 0)$ always exists. When $r_0 > d$, there exists a predator free equilibrium $E_u = (\frac{r_0 - d}{a}, 0)$. A unique positive (co-existence) equilibrium exists when

$$r_0 > \frac{a m}{c \rho(k)} + d.\tag{2.8}$$

The positive equilibrium is denoted by $E^+ = (\bar{u}, \bar{v})$ with \bar{u} and \bar{v} satisfying

$$\begin{aligned}\bar{u} &= \frac{m}{c \rho(k)}, \\ r_0 f(k, \bar{v}) - d - a \bar{u} - \rho(k) \bar{v} &= 0.\end{aligned}\tag{2.9}$$

Remark Notice that $\rho(k)$ is a decreasing function and $\lim_{k \rightarrow \infty} \rho(k) = 0$. Therefore, for any set of other parameters in (2.6), there exists a critical value $k^* \geq 0$, such that, when $k > k^*$, the condition (2.8) fails, implying that there is no positive solution when $k > k^*$.

Local stability and Hopf bifurcation

In this section, we study the local stability for each of the equilibrium solution. The linearization of (2.6) near an equilibrium (u^*, v^*) is given by

$$\begin{aligned} \frac{du}{dt} &= [r_0 f(k, v^*) - d - 2a u^*] u(t) - \rho(k) u^* v(t) - \rho(k) v^* u(t) + \left(r_0 u^* \frac{\partial f}{\partial v} \Big|_{v^*} \right) v(t), \\ \frac{dv}{dt} &= c \rho(k) u^* v(t - \tau) + c \rho(k) v^* u(t - \tau) - m v(t), \end{aligned} \quad (2.10)$$

where (u^*, v^*) denotes the corresponding equilibrium.

The characteristic equation of (2.10) at $E_0 = (0, 0)$ is

$$(r_0 - d - \lambda)(-m - \lambda) = 0. \quad (2.11)$$

Therefore, if $r_0 < d$, E_0 is locally asymptotically stable. If $r_0 > d$, E_0 is unstable.

Now if $r_0 > d$, there exists a predator free (semi-trivial) equilibrium $E_u = (\frac{r_0-d}{a}, 0)$, the characteristic equation of which is given by

$$(-r_0 + d - \lambda) \left[c \rho(k) e^{-\lambda \tau} \frac{r_0 - d}{a} - m - \lambda \right] = 0. \quad (2.12)$$

Since $r_0 - d > 0$, $-r_0 + d - \lambda = 0$ only has a negative root. Other roots are determined by the equation

$$c \rho(k) e^{-\lambda \tau} \frac{r_0 - d}{a} - m - \lambda = 0. \quad (2.13)$$

This transcendental equation is in the form of the Hayes equation and hence, the existing results for this equation can be employed. Note that $c \rho(k) \frac{r_0-d}{a} > 0 > -m$ provided that $r_0 > d$, by Hayes [10] (also see Hale and Verdyun Lundel [9] or Smith [21]), E_u is locally asymptotically stable if $c \rho(k) \frac{r_0-d}{a} - m < 0$ and E_u is unstable if $c \rho(k) \frac{r_0-d}{a} - m > 0$. In other words, $r_0 < \frac{am}{c \rho(k)} + d$ (reverse of (2.8)) is a necessary and sufficient condition for E_u to be locally asymptotically stable.

When condition (2.8) holds, there is a unique positive equilibrium $E^+ = (\bar{u}, \bar{v})$, at which,

the corresponding characteristic equation reads

$$\lambda^2 + (a\bar{u} + m)\lambda + ma\bar{u} + e^{-\lambda\tau} \left[-m\lambda + m\rho(k)\bar{v} - r_0 m\bar{v} \frac{\partial f}{\partial v} \Big|_{\bar{v}} - am\bar{u} \right] = 0. \quad (2.14)$$

When $\tau = 0$, since $a\bar{u} > 0$ and $m\rho(k)\bar{v} - r_0 m\bar{v} \frac{\partial f}{\partial v} \Big|_{\bar{v}} > 0$, by the Routh–Hurwitz criterion, all roots of the resulting quadratic equation have negative real parts. Now we check if pure imaginary roots are possible for $\tau > 0$. Plugging $\lambda = \omega i$ ($\omega > 0$) into (2.13) and separating the real and imaginary parts, we obtain

$$\begin{cases} m\omega \sin(\omega\tau) - \left[m\rho(k)\bar{v} - r_0 m\bar{v} \frac{\partial f}{\partial v} \Big|_{\bar{v}} - am\bar{u} \right] \cos(\tau\omega) = -\omega^2 + ma\bar{u}, \\ m\omega \cos(\omega\tau) + \left[m\rho(k)\bar{v} - r_0 m\bar{v} \frac{\partial f}{\partial v} \Big|_{\bar{v}} - am\bar{u} \right] \sin(\tau\omega) = (a\bar{u} + m)\omega, \end{cases} \quad (2.15)$$

By eliminating the trigonometric functions in (2.15), we obtain the following equation for $\omega > 0$:

$$\omega^4 + (p_1^2 - q_1^2 - 2p_0)\omega^2 + p_0^2 - q_0^2 = 0 \quad (2.16)$$

where $p_0 = ma\bar{u}$, $p_1 = a\bar{u} + m$, $q_0 = m\rho(k)\bar{v} - r_0 m\bar{v} \frac{\partial f}{\partial v} \Big|_{\bar{v}} - am\bar{u}$ and $q_1 = -m$. Simple calculation shows $p_1^2 - q_1^2 - 2p_0 = (a\bar{u})^2 > 0$. Now we distinguish two exclusive cases: (A) $p_0^2 > q_0^2$; and (B) $p_0^2 < q_0^2$.

For (A), the equation (2.16) has no positive solution, implying that (2.14) can not have pure imaginary roots for all $\tau > 0$. Therefore, the co-existence equilibrium is locally asymptotically stable for all $\tau > 0$.

For (B), (2.16) has a unique positive root

$$\omega_0 = \left(\frac{-a^2\bar{u}^2 + \sqrt{a^4\bar{u}^4 - 4p_0^4 + 4q_0^4}}{2} \right)^{\frac{1}{2}}. \quad (2.17)$$

Plugging $\omega = \omega_0$ into (2.15) and solving the resulting equation for $\sin \omega_0\tau$ and $\cos \omega_0\tau$, we

obtain

$$\begin{cases} \cos(\omega_0 \tau) = \frac{q_0 \omega_0^2 - q_0 p_0 - p_1 q_1 \omega_0^2}{q_0^2 + q_1^2 \omega_0^2} =: P_0 \\ \sin(\omega_0 \tau) = \frac{p_1 \omega_0 + q_1 \omega_0 P_0}{q_0} =: Q_0 \end{cases} \quad (2.18)$$

From this, we obtain a sequence of critical values for the delay parameter τ :

$$\tau_n = \begin{cases} \frac{1}{\omega_0} \arccos \frac{q_0 \omega_0^2 - q_0 p_0 - p_1 q_1 \omega_0^2}{q_0^2 + q_1^2 \omega_0^2} + \frac{2n\pi}{\omega_0}, & n = 0, 1, \dots, \text{ if } Q_0 > 0; \\ \frac{1}{\omega_0} \left[2\pi - \arccos \frac{q_0 \omega_0^2 - q_0 p_0 - p_1 q_1 \omega_0^2}{q_0^2 + q_1^2 \omega_0^2} \right] + \frac{2n\pi}{\omega_0}, & n = 0, 1, \dots, \text{ if } Q_0 < 0. \end{cases} \quad (2.19)$$

Therefore, in this case, the co-existence equilibrium is locally asymptotically stable when $\tau < \tau_0$. At $\tau = \tau_0$, (2.13) has a pair of pure imaginary roots $\pm i\omega_0$. We now verify the transversality condition at $\tau = \tau_0$. We claim that

$$\left. \frac{d(\Re(\lambda))}{d\tau} \right|_{\tau=\tau_0} > 0. \quad (2.20)$$

Indeed, differentiating equation (2.14) with respect to τ , we obtain

$$\left(\frac{d\lambda}{d\tau} \right)^{-1} = \frac{2\lambda + p_1 + q_1 e^{-\lambda\tau}}{e^{-\lambda\tau} \lambda(q_1 \lambda + q_0)} - \frac{\tau}{\lambda}. \quad (2.21)$$

Thus, at $\tau = \tau_0$ ($\lambda = i\omega_0$), we have

$$\begin{aligned} \operatorname{sgn} \left(\left. \frac{d\Re(\lambda)}{d\tau} \right|_{\tau=\tau_0} \right) &= \operatorname{sgn} \left(\Re \left. \frac{d(\lambda)}{d\tau} \right|_{\tau=\tau_0} \right) = \operatorname{sgn} \left(\Re \left(\left. \frac{d(\lambda)}{d\tau} \right|_{\tau=\tau_0} \right)^{-1} \right) \\ &= \operatorname{sgn} \left(\Re \left[\frac{2\lambda + p_1 + q_1 e^{-\lambda\tau}}{e^{-\lambda\tau} \lambda(q_1 \lambda + q_0)} - \frac{\tau}{\lambda} \right] \Big|_{\lambda=i\omega_0} \right) \\ &= \operatorname{sgn} \left(\frac{-\omega_0(p_1 q_1 - 2q_0) \cos(\omega_0 \tau) + (2q_1 \omega_0^2 + p_1 q_0) \sin(\omega_0 \tau) - q_1^2 \omega_0}{\omega_0(q_1^2 \omega_0^2 + q_0^2)} \right). \end{aligned} \quad (2.22)$$

Plugging (2.18) into (2.22) and simplifying, we obtain

$$\Re \left(\left. \frac{d(\lambda)}{d\tau} \right|_{\tau=\tau_0} \right)^{-1} = \frac{p_1^2 - q_1^2 - 2p_0 + 2\omega^2}{q_1^2 \omega_0^2 + q_0^2} = \frac{a^2 \bar{u}^2 + 2\omega^2}{q_1^2 \omega_0^2 + q_0^2} > 0, \quad (2.23)$$

implying

$$\left. \frac{d(\Re(\lambda))}{d\tau} \right|_{\tau=\tau_0} > 0.$$

This verifies the transversality condition at $\tau = \tau_0$. Therefore, when τ increases to pass τ_0 , Hopf bifurcation occurs.

Summarizing the above analysis, we have proved the following theorem.

Theorem 2.3.1 *For model system (2.6), the following results hold.*

- (i) *When $r_0 < d$, there is only the trivial equilibrium $E_0 = (0, 0)$ and it is locally asymptotically stable.*
- (ii) *When $d < r_0 < d + \frac{am}{c\rho(k)}$, then $E_0 = (0, 0)$ becomes unstable and there is the predator free equilibrium $E_u = \left(\frac{r_0-d}{a}, 0\right)$ which is locally asymptotically stable.*
- (iii) *When $r_0 > d + \frac{am}{c\rho(k)}$, both E_0 and E_u are unstable and there is a third equilibrium, the positive (or co-existence) equilibrium E^+ . Moreover,*
 - (iii)-1 *if $p_0 > q_0$, then $E^+ = (\bar{u}, \bar{v})$ is locally asymptotically stable for all $\tau > 0$;*
 - (iii)-2 *if $p_0 < q_0$, there is a $\tau_0 > 0$ such that $E^+ = (\bar{u}, \bar{v})$ is locally asymptotically stable when $0 < \tau < \tau_0$ and is unstable when $\tau > \tau_0$. Furthermore, there is a Hopf bifurcation of E^+ at $\tau = \tau_0$, leading to the occurrence of periodic solutions.*

Remark By Theorem (3.2) in [24], we know that the ODE model (2.2) with the linear functional response can never have periodic solutions. But in our modified model (2.6) with both cost and benefit of the anti-predation response and biomass transfer delay incorporated, even for the linear functional response, within certain range of other parameters and time delay, the stability of the co-existence equilibrium can be destroyed, leading to the occurrence of periodic solutions through Hopf bifurcation. Although we used the delay τ as the bifurcation parameter, we can also use an alternative parameter as the bifurcation parameter. For example, if we use k as bifurcation parameter, we can also confirm Hopf bifurcation when k passes some critical value. We will discuss this in more details in Section 5.

Global stability of the boundary equilibria E_0 and E_u

Theorem 2.3.1-(i) and (ii) established the *local* asymptotical stability of E_0 and E_u respectively. In this subsection, we show that E_0 and E_u are actually *globally* asymptotically stable under the respective condition.

Theorem 2.3.2 *When $r_0 < d$, there is only one trivial equilibrium $E_0 = (0, 0)$ and it is globally asymptotically stable.*

Proof Consider the Lyapunov functional $V(t) = u(t) + \frac{v(t)}{c} + \rho(k) \int_{t-\tau}^t u(s) v(s) ds$. Calculating the derivative of V along the trajectory of (2.6) yields

$$\dot{V} = r_0 u(t) f(k, v(t)) - d u(t) - a u^2(t) - \frac{m v(t)}{c}. \quad (2.24)$$

Therefore $\dot{V} \leq 0$ provided $r_0 < d$ (note that $f(k, v(t)) \leq 1$ by (2.4)). $\dot{V} = 0$ if and only if $u(t) = v(t) = 0$. Thus, $u(t) \rightarrow 0$ and $v(t) \rightarrow 0$ as $t \rightarrow \infty$, implying that $E_0 = (0, 0)$ is globally asymptotically stable.

Theorem 2.3.3 *When $d < r_0 < d + \frac{am}{c\rho(k)}$, $E_u = \left(\frac{r_0-d}{a}, 0\right)$ is globally asymptotically stable.*

Proof Note that

$$\frac{du}{dt} = r_0 u(t) f(k, v(t)) - d u(t) - a u^2(t) - \rho(k) u(t) v(t) \leq r_0 u(t) - d u(t) - a u^2(t)$$

since $f(k, v(t)) \leq 1$. By the property of the logistic equation and the comparison theorem, for any $\epsilon > 0$, there exist a $T = T(\epsilon) > 0$, such that $u(t) < \frac{r_0-d}{a} + \epsilon$ when $t > T$. Then for $t > T + \tau$, the DDE for $v(t)$ satisfies

$$\frac{dv}{dt} = c\rho(k) u(t-\tau) v(t-\tau) - m v(t) < c\rho(k) \left(\frac{r_0-d}{a} + \epsilon\right) v(t-\tau) - m v(t). \quad (2.25)$$

This establishes the following comparison (from above) equation for the variable $v(t)$

$$\frac{dx}{dt} = c\rho(k) \left(\frac{r_0-d}{a} + \epsilon\right) x(t-\tau) - m x(t). \quad (2.26)$$

Since $r_0 < d + \frac{am}{c\rho(k)}$ and ϵ is arbitrary, we can choose $\epsilon < \frac{m}{c\rho(k)} - \frac{r_0-d}{a}$ so that $c\rho(k) \left(\frac{r_0-d}{a} + \epsilon \right) - m < 0$ and $c\rho(k) \left(\frac{r_0-d}{a} + \epsilon \right) > 0 > -m$. For such chosen ϵ , by Theorem 4.7 in [21], the trivial solution $x = 0$ of (2.26) is globally asymptotically stable, meaning that every solution $x(t)$ of (2.26) satisfies $x(t) \rightarrow 0$ as $t \rightarrow \infty$. Since (2.26) is linear and cooperative, by (2.25) and the comparison theorem (see, e.g., Theorem 4.1 in [20]), we have $0 \leq v(t) \leq x(t)$, implying that $v(t) \rightarrow 0$ as $t \rightarrow \infty$. Now by the theory of asymptotically autonomous systems in [3], the behavior of u is governed by the limiting equation

$$\frac{du}{dt} = r_0 u(t) - d u(t) - a u^2(t).$$

By the result on a logistic equation, we then conclude that $u(t) \rightarrow \frac{r_0-d}{a}$ as $t \rightarrow \infty$. Therefore, we have proved that $E_u = \left(\frac{r_0-d}{a}, 0 \right)$ is globally asymptotically stable.

2.3.2 Model with the Holling Type II functional response

In this subsection, we study the model system (2.3) with Holling Type II functional response

$$g(u(t), k) = \rho(k) \frac{p u(t)}{1 + q u(t)}. \quad (2.27)$$

To make the model more mathematically tractable, in this subsection we also choose some particular forms for the functions $\rho(k)$ and $f(v, k)$ that represent the fear effect through the the response level parameter k as below:

$$\rho(k) = \frac{1}{1 + c_1 k}, \quad f(v(t), k) = \frac{1}{1 + c_2 k v(t)}. \quad (2.28)$$

With the above adoptions, model (2.3) becomes

$$\begin{cases} \frac{du}{dt} = \frac{r_0 u(t)}{1 + c_2 k v(t)} - d u(t) - a u^2(t) - \frac{p u(t) v(t)}{1 + q u(t)} \cdot \frac{1}{1 + c_1 k}, \\ \frac{dv}{dt} = \frac{c}{1 + c_1 k} \cdot \frac{p u(t - \tau) v(t - \tau)}{1 + q u(t - \tau)} - m v(t), \end{cases} \quad (2.29)$$

Here we introduce two constants c_1 and c_2 to describe the decreasing rate of reproduction and predation respectively, with respect to the response level k .

This system also has three possible equilibrium solutions. The trivial equilibrium $E_0 = (0, 0)$ always exists. When $r_0 > d$, there exists the predator free equilibrium $E_u = (\frac{r_0-d}{a}, 0)$. A positive (co-existence) equilibrium is determined by solving the system

$$\begin{cases} 0 = \frac{r_0}{1 + c_2 k \bar{v}} - d - a \bar{u} - \frac{p \bar{v}}{1 + q \bar{u}} \cdot \frac{1}{1 + c_1 k}, \\ 0 = \frac{c}{1 + c_1 k} \cdot \frac{p \bar{u}}{1 + q \bar{u}} - m. \end{cases} \quad (2.30)$$

The second equation does not contain variable v , and it has a positive solution for u if and only if

$$c p > m q (1 + c_1 k), \quad (2.31)$$

and the solution is given by

$$\bar{u} = \frac{m(1 + c_1 k)}{c p - m q (1 + c_1 k)}.$$

Plugging this \bar{u} into the first equation in (2.30) gives the following quadratic equation for the variable v :

$$a_2 v^2 + a_1 v + a_0 = 0 \quad (2.32)$$

where

$$\begin{cases} a_2 = c_2 k p, \\ a_1 = p + (d + a \bar{u})(1 + q \bar{u})(1 + c_1 k) c_1 k, \\ a_0 = (1 + q \bar{u})(1 + c_1 k)(d + a \bar{u} - r_0). \end{cases}$$

Note that under (2.31), both a_1 and a_2 are positive, and $a_0 < 0$ if and only if $d + a \bar{u} - r_0 < 0$ which is equivalent to

$$\frac{m(1 + c_1 k)}{c p - m q (1 + c_1 k)} < \frac{r_0 - d}{a}. \quad (2.33)$$

By the property of quadratic functions, we conclude that (2.32) has a positive solution \bar{v} if and only if (2.33) holds. Summarizing the above, when $r_0 > d$, there exists a unique positive equilibrium (\bar{u}, \bar{v}) if and only if

$$0 < \frac{m(1 + c_1 k)}{c p - m q (1 + c_1 k)} < \frac{r_0 - d}{a}. \quad (2.34)$$

Local stability and Hopf bifurcation

In this subsection, we study the local stability for each of the equilibrium solutions. The linearization of (2.29) at an equilibrium (u^*, v^*) is given by

$$\begin{pmatrix} \frac{du}{dt} \\ \frac{dv}{dt} \end{pmatrix} = \begin{pmatrix} J_{11} & J_{12} \\ 0 & -m \end{pmatrix} \begin{pmatrix} u(t) \\ v(t) \end{pmatrix} + \begin{pmatrix} 0 & 0 \\ K_{21} & K_{22} \end{pmatrix} \begin{pmatrix} u(t - \tau) \\ v(t - \tau) \end{pmatrix} \quad (2.35)$$

where

$$\begin{aligned} J_{11} &= \frac{r_0}{1 + c_2 k v^*} - d - 2 a u^* - \frac{p v^*}{(1 + c_1 k)(1 + q u^*)^2}, \\ J_{12} &= -\frac{c_2 k r_0 u^*}{(1 + c_2 k v^*)^2} - \frac{p u^*}{(1 + c_1 k)(1 + q u^*)}, \\ K_{21} &= \frac{c p v^*}{(1 + c_1 k)(1 + q u^*)^2}, \\ K_{22} &= \frac{c p u^*}{(1 + c_1 k)(1 + q u^*)}. \end{aligned}$$

From (2.35) we can derive the characteristic equation as

$$(\lambda - J_{11})(\lambda + m - K_{22}e^{-\tau\lambda}) - J_{12} K_{21}e^{-\tau\lambda} = 0. \quad (2.36)$$

At $E_0 = (0, 0)$, $J_{11} = r_0 - d$, $J_{12} = J_{21} = K_{12} = K_{22} = 0$, and hence, the characteristic equation of (2.36) becomes

$$(\lambda - r_0 + d)(\lambda + m) = 0.$$

Therefore, if $r_0 < d$, E_0 is locally asymptotically stable. If $r_0 > d$, E_0 is unstable.

Now if $r_0 > d$, there exists the predator free (semi-trivial) equilibrium $E_u = (\frac{r_0-d}{a}, 0)$, at which the characteristic equation is given by

$$(\lambda - d + r_0) \left(\lambda + m - \frac{c p \hat{u}}{(1 + c_1 k)(1 + q \hat{u})} e^{-\tau\lambda} \right) = 0 \quad (2.37)$$

where $\hat{u} = \frac{r_0-d}{a}$. Since $r_0 - d > 0$, $\lambda - d + r_0 = 0$ only has a negative root. Other roots of (2.37)

are determined by the equation

$$\lambda + m - \frac{c p \hat{u}}{(1 + c_1 k)(1 + q \hat{u})} e^{-\tau \lambda} = 0. \quad (2.38)$$

Noting that $\frac{c p \hat{u}}{(1 + c_1 k)(1 + q \hat{u})} > 0 > -m$, again by the results for the Hayes equation given in Hayes [10] (also see Hale and Verdyun Lunel [9] or Smith [21]), E_u is locally asymptotically stable if

$$\frac{c p \hat{u}}{(1 + c_1 k)(1 + q \hat{u})} - m < 0, \quad (2.39)$$

and E_u is unstable if (2.39) is reversed. Calculation shows that (2.39) is equivalent to

$$m(1 + c_1 k) > [c p - m q(1 + c_1 k)] \frac{r_0 - d}{a},$$

which holds if

$$\begin{aligned} & \text{either } \{c p < m q(1 + c_1 k)\}, \\ & \text{or } \left\{ c p > m q(1 + c_1 k) > 0 \quad \text{and} \quad \frac{m(1 + c_1 k)}{c p - m q(1 + c_1 k)} > \frac{r_0 - d}{a} \right\}. \end{aligned} \quad (2.40)$$

Note that (2.40) is nothing but precisely the violation of (2.34). Therefore, it is the loss of stability of E_u that leads to the occurrence of the positive equilibrium $E^+ = (\bar{u}, \bar{v})$.

When condition (2.34) holds, there is a unique positive equilibrium $E^+ = (\bar{u}, \bar{v})$ with the following characteristic equation

$$\lambda^2 + (m - J_{11})\lambda - J_{11} m + e^{-\lambda \tau} (-m \lambda + J_{11} m - J_{12} K_{21}) = 0 \quad (2.41)$$

where K_{22} has been simplified to m for this case.

When $\tau = 0$, (2.41) reduces to

$$\lambda^2 - J_{11} \lambda - J_{12} K_{21} = 0. \quad (2.42)$$

Note that $J_{12} < 0$ and $K_{21} > 0$. Thus, if $J_{11} < 0$, then by the Routh–Hurwitz criterion, the above quadratic equation only has roots with negative real parts. Now we check, under the condition

$J_{11} < 0$, if the roots of (2.41) will cross the pure imaginary axis to enter the right half plane in the complex plane as τ increases.

Plugging $\lambda = \omega i$ into (2.41) and separating the real and imaginary parts, we obtain

$$\begin{cases} m \omega \sin(\omega \tau) - (J_{11} m - J_{12} K_{21}) \cos(\tau \omega) = -\omega^2 - J_{11} m, \\ m \omega \cos(\omega \tau) + (J_{11} m - J_{12} K_{21}) \sin(\tau \omega) = (-J_{11} + m)\omega, \end{cases} \quad (2.43)$$

Eliminating the cosine and sine functions by trigonometric identity leads to the following equation for ω :

$$\omega^4 + J_{11}^2 \omega^2 + (2 m J_{11} J_{12} K_{21} - J_{12}^2 K_{21}^2) = 0. \quad (2.44)$$

Note that this is indeed a quadratic equation for ω^2 and $J_{11}^2 > 0$. Thus, when

$$2 m J_{11} J_{12} K_{21} - J_{12}^2 K_{21}^2 > 0, \quad (2.45)$$

then (2.44) has no positive solution, implying that no root of (2.41) will cross the pure imaginary axis for all $\tau \geq 0$; that is, all roots remain in the left half complex plane for all $\tau \geq 0$. Therefore, the co-existence equilibrium is locally asymptotically stable for all $\tau \geq 0$, provided that $J_{11} < 0$ and (2.45) holds.

If $J_{11} < 0$ but (2.45) is reversed, then (2.43) has a unique positive root

$$\omega_0 = \sqrt{\frac{-J_{11}^2 + \sqrt{J_{11}^4 - 4 \cdot (2 m J_{11} J_{12} K_{21} - J_{12}^2 K_{21}^2)}}{2}},$$

corresponding to which, τ has a sequence of values

$$\tau_n = \frac{1}{\omega_0} \arccos \frac{\omega_0^2 m(-J_{11} + m) + (\omega_0^2 + J_{11} m)(J_{11} m - J_{12} K_{21})}{m^2 \omega_0^2 + (J_{11} m - J_{12} K_{21})^2} + \frac{2 n \pi}{\omega_0}, \quad n = 0, 1, 2, \dots,$$

which are possible critical values for τ at which Hopf bifurcation may occur. Therefore, the co-existence equilibrium is locally asymptotically stable when $\tau < \tau_0$ where

$$\tau_0 = \frac{1}{\omega_0} \arccos \frac{\omega_0^2 m(-J_{11} + m) + (\omega_0^2 + J_{11} m)(J_{11} m - J_{12} K_{21})}{m^2 \omega_0^2 + (J_{11} m - J_{12} K_{21})^2}. \quad (2.46)$$

When $\tau = \tau_0$, (2.41) has a pair of pure imaginary roots $\pm i\omega_0$. In order to confirm Hopf bifurcation at the first critical value $\tau = \tau_0$, we need to verify the transversality condition, that is,

$$\left. \frac{d\Re(\lambda)}{d\tau} \right|_{\tau=\tau_0} > 0. \quad (2.47)$$

Indeed, differentiating equation (2.41) with respect to τ , we have

$$\left(\frac{d\lambda}{d\tau} \right)^{-1} = \frac{m - J_{11} + 2\lambda - m e^{-\lambda\tau}}{e^{-\lambda\tau} \lambda(-m\lambda + J_{11}m - J_{12}K_{21})} - \frac{\tau}{\lambda}.$$

Hence, at $\tau = \tau_0$ ($\lambda = i\omega_0$),

$$\begin{aligned} \operatorname{sgn} \left(\left. \frac{d\Re(\lambda)}{d\tau} \right|_{\tau=\tau_0} \right) &= \operatorname{sgn} \left(\Re \left. \frac{d(\lambda)}{d\tau} \right|_{\tau=\tau_0} \right) = \operatorname{sgn} \left(\Re \left(\left. \frac{d(\lambda)}{d\tau} \right|_{\tau=\tau_0} \right)^{-1} \right) \\ &= \operatorname{sgn} \left(\Re \left[\frac{m - J_{11} + 2\lambda - m e^{-\lambda\tau}}{e^{-\lambda\tau} \lambda(-m\lambda + J_{11}m - J_{12}K_{21})} - \frac{\tau}{\lambda} \right] \Big|_{\lambda=i\omega_0} \right) \\ &= \operatorname{sgn} \left(\frac{k_1 \cos(\omega_0 \tau) + k_2 \sin(\omega_0 \tau) - m^2 \omega_0}{\omega_0 [(J_{11}^2 + \omega_0^2) m^2 - 2m J_{11} J_{12} K_{21} + J_{12}^2 K_{21}^2]} \right) \end{aligned}$$

where $k_1 = \omega_0(I_{11}m - 2J_{12}K_{21} + m^2)$ and $k_2 = m^2 J_{11} + m(-J_{11}^2 - J_{12}K_{21} - 2\omega_0^2) + J_{11}J_{12}K_{21}$.

From system (2.43), we have

$$\begin{aligned} \cos(\omega_0 \tau) &= \frac{\omega_0^2 m(-J_{11} + m) + (\omega_0^2 + J_{11}m)(J_{11}m - J_{12}K_{21})}{m^2 \omega_0^2 + (J_{11}m - J_{12}K_{21})^2}, \\ \sin(\omega_0 \tau) &= \frac{-\omega_0^2 - J_{11}m + (J_{11}m - J_{12}K_{21})\cos(\omega_0 \tau)}{m\omega_0}. \end{aligned} \quad (2.48)$$

Consequently,

$$\Re \left(\left. \frac{d(\lambda)}{d\tau} \right|_{\tau=\tau_0} \right)^{-1} = \frac{J_{11}^2 + 2\omega_0^2}{(J_{11}^2 + \omega_0^2)m^2 - 2m J_{11} J_{12} K_{21} + J_{12}^2 K_{21}^2} > 0. \quad (2.49)$$

Therefore, the transversal condition holds and there occurs a Hopf bifurcation at $\tau = \tau_0$.

If (2.34) holds but $J_{11} > 0$, then equation (2.41) only has roots with positive real parts when $\tau = 0$, meaning that the positive equilibrium $E^+ = (\bar{u}, \bar{v})$ is unstable when $\tau = 0$. Now we follow the same procedure to check if the roots of (2.41) will cross the pure imaginary axis

to enter the left half plane in the complex plane as τ increases.

Plugging $\lambda = \omega i$ into (2.41) and separating the real and imaginary parts, we still obtain the system (2.43) and the equation (2.44) for ω . But now, since $J_{11} > 0$, the condition (2.45) is reversed, and thus, (2.43) has a unique positive root ω_0 . Differentiating equation (2.41) and evaluating at $\lambda = i\omega_0$, we find that (2.49) still holds, implying that any roots on the right half of the complex plane will remain on the right half plane as τ increases. This means that the positive equilibrium $E^+ = (\bar{u}, \bar{v})$ remains unstable for all $\tau > 0$.

Summarizing the above analysis, we have proven the following theorem,

Theorem 2.3.4 *For model system (2.29), the following hold.*

- (i) *When $r_0 < d$, there is only the trivial equilibrium $E_0 = (0, 0)$ and it is locally asymptotically stable; when $r_0 > d$, it becomes unstable and there is the predator free equilibrium E_u .*
- (ii) *For E_u , when (2.34) is violated (i.e., (2.40) holds), E_u is locally asymptotically stable; when (2.34) holds, then E_u becomes unstable and there is the positive (co-existence) equilibrium E^+ .*
- (iii) *Assume (2.34) holds so that E^+ exists and suppose $J_{11} < 0$ holds.*
 - (iii)-1 *If (2.45) is satisfied, then $E^+ = (\bar{u}, \bar{v})$ is locally asymptotically stable for all $\tau > 0$*
 - (iii)-2 *If (2.45) is reversed, then there is a $\tau_0 > 0$ such that $E^+ = (\bar{u}, \bar{v})$ is locally asymptotically stable when $0 < \tau < \tau_0$ and unstable when $\tau > \tau_0$. Furthermore, there is a Hopf bifurcation around E^+ at $\tau = \tau_0$, causing periodic solutions around E^+ .*
- (iv) *Assume (2.34) holds so that E^+ exists and suppose $J_{11} > 0$ holds, then $E^+ = (\bar{u}, \bar{v})$ is unstable for all $\tau > 0$.*

Remark Comparing with the results for the case with linear functional response (i.e., (2.6)) in Subsection 3.1, as far as the stability of the co-existence equilibrium is concerned, we have required a condition “ $J_{11} < 0$ ” which is needed for the corresponding ODE when $\tau = 0$ to

have its co-existence equilibrium being stable. This should not be surprising as it is well-known that for an ODE predator-prey model (i.e., without delay) with a functional response of Holling Type II, the positive equilibrium may also lose its stability to periodic solutions through Hopf bifurcation. It is very natural to expect Hopf bifurcation to occur as well when J_{11} changes signs. But this is quite analytically demanding, hence we will explore along this line numerically in Section 4.

Global stability of the boundary equilibria E_0 and E_u

Parallel to Subsection 3.1.2, in this subsection, we study the global asymptotical stability of the equilibria E_0 and E_u .

Theorem 2.3.5 *When $r_0 < d$, the trivial equilibrium $E_0 = (0, 0)$ is indeed globally asymptotically stable.*

Proof Consider

$$V(t) = u(t) + \frac{v(t)}{c} + \frac{1}{1 + c_1 k} \int_{t-\tau}^t \frac{p u(s) v(s)}{1 + q u(s)} ds.$$

Then

$$\dot{V} = \frac{r_0 u(t)}{1 + c_2 k v(t)} - d u(t) - a u^2(t) - \frac{m v(t)}{c}. \quad (2.50)$$

Therefore $\dot{V} \leq 0$ provided $r_0 < d$, and $\dot{V} = 0$ if and only if $u(t) = v(t) = 0$. Thus, $u(t) \rightarrow 0$ and $v(t) \rightarrow 0$ as $t \rightarrow \infty$, and hence, $E_0 = (0, 0)$ is globally asymptotically stable.

Theorem 2.3.6 *When $d < r_0$ and (2.39) holds (i.e., (2.34) is violated), $E_u = \left(\frac{r_0-d}{a}, 0\right)$ is globally asymptotically stable.*

Proof Consider

$$\frac{du}{dt} = \frac{r_0 u(t)}{1 + c_2 k v(t)} - d u(t) - a u^2(t) - \frac{p u(t) v(t)}{(1 + q u(t))(1 + c_1 k)} \leq r_0 u(t) - d u(t) - a u^2(t).$$

By the property of logistic equation and the comparison theorem, for any $\epsilon > 0$, there exist a $T = T(\epsilon) > 0$, such that when $t > T$, $u(t) < \frac{r_0-d}{a} + \epsilon$. Then for $t > T + \tau$, the DDE for $v(t)$

satisfies

$$\begin{aligned} \frac{dv}{dt} &= \frac{c}{1 + c_1 k} \cdot \frac{p u(t - \tau) v(t - \tau)}{1 + q u(t - \tau)} - m v(t) \\ &< \frac{c}{1 + c_1 k} \cdot \frac{p \left(\frac{r_0 - d}{a} + \epsilon \right)}{1 + q \left(\frac{r_0 - d}{a} + \epsilon \right)} v(t - \tau) - m v(t). \end{aligned} \quad (2.51)$$

By (2.39), we can choose $\epsilon > 0$ sufficiently small so that

$$\frac{c}{1 + c_1 k} \cdot \frac{p (\hat{u} + \epsilon)}{1 + q (\hat{u} + \epsilon)} - m < 0.$$

By [21], the trivial solution of

$$\frac{dx}{dt} = \frac{c}{1 + c_1 k} \cdot \frac{p (\hat{u} + \epsilon) x(t - \tau)}{1 + q (\hat{u} + \epsilon)} - m x(t), \quad (2.52)$$

is globally asymptotically stable. Note that (2.52) is monotone, by (2.51) and the comparison theorem, $v(t) \rightarrow 0$ as $t \rightarrow \infty$. This means that the first equation in (2.29) is asymptotically autonomous having the following logistic equation as its limit equation:

$$\frac{du}{dt} = r_0 u(t) - d u(t) - a u^2(t).$$

Since $\hat{u} = (r_0 - d)/a$ attracts every positive solution to this logistic equation, by the theory of asymptotically autonomous systems (see, e.g.[3]), we conclude that in the system (2.29) $u(t) \rightarrow \hat{u} = \frac{r_0 - d}{a}$ as $t \rightarrow \infty$. Therefore, every positive solution of (2.29) converges to $E_u = (\hat{u}, 0)$. This together with the local stability established in Theorem 2.3.4 implies that E_u is globally asymptotically stable.

2.4 Numerical simulations

In this section, we present some numerical simulations to illustrate the main analytic results obtained in Section 3, and also to more visually explore the impact of the anti-predation response level and the biomass transfer time.

We begin with the model (2.6) that adopts the linear functional response, with two response functions $f(k, v)$ and $\rho(k)$ given by (2.28), that is, the following system:

$$\begin{cases} \frac{du}{dt} = \frac{r_0 u(t)}{1 + c_2 k v(t)} - d u(t) - a u^2(t) - \frac{u(t) v(t)}{1 + c_1 k}, \\ \frac{dv}{dt} = \frac{c u(t - \tau) v(t - \tau)}{1 + c_1 k} - m v(t). \end{cases} \quad (2.53)$$

We fix the parameters

$$r_0 = 0.03, \quad d = 0.01, \quad a = 0.01, \quad m = 0.05, \quad c = 0.4, \quad c_1 = 1, \quad c_2 = 1, \quad (2.54)$$

and demonstrate how k and τ impact the population dynamics. To this end, we transfer the threshold for r_0 in comparison with $d + am/c\rho(k)$ for the stability of E_u in (ii) and (iii) of Theorem 2.3.1 to a threshold value for k . By setting $r_0 = d + \frac{am}{c\rho(k)}$ and using the parameter values in (2.54), we obtain $k^* = 15$. By Theorem 2.3.1, when $k > 15$, the predator free equilibrium E_u is stable (as demonstrated in Figure 2.1-(a) for $k = 20$); when $k < 15$, E_u becomes unstable and there occurs the unique co-existence equilibrium E^+ . For $k = 11 < k^*$ and with the above parameters, we can numerically calculate to obtain $p_0 = 0.00075$ and $|q_0| = 0.0005250388635$, giving a situation of $p_0 > |q_0|$ (Theorem 2.3.1-(iii)-1), and hence, E^+ is asymptotically stable for any $\tau > 0$, as demonstrated in Figure 2.1-(b).

When k is further decreased to $k = 1$, we still have the co-existence equilibrium E^+ , and p_0 and q_0 are numerically computed to be $p_0 = 0.000125$ and $q_0 = 0.0007484621132$, corresponding to the scenario in Theorem 2.3.1-(iii)-(2). Further calculations reveal that $\tau_0 = 3.678038406$. The numeric solutions are illustrated in Figure 2.2, for $\tau < \tau_0$ and $\tau > \tau_0$ respectively in (a) and (b). For latter case ($\tau = 4 > \tau_0$), the periodic solutions are also illustrated in the $u - v$ plane in Figure 2.3. With the parameters given in (2.54), we also plot the bifurcation diagrams with respect to time delay τ (with $k = 1$ fixed) and anti-predation strategy k (with $\tau = 2$ fixed) respectively in Figure 2.4-(a) and Figure 2.4-(b). There, the curve represents either the predator population of the stable positive equilibrium point, or the maximum and the minimum value of the predator population in the bifurcated periodic solution.

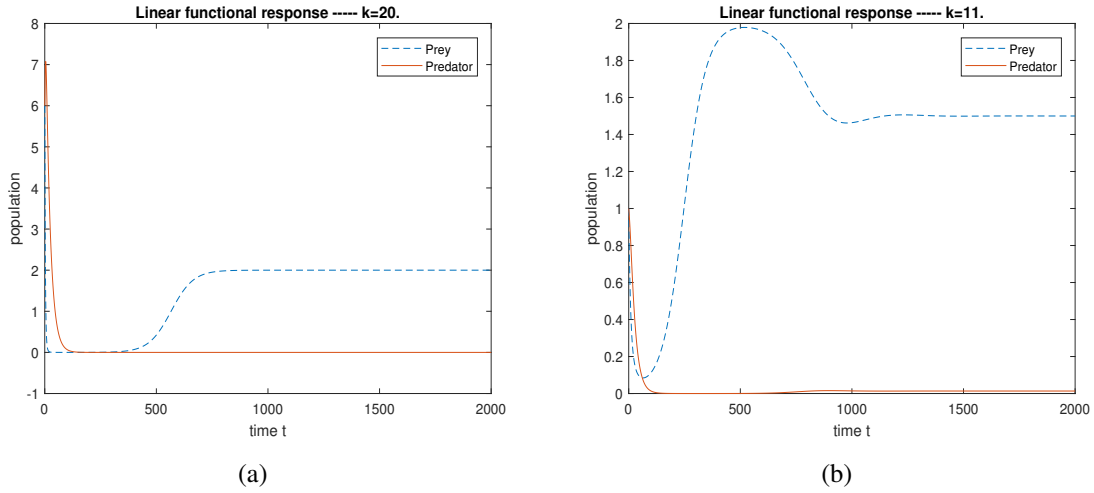


Figure 2.1: Population dynamics of (2.53). (a) When $k = 20 > k^* = 15$, the predator free equilibrium E_u is stable, the predator species goes extinct and the prey species eventually goes to its carrying capacity. (b) When $k = 11 < k^* = 15$, E_u is unstable and there is the co-existence equilibrium E^+ which is asymptotically stable for all $\tau \geq 0$ since $p_0 = 0.00075 > |q_0| = 0.0005250388635$.

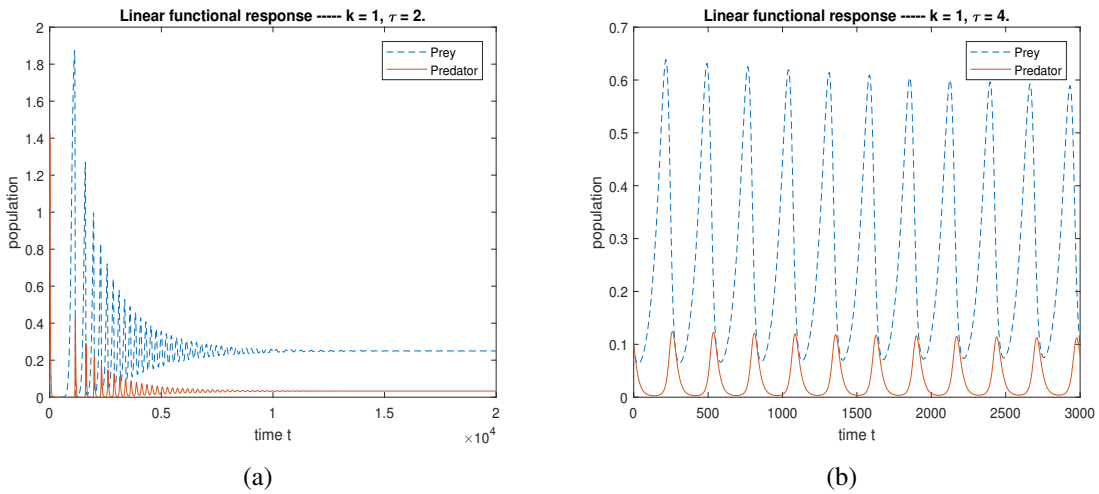


Figure 2.2: Population dynamics of (2.53). (a) When $k = 1 < k^*$, $p_0 = 0.000125 < q_0 = 0.0007484621132$, $\tau = 2 < \tau_0 = 3.678038406$, the co-existence equilibrium is stable. (b) $\tau = 4 > \tau_0 = 3.678038406$, there occurs a periodic solution.

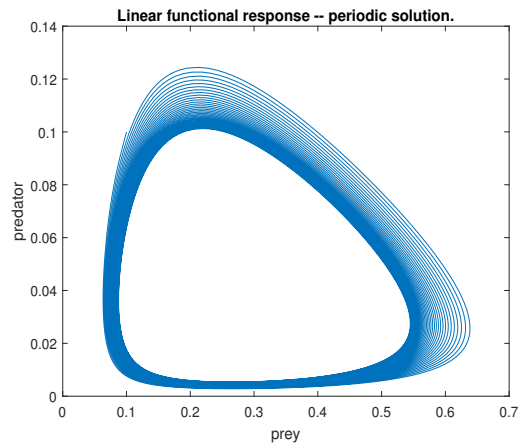


Figure 2.3: Plot of periodic orbit of (2.53) in $u = v$ plane when $k = 1$ and $\tau = 4 > \tau_0 = 3.678038406$.

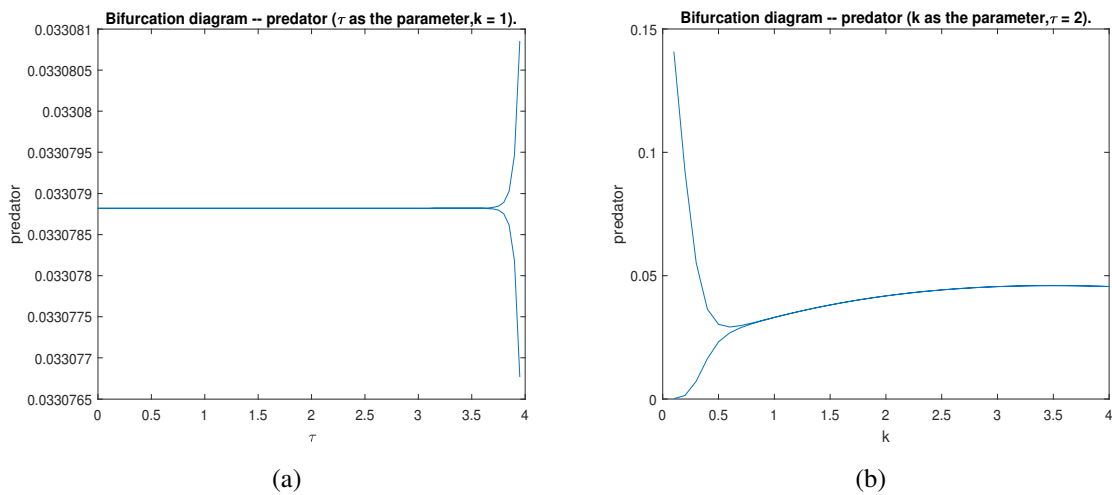


Figure 2.4: Bifurcation diagram for (2.53) : (a) fixing $k = 1$ and choosing τ as the bifurcation parameter; (b) fixing $\tau = 2$ and choosing k as the bifurcation parameter.

Next demonstrate the results for the model system (2.29) with the following parameter values

$$r_0 = 0.03, d = 0.01, a = 0.01, m = 0.05, c = 0.4, c_1 = 1, c_2 = 1, p = 0.5, q = 0.6. \quad (2.55)$$

Since $r_0 > d$, the predator free equilibrium E_u exists. For its stability, we can similarly transfer the threshold value for r_0 in Theorem (2.3.4) to a critical value k^* of k , by setting

$$r_0 = \frac{a m (1 + c_1 k)}{c p - m q (1 + c_1 k)} + d$$

and solving it for k , leading to the a numeric value $k^* = 2.636363636$. Thus, by Theorem (2.3.4), when $k > 2.636363636$, the predator free equilibrium E_u is stable (as demonstrated in Figure 2.5-(a)), and when $k < 2.636363636$, E_u becomes unstable and there occurs the unique co-existence equilibrium E^+ . As far as the stability of E^+ is concerned under $k < k^* = 2.636363636$, it depends on whether $J_{11} < 0$ or $J_{11} > 0$. When $k = 2$, numeric calculations give $J_{11} = -0.01184921799 < 0$ and $2 m J_{11} J_{12} K_{21} - J_{12}^2 K_{21}^2 = 1.723290120 \times 10^{-7} > 0$ (i.e., (2.45) holds). By Theorem 2.3.4-(iii)-1, E^+ is asymptotically stable (see Figure 2.5-(b)).

However, when k is further decreased to $k = 1$, computations give $J_{11} = -0.003821249991 < 0$ (still negative) but $2 m J_{11} J_{12} K_{21} - J_{12}^2 K_{21}^2 = -2.86322377 \times 10^{-8} < 0$ (i.e., (2.45) is reversed now). This is the scenario of Theorem 2.3.4-(iii)-2, meaning that the stability of E^+ further depends on the size of delay τ . By (2.46) we compute to obtain $\tau_0 = 33.27610729$. The numeric solutions for $\tau < \tau_0$ and $\tau > \tau_0$ are shown in Figure 2.6-(a)-(b) respectively for $\tau = 4$ and $\tau = 120$; and plotting in the $u - v$ plane for the case of Figure 2.6-(b) is given in Figure 2.7.

Parallel to Figure 2.4, we also plot the bifurcation diagrams with respect to delay τ (with $k = 1$ fixed) and anti-predation response level k (with $\tau = 2$ fixed) respectively in Figure 2.8-(a) and Figure 2.8-(b), with the parameters given in (2.55).

We have seen in Theorem 2.3.4 and mentioned in Remark 2.3.2 that when $J_{11} > 0$, the system has no stable equilibrium for all $\tau > 0$. In such a case, periodic behaviour is the outcome. This is demonstrated in Figure 2.9. Indeed, we not only observe the periodic behaviours, but also find that the magnitude of the sustained oscillations (periodic solutions) is enlarged by

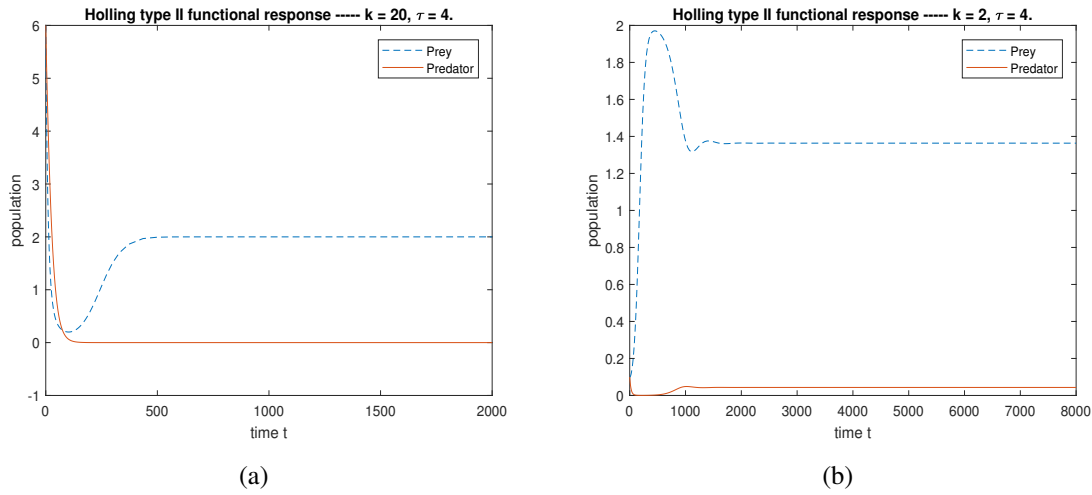


Figure 2.5: Population dynamics of (2.29). (a) When $k = 20 > k^* = 2.636363636$, the predator free equilibrium E_u is stable. (b) When $k = 2 < k^*$, E_u becomes unstable and there occurs the positive equilibrium E^+ which is asymptotically stable for all $\tau > 0$ because $J_{11} = -0.01184921799 < 0$ and $(2m J_{11} J_{12} K_{21} - J_{12}^2 K_{21}^2) = 1.723290120 \cdot 10^{-7} > 0$.

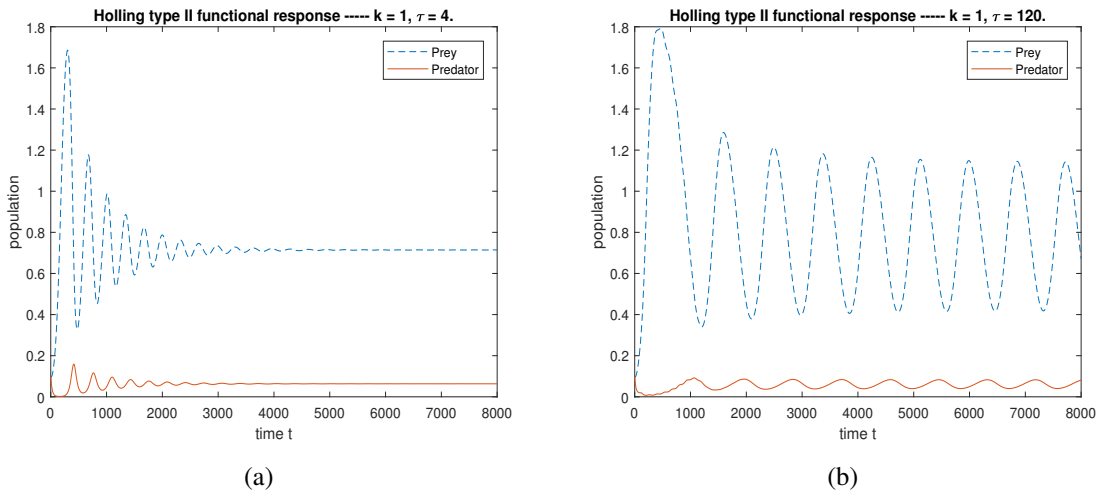


Figure 2.6: When $k = 1 < k^*$, $J_{11} = -0.003821249991 < 0$, $(2m J_{11} J_{12} K_{21} - J_{12}^2 K_{21}^2) = -2.86322377 \cdot 10^{-8} < 0$. (a) When $\tau = 4 < \tau_0 = 33.27610729$, the co-existence equilibrium E^+ is still stable; (b) When $\tau = 120 > \tau_0 = 33.27610729$, E^+ loses its stability and a periodic solution occurs.

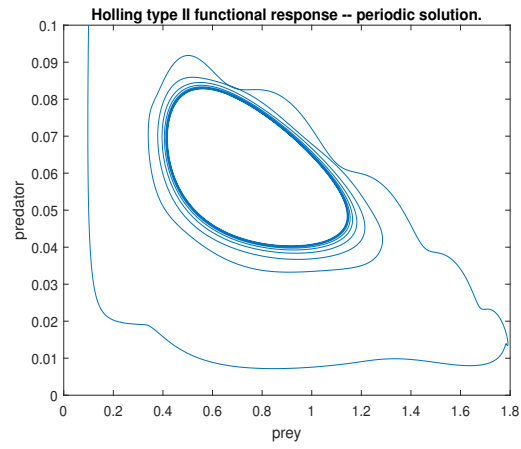


Figure 2.7: Periodic orbits when $k = 1$ and $\tau = 120$.

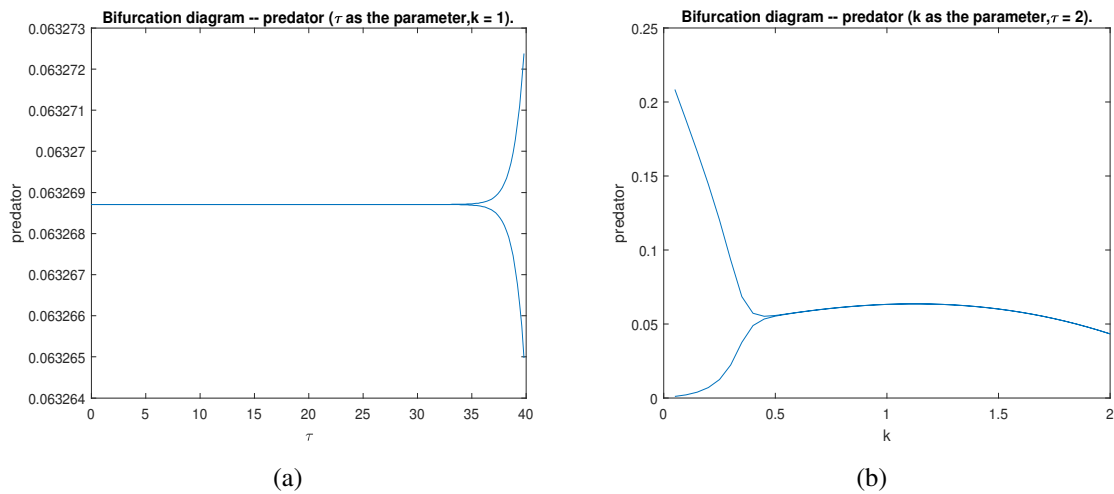


Figure 2.8: Bifurcation diagram for (a) fix $k = 1$, choose τ as the bifurcation parameter. (b) fix $\tau = 2$, choose k as the bifurcation parameter.

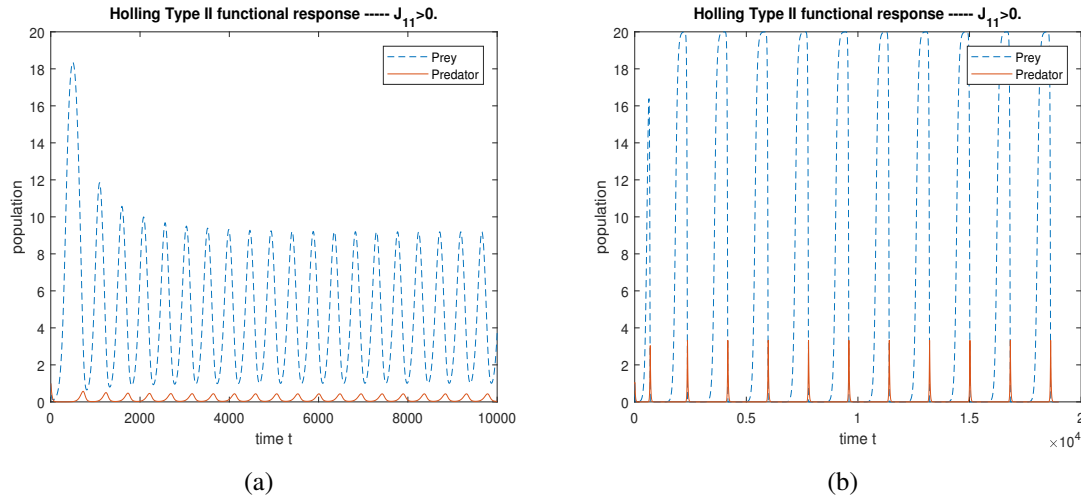


Figure 2.9: By setting $k = 3.4$, $J_{11} = 0.00084875902838911633 > 0$. (a) Solutions approach to a periodic solution for $\tau = 0$ (periodic solutions for the ODE). (b) Periodic behaviours are preserved for $\tau > 0$ and are actually magnified by $\tau > 0$.

$\tau > 0$.

2.5 Conclusion and discussions

Recent field studies on the fear effect in predator-prey interactions have triggered the need to modify existing predator-prey models that do not consider the fear effect. In a recent work Wang et al [24], the authors incorporated an anti-predation mechanism into an ODE model to account for the fear effect which leads to a cost in reproduction; analyzing the model, they have obtained some results on the effect of such an anti-predation response. In this chapter, based on the fact that in addition to cost, there is also a benefit for an anti-predation response; and meanwhile, there is also a time delay in biomass transfer from prey to predator after predation, we have further modified the model studied in [24] to explore the joint effects of both biomass transfer delay and the fear effect.

Following [24], we have considered two types of functional responses: Holling Type I and Holling Type II. In both cases, we have obtained and stated our main results *more explicitly* in terms of some parameters such as r_0 and d , but they can be translated into statements in terms of the two main parameters k and τ . Such a translation will lead to loss of some explicitness, but this can be easily achieved numerically, as demonstrated in Section 4. For example, when

Holling Type I (linear) functional response is adopted, Theorem 2.3.1 can be restated in terms of k and τ as below:

Theorem 2.5.1 *For the predator-prey system (2.6) with linear functional response under condition $r_0 > d$, there may exist two critical values of the anti-predation level k that $0 < \hat{k} < k^*$, such that,*

- (i) *When $k > k^*$, $E_u = \left(\frac{r_0-d}{a}, 0\right)$ is globally asymptotically stable. When $k < k^*$, $E_u = \left(\frac{r_0-d}{a}, 0\right)$ is unstable and there occurs a unique co-existence equilibrium E^+ .*
- (ii) *When $k^* > k > \hat{k}$, the unique co-existence equilibrium $E^+ = (\bar{u}, \bar{v})$ is locally asymptotically stable for all $\tau > 0$. If $0 < k < \hat{k}$, there is a $\tau_0 > 0$ such that $E^+ = (\bar{u}, \bar{v})$ is locally asymptotically stable when $0 < \tau < \tau_0$ and unstable when $\tau > \tau_0$; furthermore, there is a Hopf bifurcation about E^+ at $\tau = \tau_0$.*

When Holling Type II functional response is adopted, Theorem 2.3.4 can be restated in terms of k and τ as below.

Theorem 2.5.2 *Consider the predator-prey system (2.29) with Holling Type II functional response under condition $r_0 > d$.*

- (i) *There exists a critical value $k^* > 0$ such that for $k > k^*$, $E_u = \left(\frac{r_0-d}{a}, 0\right)$ is globally asymptotically stable. When $k < k^*$, $E_u = \left(\frac{r_0-d}{a}, 0\right)$ is unstable and there occurs a unique co-existence equilibrium $E^+ = (\bar{u}, \bar{v})$.*
- (ii) *When $k < k^*$ and $J_{11} < 0$, there exists another critical value $0 < \hat{k} < k^*$ such that*
 - (ii)-1 *if $\hat{k} < k < k^*$, the unique co-existence equilibrium E^+ is locally asymptotically stable for all $\tau > 0$;*
 - (ii)-2 *if $0 < k < \hat{k}$, there is a $\tau_0 > 0$ such that E^+ is locally asymptotically stable only when $0 < \tau < \tau_0$ and it becomes unstable when $\tau > \tau_0$; furthermore, there is a Hopf bifurcation about E^+ at $\tau = \tau_0$.*
- (iii) *When $k < k^*$ and $J_{11} > 0$, a periodic solution occurs even if $\tau = 0$, and it does not vanish for all $\tau > 0$.*

We point out that the critical values k^* and \hat{k} in the above translated theorems are defined implicitly by equations in Theorem 2.3.4-(ii) corresponding to the thresholds for the inequalities there, which in general cannot be solved explicitly. However, as demonstrated in Section 4, given the values of other parameters, they can be numerically calculated.

From the above theorems, we find that the anti-predation strategy k and the digestion delay τ play important roles in both models. As long as r_0 (the natural growth rate of prey) is greater than d (the natural death rate of prey), the trivial equilibrium solution is unstable and the populations of the predator and prey are determined by k and τ , in terms of the critical values k^* , \hat{k} and τ_0 , as classified in the theorems. Note that τ_0 depends on k , as illustrated in Figure 2.10 for both functional responses considered for the given set of parameter values in (2.55). Also from the equations that determine the critical values k^* ($r_0 = d + am/c\rho(k)$ in Theorem 2.3.1 and (2.34) in Theorem 2.3.4), we can see the impact of the incorporated benefit factor $\rho(k)$ as a function of the anti-predation response level k . This shows the *trade-off effect* of cost and benefit of the response k , and is *in strong contrast* to the corresponding models considered in [24], where *no benefit* was considered ($\rho(k) = 1$) and hence small k favours the prey population since k only leads to a cost of reducing the reproduction of the prey. Also, in the ODE model in [24] with Holling Type I functional response, there is no periodic solution for any values of the parameter set; however, with the digestion delay incorporated, periodic phenomenon becomes possible.

We also point out an important difference of the model with Holling Type II functional response from that with Holling Type I functional response. For the former, when $k < k^*$, delay caused oscillations can occur only in the case when $J_{11} < 0$; and when $J_{11} > 0$, there is also a periodic solution but that is not caused by the delay τ . This indicates that the sign change of J_{11} from negative to positive also leads to Hopf bifurcation, and this is in agreement with the periodic solution observed in the ODE model with Holling Type II functional response in [24]. Accordingly, one can also explore the sign change numerically by the formula defining J_{11} and the equations in (2.30) that determine the co-existence equilibrium $E^+ = (\bar{u}, \bar{v})$.

The differences between the two functional responses considered in our model are illustrated in Section 4 by using the same set of parameter values. It has been seen that for a given

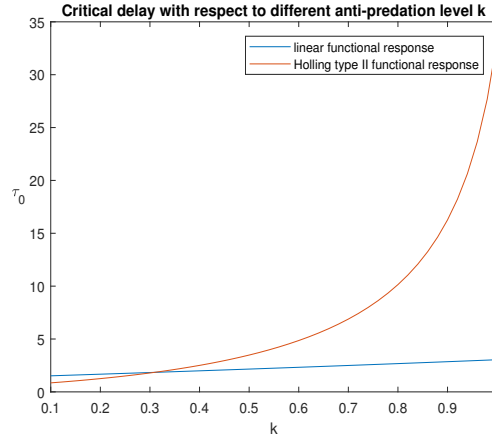


Figure 2.10: Critical value of time delay for fixed anti-predation level k for both functional responses

$\tau > 0$, the critical value k^* in Holling Type II model is much less than that in the model with linear functional response (2.636363636 vs 15 in our numeric results). This seems to suggest that anti-predation strategy is more sensitive to the population of predator with Holling Type II functional response than with Holling Type I. Similarly, for a given k , the critical delay τ_0 in Holling Type II model is much greater than that in the model with linear functional response (see Fig. 2.10). Thus, the results are actually specific to the particular choice of the functional response function. This is not surprising to predator-prey modellers as it has been widely known that different kinds of predation between species have different characteristics and hence, needs to use different functional responses to capture the main feature. Exploring the joint impacts of anti-predation response and biomass transfer delay on the population dynamics with other types of functional responses remains an interesting and worthwhile topic for future research. We point out that in both cases, we have only explored the Hopf bifurcation at the first critical value τ_0 for the delay parameter. This is because this value is most important, serving as a threshold for the stability of the positive equilibrium E^+ and carrying information about the consequence of E^+ becoming unstable. Investigation of the bifurcations at the subsequent critical values τ_n , $n = 1, 2, \dots$ is more involving, demanding theory and methods on global bifurcation and hence could be very lengthy. Therefore, we decide not to explore in this chapter.

We have chosen the ODE model (2.2) from [24] as the basic model into which a bene-

fit coming from the anti-predation response and a delay in biomass transfer are incorporated. Note that this basic model uses the *logistic growth* for the prey population and assumes that the predator is a *specialist*. Other types of growth for prey population and the predation by generalist predators are also important topics to investigate, when the fear effect and the biomass transfer delay are incorporated. We remark that, also based on (2.2), Das and Samanta [7] incorporated an extra food source for the predator and added a white noise to the death rates of the prey and predator and they analyzed the resulting stochastic model. Mondal *et al* [17] further considered a digestion delay in addition to the cost of fear, white noise in the death rates, and extra food for the predator; however, the benefit of the anti-predation response was not considered.

Bibliography

- [1] Abrams, P. A., Ginzburg, L. R., *The nature of predation: prey dependent, ratio dependent or neither ?*, Trends in Ecology and Evolution **15**(2000), 337-341.
- [2] Arditi, R., Ginzburg, L. R., *Coupling in predator-prey dynamics: ratio dependence*, Journal of Theoretical Biology **139**(1989), 311-326.
- [3] Castillo-Chavez, C., Thieme, H. R., *Asymptotically autonomous epidemic models*, In: O. Arino et al: Mathematical Population Dynamics: Analysis of Heterogeneity, I. Theory of Epidemics (pp. 33-50). Wuerz, Canada, 1995
- [4] Creel, S., Christianson, D., *Relationships between direct predation and risk effects*, Trends Ecol Evolut **23**(2008), 194-201.
- [5] Cresswell, W., *Predation in bird populations*, J Ornithol **152**(2011), 251-263.
- [6] Cushing, J. M., *Integro-differential equations and delay models in population dynamics*, Lecture Notes in Biomathematics, Springer-Verlag, Berlin, Heidelberg, New York, **Vol. 20**, 1977.
- [7] Das, A, Samanta G. P., *Modeling the fear effect on a stochastic prey-predator system with additional food for the predator*, J. Phys. A: Math. Theor. **51** (2018) 465601 (26pp).
- [8] Holling, C. S., *The functional response of predator to prey density and its role in mimicry and population regulation*, Mem. Ent. Sec. Can. **45**(1965), 1-60.
- [9] Hale, J. K., Verduyn Lunel, S. M., *Introduction to Functional Differential Equations*, Springer-Verlag New York, 1993.

- [10] Hayes, N. D., *Roots of the transcendental equations associated with a certain differential-difference equation*, J London Math Soc **25**(1950), 226-232.
- [11] Jeschke, J. M., Kopp, M., Tollrian, R., *Predator function responses: discriminating between handling and digesting prey*, Ecological Monographs **72**(1) (2002), 95-112.
- [12] Li, F., Li, H., *Hopf bifurcation of a predator-prey model with time delay and stage structure for the prey*, Mathematical and Computer Modelling **55**(2012), 672-679.
- [13] Lima, S. L., *Nonlethal effects in the ecology of predator-prey interactions*, Bioscience **48**(1998), 25-34.
- [14] Lima, S. L., *Predators and the breeding bird: behavioural and reproductive flexibility under the risk of predation*, Biol Rev **84**(2009), 85-513.
- [15] Lotka, A. J., *Analytical Note on Certain Rhythmic Relations in Organic Systems*, Proc. Natl. Acad. Sci. U.S.A. **6**(1920), 410-415 .
- [16] Lotka, A. J., *Elements of Physical Biology*, Williams and Wilkins (1925).
- [17] Mondal, S., Maiti, A. Samanta, G. P., *Effects of Fear and Additional Food in a Delayed Predator-Prey Model*, Biophysical Reviews and Letters, **13** (2018), 157-177.
- [18] Rosenzweig, M. L., MacArthur, R. H., *Graphical representation and stability conditions of predator-prey interactions*, American Naturalist **97** (1963), 209-223.
- [19] Skalski, G. T., Gilliam, J. F., *Functional responses with predator interference: viable alternatives to the Holling Type II model*, Ecology **82**(2001), 3083-3092.
- [20] Smith, H., *Monotone Dynamical Systems: An Introduction to the Theory of Competitive and Cooperative Systems*, Amer. Math. Soc. Math. Surveys and Monographs **Vol. 41**, 1995.
- [21] Smith, H., *An Introduction to Delay Differential Equations with Applications to the Life Sciences*, Springer-Verlag New York, 2010.
- [22] Volterra, V., *Variazioni e fluttuazioni del numero d'individui in specie animali conviventi*, Mem. Acad. Lincei Roma. **2**(1926), 31-113.

- [23] Volterra, V., *Variations and fluctuations of the number of individuals in animal species living together*, In Chapman, R. N. *Animal Ecology*. McGraw-Hill, 1931.
- [24] Wang, X., Zanette, L. Y., Zou, X., *Modelling the fear effect in predator-prey interactions*, *J Math Biol.* **73**(2016), 1179-1204.
- [25] Wang, X., Zou, X., *Modeling the Fear Effect in Predator-Prey Interactions with Adaptive Avoidance of Predators*, *Bull Math Biol* **79**(2017), 1325-1359.
- [26] Wang, X., Zou, X., *Pattern formation of a predator-prey model with the cost of anti-predator behaviours*, *Mathematical Biosciences and Engineering*, **15**(2018), 775-805.
- [27] Wangersky, P. J., Cunningham, W. J., *Time Lag in Prey-Predator Population Models*, *Ecology*, **38**(1957), 136-139.
- [28] Xu, R., *Global dynamics of a predator-prey model with time delay and stage structure for the prey*, *Nonlinear Anal. RWA* **12**(2011), 2151-2162.
- [29] Zanette, L. Y., White, A. F., Allen, M. C., Clinchy, M., *Perceived predation risk reduces the number of offspring songbirds produce per year*, *Science* **334** (6061)(2011), 1398-1401.

Chapter 3

On mechanisms of trophic cascade caused by anti-predation response in food chain systems

3.1 Introduction

Predator-prey interactions have attracted the great attention of both ecologists and mathematical biologists, not only because of their vast existence in nature but also because of their diversified forms and rich consequences in the real world. Mathematically, if only considering direct interaction through predation, a classic predator-prey model can be generally described by a system of ordinary differential equations of the form:

$$\begin{cases} \frac{du}{dt} = f_1(u(t)) - p(u(t), v(t))v(t), \\ \frac{dv}{dt} = f_2(v(t)) + cp(u(t), v(t))v(t). \end{cases} \quad (3.1)$$

See, e.g., [16, 17, 29, 30]. Here $u(t)$ and $v(t)$ are the populations of the prey and predator respectively, $f_1(u)$ and $f_2(v)$ denote growth functions of the prey and the predator respectively, $p(u, v)$ is the functional response which accounts for the predation rate and biomass transfer from the prey to the predator after predation, and the constant c explains the efficiency in biomass transfer.

Predator-prey ODE models of the above form only consider interactions of two species with direct effect reflected by the predation term. However, since 1990s, more and more ecologists have realized the existence of indirect effects (e.g., fear effect), and observed impact of such effects; see, e.g. [1, 14, 21, 27]. Recent field experiments have found the presence of predator itself, can have significant influence on prey's population through changes in reproduction [15, 36], habitat selection [4, 28] and physiology [3, 5, 35]. In contrast, as far as mathematical modeling is concerned, indirect effects have been largely (if not all) ignored in those existing models describing predator-prey interactions and those on conservation and management of the ecosystem.

Motivated by the field study in [36] which observed an as high as 40% decrease in prey's reproduction rate when the prey perceived a risk of predator coming from the playback of the predator's voice, [31] formulated a mathematical model in the form of the following ordinary differential equations

$$\begin{cases} \frac{du}{dt} = f(k, v(t)) r_0 u(t) - d u(t) - a u^2(t) - p(u(t)) v(t), \\ \frac{dv}{dt} = c p(u(t)) v(t) - m v(t). \end{cases} \quad (3.2)$$

Here u is the population of the prey species and v is the population of predator species, and the prey's growth follows a logistic growth with the intrinsic growth rate being split into the net growth rate r_0 and natural death rate d , given by $r_0 - d$. To mimic the scenario of the field experimental study in [36] in which predation actually did not occur due to the use of electronic fence, in (3.2) the fear effect is only incorporated into the production term by the function $f(k, v(t))$ accounting for a cost. The term $au^2 = (au)u$ reflects the self-limiting mechanism of u (due to intra-species competition) and c is the biomass transform efficiency constant. The function $p(u)$ is the functional response which is assumed to depend on the prey population only. Analysis of (3.2), both analytical and numerical, have revealed some interesting dynamics that would have not occurred without considering the fear effect.

Since [31], there have been some follow-up modelling works that extend the model (3.2) to accommodate various aspects of fear effect. For example, [32] considered *age structure* and discussed different impacts of fear effect on different age stages; [33] explored the fear effect

reflected thought the *dispersals* and its impact on the pattern formation. [8] incorporated an extra food source for the predator in (3.2) and also added a white noise to the death rates of the prey and predator, and analyzed the resulting stochastic model. [18] further considered a digestion delay in addition to the cost of fear, white noise in the death rates, and extra food for the predator but ignored the benefit of the anti-predation response. More recently, in addition to a digestion delay and a cost in prey's production due to the anti-predation response, [34] further incorporated a benefit term from the anti-predation response, and explored the joint impact of the fear effect and the digestion delay on the population dynamics for both predator and prey.

In the real world, it is quite common that a species can predate on one species and in the mean time, it can be a prey of other species. This leads to occurrence of food chains between multiple species, consisting of cascading predator-prey interactions. One may naturally ask how a fear effect arising from one or more species in the chain will affect the dynamics of the whole cascaded populations? In a more recent field experimental study [26], the authors tested a meso-predator cascade by manipulating the large carnivores playback, which resulted in a decrease in the population of meso-carnivore and increase in the population of its prey. That is, the fear effect on the top species in that chain of three species actually affects every species in the ecosystem explicitly or implicitly.

To better understand the above mentioned propagation of the fear effect from top layer to the bottom layer in that food chain ecosystem reported in [26], we incorporate a fear effect on the top species into a Lotka-Volterra type food chain model, formulated by the following system of ordinary differential equations

$$\begin{cases} \frac{dN_1}{d\tau} = N_1 (R_1 - a_{11}N_1 - a_{12}N_2), \\ \frac{dN_2}{d\tau} = N_2 (R_2 - a_{22}N_2 - a_{23}N_3 + a_{21}N_1), \\ \frac{dN_3}{d\tau} = N_3 (B(\alpha) - D - a_{33}N_3 + a_{32}N_2), \\ N_1(0) \geq 0, \quad N_2(0) \geq 0, \quad N_3(0) \geq 0. \end{cases} \quad (3.3)$$

Here, N_3 is the population of the meso-carnivore (e.g., racoon) which is affected by the large carnivore's (e.g., wolf, bear) *playback*; N_2 is the prey (e.g., crab) of the meso-carnivore N_3 ,

and N_1 is the prey of N_2 . Each species is assumed to follow a logistic growth with growth rates R_1 , R_2 and $B(\alpha) - D$ respectively. The population of the large carnivores does not appear in the system because in the field study [26], only their voices are played, and hence they only have fear (indirect) effect on the meso-carnivores represented by $B(\alpha)$, where the net birth (production) rate $B(\alpha)$ depends on a parameter α standing for the meso-carnivore's anti-predation response level. By its biological meaning, $B(\alpha)$ is assumed to satisfy

$$B'(\alpha) < 0, \quad B(0) = B_3 > 0 \quad \text{and} \quad \lim_{\alpha \rightarrow \infty} B(\alpha) = 0. \quad (3.4)$$

The constant D is the natural death rate of N_3 , a_{ii} ($i = 1, 2, 3$) are the intra-species competition coefficients. a_{12} and a_{23} are the predation rates, while a_{21} and a_{32} are the conversion rate of the biomass from N_1 to N_2 and from N_2 to N_3 respectively; thus, a_{12}/a_{21} and a_{23}/a_{32} actually account for the efficiency of biomass transfer from the predations. We point out that this type of three dimensional food chain models have been intensive and extensively studied by some researchers, see, e.g., [9, 11, 12, 13] and the references therein. As far as fear effect in food chains is concerned, two recent papers [19, 20] have also followed line of [31] to consider fear effect in food chain of three species; their scenario is different from ours: they considered other types of functional responses, they incorporated fear effects in the bottom and middle species, and they assumed that the top and middle species are specialist predators. The *first goal* of this chapter is to explore the dynamics of (3.3), particularly, the impact of the meso-carnivore's anti-predation response level α on the dynamics.

In (3.3), only the cost for the meso-carnivore's anti-predation response is considered. For such a response, in addition to cost, there should also be a benefit (see, e.g., [6, 27]), typically reflected by the decrease in the chance of being predated. A response strategy is expected to seek balance between cost and benefit to achieve certain optimality. In order to also add the benefit into the interplay in the above model system (3.3), we need the term of predation on the meso-carnivore by a large carnivore, which inevitably requires us to add the the population of that large carnivore into the system. This leads to the following four dimensional food chain

model

$$\begin{cases} \frac{dN_1}{d\tau} = N_1 (R_1 - a_{11}N_1 - a_{12}N_2), \\ \frac{dN_2}{d\tau} = N_2 (R_2 - a_{22}N_2 - a_{23}N_3 + a_{21}N_1), \\ \frac{dN_3}{d\tau} = N_3 (B(\alpha, N_4) - D_3 - a_{33}N_3 + a_{32}N_2 - a_{34}(\alpha)N_4), \\ \frac{dN_4}{d\tau} = N_4 (-D_4 + \bar{c} a_{34}(\alpha)N_3), \\ N_1(0) \geq 0, N_2(0) \geq 0, N_3(0) \geq 0, N_4(0) \geq 0, \end{cases} \quad (3.5)$$

where N_4 is the population of the restored top predator (large carnivore) which is assumed to be a specialist predator with the mortality rate D_4 . Now the net growth function of N_3 depends not only on the anti-predation response level α but also on the population of its predator N_4 . The function $a_{34}(\alpha)$ denotes the encounter rate between N_3 and N_4 which is affected by the protective behaviours of N_3 species characterized by its dependence on the anti-predation response level α . By their biological meanings of $B(\alpha, N_4)$ and $a_{34}(\alpha)$, they are assumed to satisfy the following conditions:

$$\begin{cases} B(\alpha, N_4) \text{ is decreasing in } \alpha \text{ and } N_4, B(0, N_4) = B(\alpha, 0) = B_3 > 0, \\ \lim_{\alpha \rightarrow \infty} B(\alpha, N_4) = \lim_{N_4 \rightarrow \infty} B(\alpha, N_4) = 0, \end{cases} \quad (3.6)$$

and

$$a_{34}(\alpha) \text{ is decreasing, } a_{34}(0) = a_0 > 0, \lim_{\alpha \rightarrow \infty} a_{34}(\alpha) = 0. \quad (3.7)$$

Finally, \bar{c} is the efficiency of biomass transform. So in this model, we consider both the complex multi-trophic predator-prey structure and the trade-off from anti-predation response.

The remainder of this chapter is organized as follows. In Section 2, we analyze the model system (3.3). We establish the well-posedness of system (3.3) and find the condition for existence and stability for all its equilibrium solutions. We also discuss the relationship between the anti-predation level and the final population size. In the end, some numerical examples, together with some discussions, are given to demonstrate our results. In Section 3, we investigate the dynamics of the four dimension model (3.5), including the existence and stability of equilibria as well as the continuously dependence between the final population size with respect to the anti-predation level. We also discuss the difference of the results from those for (3.3)

in Section 2. In addition, we also present some numerical examples to illustrate that different functional response functions may lead to slightly different dynamical behaviour of the solution. In Section 4, we summarize our main results and discuss their biological implications. We also discuss some possible future projects along this direction of anti-predation response in predator-prey interactions.

3.2 Analysis of the model without large carnivores

In this section, we analyze the three-species model (3.3). We first show the well-posedness of the system (3.3). Then we find all equilibrium solutions and discuss their stability in terms of the parameter values and anti-predation strategy level. As we mentioned in last section, this kind of food chain models have been studied in literatures, and thus, some technical results can be found in existing researches, e.g., [9, 11, 12, 13] and their references. But we need to associate the results to the new parameter α , the anti-predation response level of the species N_3 to shed light on influence of the fear effect for this model.

3.2.1 Preliminaries

For mathematical simplification, we first non-dimensionalize the model (3.3). Let

$$t = R_1\tau, \quad x = \frac{a_{11}N_1}{R_1}, \quad y = \frac{a_{12}N_2}{R_1}, \quad z = \frac{a_{23}N_3}{R_1},$$

then model (3.3) becomes

$$\begin{cases} \frac{dx}{dt} = x(1 - x - y), \\ \frac{dy}{dt} = y(k - d_1y - z + \beta_1x), \\ \frac{dz}{dt} = z(f(\alpha) - d_2z + \beta_2y), \end{cases} \quad (3.8)$$

where

$$k = \frac{R_2}{R_1}, \quad d_1 = \frac{a_{22}}{a_{12}}, \quad d_2 = \frac{a_{33}}{a_{23}}, \quad \beta_1 = \frac{a_{21}}{a_{11}}, \quad \beta_2 = \frac{a_{32}}{a_{12}},$$

$$f(\alpha) = \frac{B(\alpha) - D}{R_1}, \quad f(0) = \frac{B_3 - D}{R_1}, \quad \lim_{\alpha \rightarrow \infty} f(\alpha) = -\frac{D}{R_1}.$$

By the basic theory of ODE systems, we can easily show that the initial value problem for (3.8) has a unique solution; moreover, the solution is nonnegative (positive) with nonnegative (positive) initial conditions because each equation in (3.8) is of Gaussian type. Now we show that the solution to system (3.8) is bounded.

From the first equation in system (3.8) and by the non-negativity of $y(t)$, we have

$$\frac{dx}{dt} = x(1 - x - y) \leq x(1 - x).$$

By the comparison theorem [25], we can obtain $\lim_{t \rightarrow \infty} \sup x(t) \leq 1$. Therefore, for any $\epsilon_1 > 0$, there holds $x(t) \leq 1 + \epsilon_1$ for large t . Incorporating this estimate for large t into the second equation in (3.8) results in

$$\frac{dy}{dt} = y(k - d_1 y - z + \beta_1 x) \leq y(k + \beta_1(1 + \epsilon_1) - d_1 y), \quad \text{for large } t.$$

Applying the comparison theorem again, we then obtain

$$\limsup_{t \rightarrow \infty} y(t) \leq \frac{k + \beta_1(1 + \epsilon_1)}{d_1}.$$

Since $\epsilon_1 > 0$ is arbitrary small, the above inequality actually implies

$$\limsup_{t \rightarrow \infty} y(t) \leq \frac{k + \beta_1}{d_1}.$$

Incorporating the above inequality into the third equation in (3.8) and by the same argument, we can obtain

$$\limsup_{t \rightarrow \infty} z(t) \leq \max\left(\frac{f(\alpha)d_1 + \beta_2(k + \beta_1)}{d_1 d_2}, 0\right).$$

Combining the above, we have proved that the solution $(x(t), y(t), z(t))$ to (3.8) is bounded.

3.2.2 Existence and Stability of the boundary equilibria

In this section, we find all **boundary** equilibrium solutions and give the condition for their existence and stability. For the result to be biologically meaningful, we are only interested in

equilibria with nonnegative components.

An equilibrium of (3.8) solves the following system

$$\begin{cases} x(1 - x - y) = 0, \\ y(k - d_1y - z + \beta_1x) = 0, \\ z(f(\alpha) - d_2z + \beta_2y) = 0. \end{cases}$$

There are seven boundary equilibrium solutions. $E_0 = (0, 0, 0)$ is the trivial equilibrium solution which always exists. $E_1 = (1, 0, 0)$, $E_2 = (0, k/d_1, 0)$ and $E_3 = (0, 0, f(\alpha)/d_2)$ are the equilibria representing the scenario that only one species survives; E_1 and E_2 always exist, while E_3 exists only when $f(\alpha) > 0$. There are also other three *possible* equilibria corresponding to the scenario of two species coexisting, and they are given by

$$\begin{aligned} E_{12} &= \left(1 - \frac{k + \beta_1}{d_1 + \beta_1}, \frac{k + \beta_1}{d_1 + \beta_1}, 0\right), \\ E_{13} &= \left(1, 0, \frac{f(\alpha)}{d_2}\right), \\ E_{23} &= \left(0, \frac{d_2k - f(\alpha)}{d_1d_2 + \beta_2}, k - \frac{d_1d_2k - d_1f(\alpha)}{d_1d_2 + \beta_2}\right). \end{aligned}$$

By the nonnegative requirement, E_{12} exists when $k < d_1$, E_{13} exists when $f(\alpha) > 0$ and E_{23} exists when $d_2k > f(\alpha) > -\beta_2k/d_1$.

The local stability of an equilibrium is obtained by linearization at the equilibrium. The Jacobian matrix at equilibrium (x^*, y^*, z^*) is given by

$$J(E = (x^*, y^*, z^*)) = \begin{pmatrix} 1 - 2x^* - y^* & -x^* & 0 \\ \beta_1y^* & k - 2d_1y^* + \beta_1x^* - z^* & -y^* \\ 0 & \beta_2z^* & f(\alpha) - 2d_2z^* + \beta_2y^* \end{pmatrix}. \quad (3.9)$$

At $E_0 = (0, 0, 0)$, the Jacobian is given by

$$J(E_0) = \begin{pmatrix} 1 & 0 & 0 \\ 0 & k & 0 \\ 0 & 0 & f(\alpha) \end{pmatrix},$$

therefore E_0 is unstable, as there are positive eigenvalues $\lambda_1 = 1$ and $\lambda_2 = k$.

Similarly, at $E_1 = (1, 0, 0)$, the Jacobian is given by

$$J(E_1) = \begin{pmatrix} -1 & -1 & 0 \\ 0 & k + \beta_1 & 0 \\ 0 & 0 & f(\alpha) \end{pmatrix},$$

therefore E_1 is unstable, as there is a positive eigenvalue $\lambda = k + \beta_1$.

At $E_2 = (0, k/d_1, 0)$, the Jacobian is given by

$$J(E_2) = \begin{pmatrix} 1 - \frac{k}{d_1} & 0 & 0 \\ \frac{\beta_1 k}{d_1} & -k & -\frac{k}{d_1} \\ 0 & 0 & f(\alpha) + \frac{\beta_2 k}{d_1} \end{pmatrix},$$

therefore E_2 is asymptotically stable if and only if $1 - k/d_1 < 0$ and $f(\alpha) < -\beta_2 k/d_1$.

At $E_3 = (0, 0, f(\alpha)/d_2)$, the Jacobian is given by

$$J(E_3) = \begin{pmatrix} 1 & 0 & 0 \\ 0 & k - \frac{f(\alpha)}{d_2} & 0 \\ 0 & \frac{\beta_2 f(\alpha)}{\alpha_2} & -f(\alpha) \end{pmatrix},$$

hence, E_3 is unstable since there is a positive eigenvalue $\lambda = 1$.

At E_{12} , the Jacobian becomes

$$J(E_{12}) = \begin{pmatrix} \frac{k + \beta_1}{d_1 + \beta_1} - 1 & \frac{k + \beta_1}{d_1 + \beta_1} - 1 & 0 \\ \frac{\beta_1 k + \beta_1^2}{d_1 + \beta_1} & -\frac{d_1 k + d_1 \beta_1}{d_1 + \beta_1} & -\frac{k + \beta_1}{d_1 + \beta_1} \\ 0 & 0 & f(\alpha) + \frac{\beta_2 k + \beta_2 \beta_1}{d_1 + \beta_1} \end{pmatrix},$$

thus, E_{12} is asymptotically stable if and only if $f(\alpha) < -\frac{\beta_2 k + \beta_2 \beta_1}{d_1 + \beta_1}$.

At $E_{13} = (1, 0, f(\alpha)/d_2)$, the Jacobian reduces to

$$J(E_{13}) = \begin{pmatrix} -1 & -1 & 0 \\ 0 & k + \beta_1 - \frac{f(\alpha)}{d_2} & 0 \\ 0 & \frac{\beta_2 f(\alpha)}{\alpha_2} & -f(\alpha) \end{pmatrix},$$

therefore E_{13} is asymptotically stable if and only if $f(\alpha) > d_2(k + \beta_1)$.

At $E_{23} = \left(0, \frac{d_2k - f(\alpha)}{d_1d_2 + \beta_2}, k - \frac{d_1d_2k - d_1f(\alpha)}{d_1d_2 + \beta_2}\right)$, the Jacobian is given by

$$J(E_{23}) = \begin{pmatrix} 1 - \frac{d_2k - f(\alpha)}{d_1d_2 + \beta_2} & 0 & 0 \\ \frac{\beta_1d_2k - \beta_1f(\alpha)}{d_1d_2 + \beta_2} & -\frac{d_1d_2k - d_1f(\alpha)}{d_1d_2 + \beta_2} & -\frac{d_2k - f(\alpha)}{d_1d_2 + \beta_2} \\ 0 & \beta_2k - \frac{\beta_2d_1d_2k - \beta_2d_1f(\alpha)}{d_1d_2 + \beta_2} & -d_2k + \frac{d_1d_2^2k - d_1d_2f(\alpha)}{d_1d_2 + \beta_2} \end{pmatrix},$$

therefore E_{23} is asymptotically stable if and only if $f(\alpha) > d_2k - d_1d_2 - \beta_2$.

We summarize the above analysis in the following proposition.

Proposition 3.2.1 *For system (3.8), the following statement hold.*

- (i) *Equilibrium E_0 and E_1 always exist and are unstable.*
- (ii) *Equilibrium E_2 always exists; it is asymptotically stable if and only if $k > d_1$ and $f(\alpha) < -\beta_2k/d_1$.*
- (iii) *When $f(\alpha) > 0$, E_3 exists; it is unstable. E_{13} exists and is asymptotically stable if and only if $f(\alpha) > d_2(k + \beta_1)$.*
- (iv) *When $k < d_1$, E_{12} exists; it is asymptotically stable if and only if $f(\alpha) < -\beta_2(k + \beta_1)/(d_1 + \beta_1)$.*
- (v) *When $d_2k > f(\alpha) > -\beta_2k/d_1$, E_{23} exists; it is asymptotically stable if and only if $f(\alpha) < d_2k - d_1d_2 - \beta_2$.*

3.2.3 Existence and stability of a positive equilibrium solution

There is a unique positive equilibrium solution $E^* = (x^*, y^*, z^*)$ if

$$d_2(k + \beta_1) > f(\alpha) > \max\left(d_2k - d_1d_2 - \beta_2, \frac{-\beta_2(k + \beta_1)}{d_1 + \beta_1}\right). \quad (3.10)$$

Indeed, $E^* = (x^*, y^*, z^*)$ is given by

$$\begin{cases} x^* = 1 - y^*, \\ y^* = \frac{d_2(k + \beta_1) - f(\alpha)}{d_2(d_1 + \beta_1) + \beta_2}, \\ z^* = k + \beta_1 - (d_1 + \beta_1)y^*. \end{cases} \quad (3.11)$$

The conditions in (3.10) directly comes from the formulas in (3.11).

The Jacobian matrix at the positive equilibrium can be simplified as

$$J(E^*) = \begin{pmatrix} -x^* & -x^* & 0 \\ \beta_1 y^* & -d_1 y^* & -y^* \\ 0 & \beta_2 z^* & -d_2 z^* \end{pmatrix},$$

Thus, the corresponding characteristic equation is

$$\begin{aligned} \lambda^3 + (d_1 y^* + d_2 z^* + x^*) \lambda^2 + (d_1 d_2 y^* z^* + \beta_1 x^* y^* + \beta_2 y^* z^* + d_1 x^* y^* + d_2 x^* z^*) \lambda \\ + (\beta_1 d_2 + d_1 d_2 + \beta_2) x^* y^* z^* = 0. \end{aligned}$$

where

$$\begin{cases} a_1 = d_1 y^* + d_2 z^* + x^* > 0, \\ a_2 = d_1 d_2 y^* z^* + \beta_1 x^* y^* + \beta_2 y^* z^* + d_1 x^* y^* + d_2 x^* z^* > 0, \\ a_3 = (\beta_1 d_2 + d_1 d_2 + \beta_2) x^* y^* z^* > 0, \end{cases}$$

and

$$\begin{aligned} a_1 a_2 - a_3 &= d_1^2 d_2 (y^*)^2 z^* + d_1 d_2^2 y^* (z^*)^2 + \beta_1 d_1 x^* (y^*)^2 + \beta_2 d_1 (y^*)^2 z^* + \beta_2 d_2 y^* (z^*)^2 \\ &+ d_1^2 x^* (y^*)^2 + 2d_1 d_2 x^* y^* z^* + d_2^2 x^* (z^*)^2 + \beta_1 (x^*)^2 y^* + d_1 (x^*)^2 y^* + d_2 (x^*)^2 z^* > 0. \end{aligned}$$

By Routh-Hurwitz criterion, the positive equilibrium is locally asymptotically stable. Moreover, we can prove that it is actually globally asymptotically stable as long as it exists (i.e., (3.10) holds).

Theorem 3.2.2 *If (3.10) holds, then the positive equilibrium E^* is globally asymptotically stable.*

Proof Consider the Lyapunov function

$$V(x, y, z) = \beta_1 \beta_2 (x - x^* - x^* \ln \frac{x}{x^*}) + \beta_2 (y - y^* - y^* \ln \frac{y}{y^*}) + (z - z^* - z^* \ln \frac{z}{z^*}),$$

then

$$\frac{dV}{dt} = -\beta_1 \beta_2 (x - x^*)^2 - \beta_2 (y - y^*)^2 - (z - z^*)^2 \leq 0$$

and $\frac{dV}{dt} = 0$ if and only if $(x, y, z) = (x^*, y^*, z^*)$. By LaSalle's Invariant Principle, we conclude E^* is globally asymptotically stable.

For readers' convenience, we summarize the analytical results on the dynamics of the model (3.8) obtained above in the following Table 3.1.

Table 3.1: Condition of existence and stability of the equilibria in model (3.8)

Equilibrium solution	Existence	Stability
E_0	Always	Unstable
E_1	Always	Unstable
E_2	Always	$d_1 < k$ and $f(\alpha) < -\beta_2 k / d_1$
E_3	$f(\alpha) > 0$	Unstable
E_{12}	$d_1 > k$	$f(\alpha) < -\beta_2(k + \beta_1) / (d_1 + \beta_1)$
E_{13}	$f(\alpha) > 0$	$f(\alpha) > d_2(k + \beta_1)$
E_{23}	$d_2 k > f(\alpha) > -\beta_2 k / d_1$	$f(\alpha) < d_2 k - d_1 d_2 - \beta_2$
E^*	$d_2(k + \beta_1) > f(\alpha) > \max\left(d_2 k - d_1 d_2 - \beta_2, -\frac{\beta_2(k + \beta_1)}{d_1 + \beta_1}\right)$	GAS

From Theorem 3.2.2, we know that the positive equilibrium is always globally asymptotically stable as long as it exists (i.e., (3.10) holds), implying that the populations of all three species will converge to co-existence state at the respect levels x^* , y^* and z^* . Thus, it is worthwhile to investigate how the response strength α will affect these levels. Indeed, direct

calculations give

$$\begin{cases} \frac{dy^*}{d\alpha} = \frac{-f'(\alpha)}{d_2(d_1 + \beta_1) + \beta_2} > 0, \\ \frac{dx^*}{d\alpha} = -\frac{dy^*}{d\alpha} < 0, \\ \frac{dz^*}{d\alpha} = -(d_1 + \beta_1)\frac{dy^*}{d\alpha} < 0. \end{cases}$$

That is, within the range of α that guarantees (3.10), with the increase of the anti-predation response strength α , the final population sizes of the meso-carnivore, its prey and the prey's prey will decrease, increase and decrease respectively, demonstrating an alternative pattern for the fear effect in the cascade, which was observed in the field study [26]. Therefore, the model (3.3) does provide a mechanism that can explain the phenomenon of trophic cascade caused by a fear of large carnivores reported in [26].

3.2.4 Numerical simulations

In this subsection, we present some numerical simulations to illustrate the analytical results obtained above. For this purpose, we choose a particular form for the function $B(\alpha)$ given by

$$B(\alpha) = \frac{R_3}{1 + c\alpha},$$

and this sends (3.3) to the following system:

$$\begin{cases} \frac{dN_1}{d\tau} = N_1 (R_1 - a_{11}N_1 - a_{12}N_2), \\ \frac{dN_2}{d\tau} = N_2 (R_2 - a_{22}N_2 - a_{23}N_3 + a_{21}N_1), \\ \frac{dN_3}{d\tau} = N_3 \left(\frac{R_3}{1 + c\alpha} - D - a_{33}N_3 + a_{32}N_2 \right), \\ N_1(0) \geq 0, \quad N_2(0) \geq 0, \quad N_3(0) \geq 0, \end{cases} \quad (3.12)$$

We fix the parameters

$$\begin{aligned} R_1 = 1, \quad a_{11} = 1, \quad a_{12} = 0.4, \quad R_2 = 1, \quad a_{22} = 0.2, \quad a_{23} = 0.5, \quad a_{21} = 0.5, \\ R_3 = 3, \quad D = 1, \quad a_{33} = 0.5, \quad a_{32} = 0.05, \quad c = 0.4, \end{aligned} \quad (3.13)$$

and demonstrate how α impacts the population dynamics. In this case, $k = R_2/R_1 = 1$ and $d_1 = a_{22}/a_{12} = 1/2$ so $k > d_1$. According to Proposition 3.2.1, there are three threshold values for α , denoted by α_1^* , α_2^* and α_3^* , which are given by

$$\begin{cases} f(\alpha_1^*) = d_2(k + \beta_1), \\ f(\alpha_2^*) = d_2k - d_1d_2 - \beta_2, \\ f(\alpha_3^*) = -\frac{\beta_2k}{d_1}. \end{cases}$$

Using the parameter values in (3.13), we obtain $\alpha_1^* = 0.5$, $\alpha_2^* \approx 2.954545455$ and $\alpha_3^* = 7.5$. By Proposition 3.2.1, when $0 < \alpha < 0.5$, the equilibrium E_{13} is stable (as demonstrated in Figure 3.1-(a) for $\alpha = 0.4$); when $0.5 < \alpha < 2.954545455$, the coexistence equilibrium E^* is stable (as demonstrated in Figure 3.1-(b) for $\alpha = 2$); when $2.954545455 < \alpha < 7.5$ (destroying (3.10), hence E^* no longer exists), the equilibrium E_{23} is stable (as demonstrated in Figure 3.1-(c) for $\alpha = 5$); when $\alpha > 7.5$, the equilibrium E_2 is stable (as demonstrated in Figure 3.1-(d) for $\alpha = 10$). The bifurcation diagram with respect to α is given in Figure 3.2.

Now, we change R_1 to $R_1 = 3$ and a_{33} to $a_{33} = 0.1$ and keep other parameters the same as in (3.13). Then $k = R_2/R_1 = 1/3$ and $d_1 = a_{22}/a_{12} = 1/2$ leading to the scenario of $k < d_1$. According to Proposition 3.2.1, there are two threshold values for α , denoted by $\bar{\alpha}_1$ and $\bar{\alpha}_2$, which are given by

$$\begin{cases} f(\bar{\alpha}_1) = d_2(k + \beta_1), \\ f(\bar{\alpha}_2) = -\frac{\beta_2(k + \beta_1)}{d_1 + \beta_1}. \end{cases}$$

Using the parameter values in (3.13), we obtain $\bar{\alpha}_1 = 2.5$ and $\bar{\alpha}_2 \approx 8.409090911$. By Proposition 3.2.1, when $0 < \alpha < 2.5$, the equilibrium E_{13} is stable (as demonstrated in Figure 3.3-(a) for $\alpha = 2$); when $2.5 < \alpha < 8.409090911$, the coexistence equilibrium E^* is stable (as demonstrated in Figure 3.3-(b) for $\alpha = 6$); when $\alpha > 8.409090911$, the equilibrium E_{12} is stable (as demonstrated in Figure 3.3-(c) for $\alpha = 10$). The bifurcation diagram with respect to α is given in Figure 3.4.

We find that depending on the difference between k and d_1 , we have two kinds of bifurcation. In both cases, when the anti-predation response α passes a threshold, it leads to a

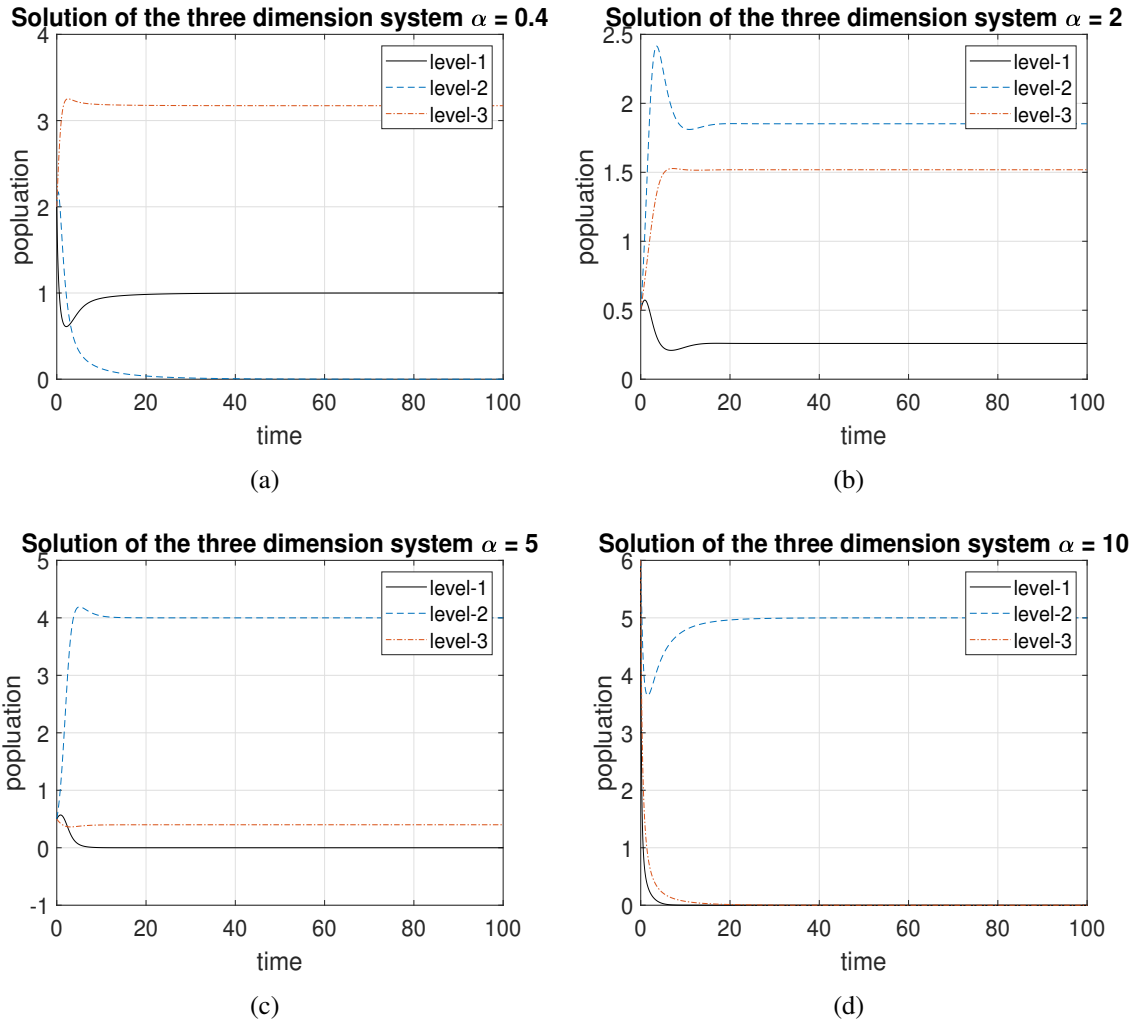


Figure 3.1: Population dynamics of (3.12) when $d_1 < k$. (a) When $0 < \alpha = 0.4 < 0.5$, the equilibrium E_{13} is stable, (b) $0.5 < \alpha = 2 < 2.954545455$, the coexistence equilibrium E^* is stable, (c) when $2.954545455 < \alpha = 5 < 7.5$, the equilibrium E_{23} is stable, (d) when $\alpha = 10 > 7.5$, the equilibrium E_2 is stable.

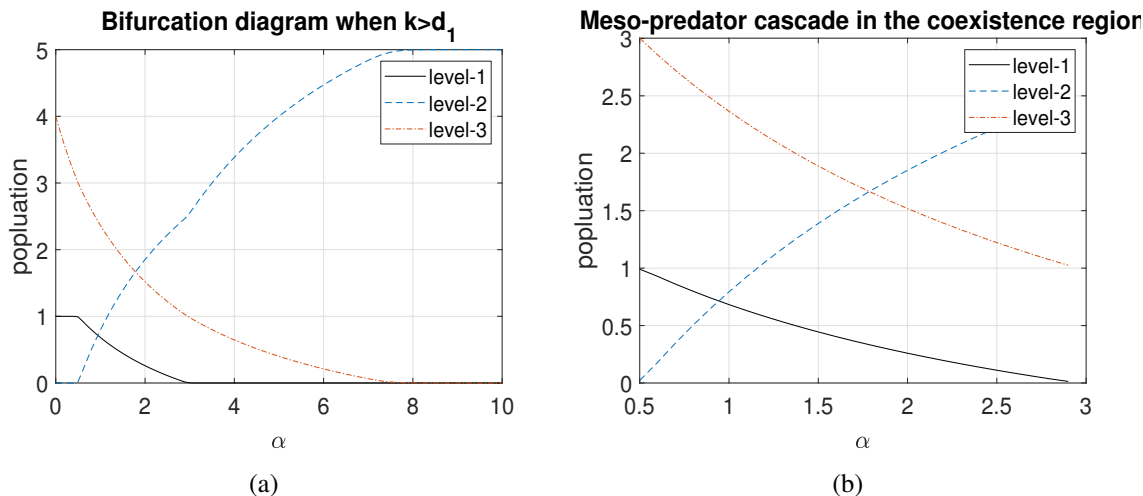


Figure 3.2: (a) Bifurcation diagram of (3.12) when $k > d_1$, (b) In the region when the coexistence equilibrium E^* is stable, we can observe a meso-predator cascade.

transcritical bifurcation and we can always observe a meso-predator cascade inside the coexistence region when increasing α : the population of meso-predator is decreasing, the population of its prey is increasing and the population of the prey's prey (bottom prey) is decreasing. However, this pattern will be dramatically changed when we restore large carnivores instead of only manipulating their playback to induce fear. In the next section, we will model the case when we also introduce the large carnivores back into the food chain, leading to a 4-D model.

3.3 Model with restoring large carnivores

In this section, we analyze (3.5) which has the population of large carnivores incorporated together with a benefit in preventing predation of the meso-carnivore by the large carnivores, in addition to the cost in the meso-carnivore's production. Parallel to Section 3.2, we first establish the well-posedness of the 4-D model (3.5), discuss all possible equilibrium solutions and find the condition for their existence and stability in terms of the parameter values and anti-predation strategy level.

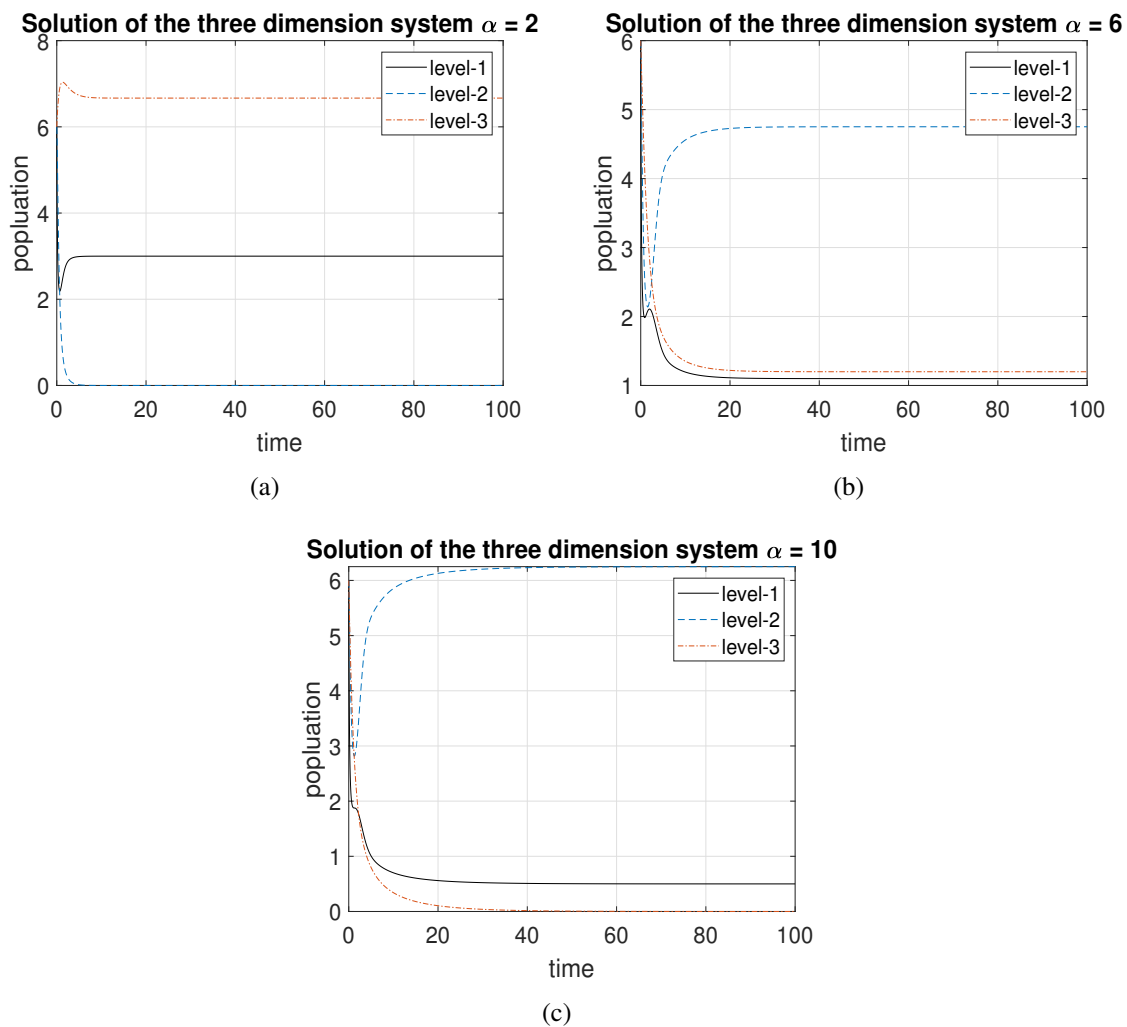


Figure 3.3: Population dynamics of (3.12) when $d_1 > k$. (a) When $0 < \alpha = 2 < 2.5$, the equilibrium E_{13} is stable, (b) $2.5 < \alpha = 6 < 8.409090911$, the coexistence equilibrium E^* is stable, (c) when $8.409090911 < \alpha = 10$, the equilibrium E_{12} is stable.

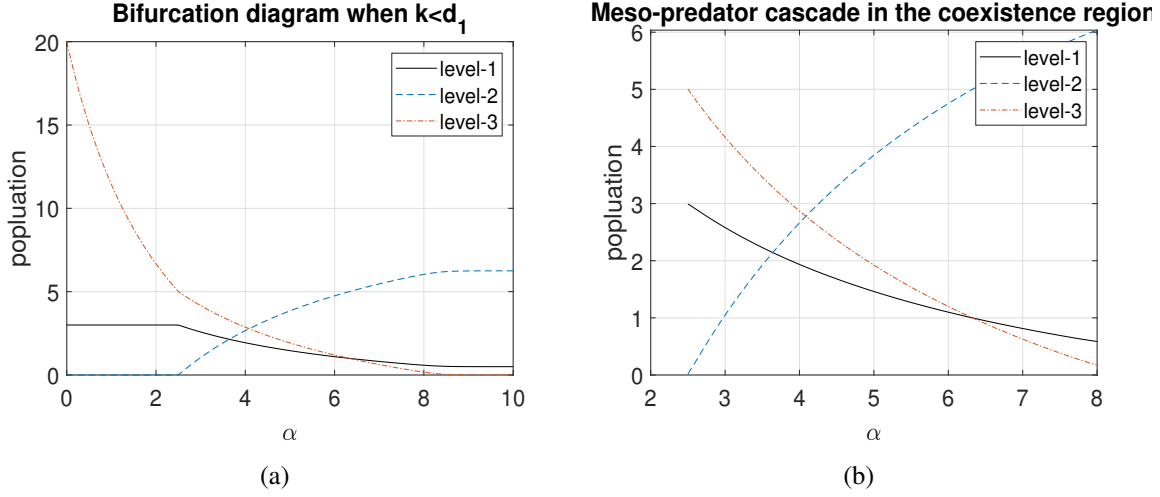


Figure 3.4: (a) Bifurcation diagram of (3.12) when $d_1 > k$, (b) In the region when the coexistence equilibrium E^* is stable, we can observe a meso-predator cascade.

3.3.1 Well-posedness

For mathematical simplification, we still apply non-dimensionalization for our model (3.5) which is a natural expansion of the non-dimensionalization for (3.3) in Section 2, given by

$$t = R_1 \tau, \quad x = \frac{a_{11} N_1}{R_1}, \quad y = \frac{a_{12} N_2}{R_1}, \quad z = \frac{a_{23} N_3}{R_1}, \quad w = \frac{a_0 N_4}{R_1},$$

with $a_0 = a_{34}(0)$. Then model (3.5) becomes

$$\begin{cases} \frac{dx}{dt} = x(1 - x - y), \\ \frac{dy}{dt} = y(k - d_1 y - z + \beta_1 x), \\ \frac{dz}{dt} = z(f(\alpha, w) - d_2 z + \beta_2 y - p(\alpha)w), \\ \frac{dw}{dt} = w(-m + cp(\alpha)z) \end{cases} \quad (3.14)$$

where

$$k = \frac{R_2}{R_1}, \quad d_1 = \frac{a_{22}}{a_{12}}, \quad d_2 = \frac{a_{33}}{a_{23}}, \quad \beta_1 = \frac{a_{21}}{a_{11}}, \quad \beta_2 = \frac{a_{32}}{a_{12}}, \quad m = \frac{D_4}{R_1}, \quad c = \frac{\bar{c}a_0}{a_{23}}.$$

For the transformed and rescaled functions $f(\alpha, w)$ and $p(\alpha)$, the conditions (3.6) and (3.7) are transformed to

$$\left\{ \begin{array}{l}
f(\alpha, w) = \frac{B(\alpha, N_4) - D_3}{R_1}, \\
f(\alpha, 0) = f(0, w) = f_0 = \frac{B_3 - D_3}{R_1}, \\
\frac{\partial f}{\partial \alpha} < 0, \quad \frac{\partial f}{\partial w} < 0, \\
\lim_{\alpha \rightarrow \infty} f(\alpha, w) = \lim_{w \rightarrow \infty} f(\alpha, w) = \frac{-D_3}{R_1}, \\
p(\alpha) = \frac{a_{34}(\alpha)}{a_0}, \\
\frac{dp}{d\alpha} < 0, \\
p(0) = 1 \quad \text{and} \quad \lim_{\alpha \rightarrow \infty} p(\alpha) = 0.
\end{array} \right. \quad (3.15)$$

By the fundamental theory of ODEs, we easily see that the initial value problem associated with (3.14) has a unique solution; moreover, the solution is nonnegative (positive) with nonnegative (positive) initial conditions. Next we show that the solution to system (3.14) is bounded.

Firstly, by the same argument as in subsection 2.2, we can obtain the same estimates for $x(t)$ and $y(t)$:

$$\limsup_{t \rightarrow \infty} x(t) \leq 1 \quad \text{and} \quad \limsup_{t \rightarrow \infty} y(t) \leq \frac{k + \beta_1}{d_1}.$$

For z and w , we consider $P = cz + w$. Then we have

$$\frac{dP}{dt} = cz(f(\alpha, w) - d_2z + \beta_2y) - mw.$$

Now for any given $\epsilon > 0$, there holds $y(t) \leq (k + \beta_1)(1 + \epsilon)/d_1$ for large t . Then for some $\mu \in (0, m)$ and large t , we have

$$\begin{aligned}
\frac{dP}{dt} + \mu P &= cz(\mu + f(\alpha, w) - d_2z + \beta_2y) - (m - \mu)w, \\
&\leq cz \left(\mu + f_0 + \frac{\beta_2(k + \beta_1)(1 + \epsilon)}{d_1} - d_2z \right) \\
&=: cz(\bar{K} - d_2z)
\end{aligned} \quad (3.16)$$

where

$$\bar{K} = \mu + f_0 + \frac{\beta_2(k + \beta_1)(1 + \epsilon)}{d_1}.$$

If $\bar{K} \leq 0$, since $z(t) \geq 0$, we can conclude that

$$\frac{dP}{dt} + \mu P \leq 0,$$

leading to $P \leq P_0 e^{-\mu t}$, where $P_0 = cz_0 + w_0$ comes from the initial condition. Thus,

$$\limsup_{t \rightarrow \infty} P(t) \leq 0.$$

If $\bar{K} > 0$, then

$$\frac{dP}{dt} + \mu P \leq \frac{c\bar{K}^2}{4d_2}.$$

By the comparison theorem [25], we can obtain

$$P \leq P_0 e^{-\mu t} + (1 - e^{-\mu t}) \frac{c\bar{K}^2}{4\mu d_2}.$$

which implies

$$\limsup_{t \rightarrow \infty} P(t) \leq \frac{c\bar{K}^2}{4\mu d_2}.$$

Thus, in both cases, P is bounded, implying that z and w are both bounded. Therefore, all four components of the solution are bounded.

3.3.2 Existence and Stability of the boundary equilibrium solutions

As in Section 2, we first analyze the boundary equilibria of the model (3.14). Again, we are only interested in the equilibria with nonnegative components.

By solving the system

$$\begin{cases} x(1 - x - y) = 0, \\ y(k - d_1y - z + \beta_1x) = 0, \\ z(f(\alpha, w) - d_2z + \beta_2y - p(\alpha)w) = 0, \\ w(-m + cp(\alpha)z) = 0, \end{cases}$$

we find that there are eleven possible boundary equilibria and they are described below. $E_0 = (0, 0, 0, 0)$ is the trivial equilibrium solution which always exists, $E_1 = (1, 0, 0, 0)$, $E_2 = (0, k/d_1, 0, 0)$ and $E_3 = (0, 0, f_0/d_2, 0)$ are the equilibria that correspond to the case of only one species surviving: E_1 and E_2 are always exist while E_3 exists only when $f_0 > 0$. There are also four possible equilibria accounting for the scenario of two species coexisting and they are

$$\begin{aligned} E_{12} &= \left(\frac{d_1 - k}{d_1 + \beta_1}, \frac{k + \beta_1}{d_1 + \beta_1}, 0, 0 \right), \\ E_{13} &= \left(1, 0, \frac{f_0}{d_2}, 0 \right), \\ E_{23} &= \left(0, \frac{d_2k - f_0}{d_1d_2 + \beta_2}, \frac{k\beta_2 + d_1f_0}{d_1d_2 + \beta_2}, 0 \right), \\ E_{34} &= \left(0, 0, \frac{m}{cp(\alpha)}, \bar{w} \right) \end{aligned}$$

where \bar{w} satisfies the equation

$$f(\alpha, \bar{w}) - \frac{d_2m}{cp(\alpha)} - p(\alpha)\bar{w} = 0. \quad (3.17)$$

Due to the requirement of non-negativity, E_{12} exists when $k < d_1$, E_{13} exists when $f_0 > 0$, and E_{23} exists when $d_2k > f_0 > -\beta_2k/d_1$. For the existence and uniqueness of E_{34} , we denote

$$F_1(w) = f(\alpha, w) - \frac{d_2m}{cp(\alpha)} - p(\alpha)w.$$

Then it is obvious that $F_1(w)$ is a decreasing function with respect to w and $\lim_{w \rightarrow \infty} F_1(w) = -\infty$. Thus, the sufficient and necessary condition for E_{34} to exist is $F_1(0) > 0$, that is $f_0 > d_2m/cp(\alpha)$.

There are three possible equilibria for the case of three species coexisting, given by

$$\begin{aligned} E_{123} &= \left(\frac{d_1 d_2 - d_2 k + \beta_2 + f_0}{\beta_1 d_2 + d_1 d_2 + \beta_2}, \frac{\beta_1 d_2 + d_2 k - f_0}{\beta_1 d_2 + d_1 d_2 + \beta_2}, \frac{\beta_1 \beta_2 + \beta_1 f_0 + \beta_2 k + d_1 f_0}{\beta_1 d_2 + d_1 d_2 + \beta_2}, 0 \right), \\ E_{134} &= \left(1, 0, \frac{m}{cp(\alpha)}, \bar{w} \right), \\ E_{234} &= \left(0, \frac{cp(\alpha)k - m}{d_1 cp(\alpha)}, \frac{m}{cp(\alpha)}, \hat{w} \right), \end{aligned}$$

where \bar{w} is as in (3.17) and \hat{w} satisfies the equation

$$f(\alpha, \hat{w}) - \frac{d_2 m}{cp(\alpha)} + \frac{\beta_2 cp(\alpha)k - \beta_2 m}{d_1 cp(\alpha)} - p(\alpha)\hat{w} = 0. \quad (3.18)$$

Thus, E_{123} exists when

$$d_2(k + \beta_1) > f_0 > \max \left(d_2 k - d_1 d_2 - \beta_2, -\frac{\beta_2(k + \beta_1)}{d_1 + \beta_1} \right),$$

The condition for E_{134} to exist is the same as for the existence of E_{34} , that is, when $f_0 > d_2 m / cp(\alpha)$. Condition for E_{234} to exist is $cp(\alpha)k - m > 0$ and

$$f_0 > \frac{d_2 m}{cp(\alpha)} - \frac{\beta_2 cp(\alpha)k - \beta_2 m}{d_1 cp(\alpha)}.$$

In order to discuss the local stability, we calculate the Jacobian matrix at equilibrium $E = (x^*, y^*, z^*, w^*)$ as

$$J(E) = \begin{pmatrix} 1 - 2x^* - y^* & -x^* & 0 & 0 \\ \beta_1 y^* & k - 2d_1 y^* + \beta_1 x^* - z^* & -y^* & 0 \\ 0 & \beta_2 z^* & J_{33} & J_{34} \\ 0 & 0 & cp(\alpha)w^* & -m + cp(\alpha)z^* \end{pmatrix}, \quad (3.19)$$

where

$$J_{33} = f(\alpha, w^*) - 2d_2z^* + \beta_2y^* - p(\alpha)w^*,$$

and

$$J_{34} = z^* \left. \frac{\partial f(\alpha, w)}{\partial w} \right|_{w=w^*} - p(\alpha)z^* < 0 \quad \text{for } z^* > 0, \quad w^* > 0.$$

At $E_0 = (0, 0, 0, 0)$, the Jacobian becomes

$$J(E_0) = \begin{pmatrix} 1 & 0 & 0 & 0 \\ 0 & k & 0 & 0 \\ 0 & 0 & f_0 & 0 \\ 0 & 0 & 0 & -m \end{pmatrix},$$

thus, E_0 is unstable.

At $E_1 = (1, 0, 0, 0)$, the Jacobian reduces to

$$J(E_1) = \begin{pmatrix} -1 & -1 & 0 & 0 \\ 0 & k + \beta_1 & 0 & 0 \\ 0 & 0 & f_0 & 0 \\ 0 & 0 & 0 & -m \end{pmatrix},$$

hence E_1 is unstable.

At $E_2 = (0, k/d_1, 0, 0)$, the Jacobian is given by

$$J(E_2) = \begin{pmatrix} 1 - \frac{k}{d_1} & 0 & 0 & 0 \\ \frac{\beta_1 k}{d_1} & -k & -\frac{k}{d_1} & 0 \\ 0 & 0 & f_0 + \frac{\beta_2 k}{d_1} & 0 \\ 0 & 0 & 0 & -m \end{pmatrix},$$

so E_2 is asymptotically stable if and only if $1 - k/d_1 < 0$ and $f_0 < -\beta_2 k/d_1$.

At $E_3 = (0, 0, f_0/d_2, 0)$, the Jacobian is now

$$J(E_3) = \begin{pmatrix} 1 & 0 & 0 & 0 \\ 0 & k - \frac{f_0}{d_2} & 0 & 0 \\ 0 & \frac{\beta_2 f_0}{\alpha_2} & -f_0 & J_{34} \\ 0 & 0 & 0 & -m + \frac{cp(\alpha)f_0}{d_2} \end{pmatrix},$$

therefore E_3 is unstable.

At E_{12} , the Jacobian is reduced to

$$J(E_{12}) = \begin{pmatrix} \frac{k-d_1}{d_1+\beta_1} & \frac{k-d_1}{d_1+\beta_1} & 0 & 0 \\ \frac{\beta_1 k + \beta_1^2}{d_1 + \beta_1} & -\frac{d_1 k + d_1 \beta_1}{d_1 + \beta_1} & -\frac{k + \beta_1}{d_1 + \beta_1} & 0 \\ 0 & 0 & f_0 + \frac{\beta_2 k + \beta_2 \beta_1}{d_1 + \beta_1} & 0 \\ 0 & 0 & 0 & -m \end{pmatrix},$$

therefore E_{12} is asymptotically stable if and only if

$$f_0 < \frac{-(\beta_2 k + \beta_2 \beta_1)}{d_1 + \beta_1}.$$

At E_{13} , the Jacobian is

$$J(E_{13}) = \begin{pmatrix} -1 & -1 & 0 & 0 \\ 0 & k + \beta_1 - \frac{f_0}{d_2} & 0 & 0 \\ 0 & \frac{\beta_2 f_0}{\alpha_2} & -f_0 & J_{34} \\ 0 & 0 & 0 & -m + \frac{cp(\alpha)f_0}{d_2} \end{pmatrix},$$

consequently, E_{13} is asymptotically stable if and only if

$$\frac{md_2}{cp(\alpha)} > f_0 > d_2(k + \beta_1).$$

At E_{23} , the Jacobian is given by

$$J(E_{23}) = \begin{pmatrix} 1 - \frac{d_2k - f_0}{d_1d_2 + \beta_2} & 0 & 0 & 0 \\ \frac{\beta_1d_2k - \beta_1f_0}{d_1d_2 + \beta_2} & -\frac{d_1d_2k - d_1f_0}{d_1d_2 + \beta_2} & -\frac{d_2k - f_0}{d_1d_2 + \beta_2} & 0 \\ 0 & \frac{k\beta_2^2 + d_1f_0\beta_2}{d_1d_2 + \beta_2} & -\frac{k\beta_2d_2 + d_1f_0d_2}{d_1d_2 + \beta_2} & J_{34} \\ 0 & 0 & 0 & -m + \frac{cp(\alpha)(k\beta_2 + d_1f_0)}{d_1d_2 + \beta_2} \end{pmatrix},$$

therefore E_{23} is asymptotically stable if and only if

$$f_0 > d_2k - d_1d_2 - \beta_2 \quad \text{and} \quad p(\alpha) < \frac{m(d_1d_2 + \beta_2)}{c(k\beta_2 + d_1f_0)}.$$

At $E_{34} = \left(0, 0, \frac{m}{cp(\alpha)}, \bar{w}\right)$, the Jacobian becomes

$$J(E_{34}) = \begin{pmatrix} 1 & 0 & 0 & 0 \\ 0 & k - \frac{m}{cp(\alpha)} & 0 & 0 \\ 0 & \frac{\beta_2m}{cp(\alpha)} & \frac{-d_2m}{cp(\alpha)} & J_{34} \\ 0 & 0 & cp(\alpha)\bar{w} & 0 \end{pmatrix},$$

therefore E_{34} is unstable.

At $E_{123} = (X_1, Y_1, Z_1, 0)$, the Jacobian is given by

$$J(E_{123}) = \begin{pmatrix} -X_1 & -X_1 & 0 & 0 \\ \beta_1 Y_1 & -d_1 Y_1 & -Y_1 & 0 \\ 0 & \beta_2 Z_1 & -d_2 Z_1 & 0 \\ 0 & 0 & 0 & -m + cp(\alpha)Z_1 \end{pmatrix},$$

where X_1 , Y_1 and Z_1 denote the three positive components in E_{123} . In Section 2, for the three dimensional model (3.8), we have proved the principle 3×3 sub-matrix of $J(E_{123})$ only has negative eigenvalues. Therefore E_{123} is asymptotically stable if and only if $-m + cp(\alpha)Z_1 < 0$, that is

$$p(\alpha) < \frac{m(\beta_1 d_2 + d_1 d_2 + \beta_2)}{c(\beta_1 \beta_2 + \beta_1 f_0 + \beta_2 k + d_1 f_0)}.$$

At $E_{134} = \left(1, 0, \frac{m}{cp(\alpha)}, \bar{w}\right)$, the Jacobian is given by

$$J(E_{134}) = \begin{pmatrix} -1 & -1 & 0 & 0 \\ 0 & k + \beta_1 - \frac{m}{cp(\alpha)} & 0 & 0 \\ 0 & \frac{\beta_2 m}{cp(\alpha)} & -\frac{d_2 m}{cp(\alpha)} & J_{34} \\ 0 & 0 & cp(\alpha)\bar{w} & 0 \end{pmatrix},$$

Since $J_{34} < 0$, E_{123} is asymptotically stable if and only if $k + \beta_1 - m/cp(\alpha) < 0$, that is $p(\alpha) < m/c(k + \beta_1)$.

At E_{234} , the Jacobian becomes

$$J(E_{234}) = \begin{pmatrix} 1 - \frac{cp(\alpha)k - m}{d_1 cp(\alpha)} & 0 & 0 & 0 \\ \frac{\beta_1 (cp(\alpha)k - m)}{d_1 cp(\alpha)} & -\frac{d_1 (cp(\alpha)k - m)}{d_1 cp(\alpha)} & -\frac{cp(\alpha)k - m}{d_1 cp(\alpha)} & 0 \\ 0 & \frac{\beta_2 m}{cp(\alpha)} & -\frac{d_2 m}{cp(\alpha)} & J_{34} \\ 0 & 0 & cp(\alpha)\hat{w} & 0 \end{pmatrix},$$

the lower 3×3 principle sub-matrix can be written as

$$A = \begin{pmatrix} -d_1 Y_2 & Y_2 & 0 \\ \beta_2 Z_2 & -d_2 Z_2 & J_{34} \\ 0 & cp(\alpha)\hat{w} & 0 \end{pmatrix},$$

where

$$Y_2 = \frac{cp(\alpha)k - m}{d_1 cp(\alpha)} \quad \text{and} \quad Z_2 = \frac{m}{cp(\alpha)}.$$

Then the characteristic polynomial of matrix A is

$$\lambda^3 + (d_1 Y_2 + d_2 Z_2)\lambda^2 + (-cp(\alpha)\hat{w}J_{34} + d_2 Z_2 d_1 Y_2 + \beta_2 Z_2 Y_2)\lambda - cp(\alpha)J_{34}d_1 \hat{w}Y_2 = 0,$$

where

$$\begin{cases} a_1 = d_1 Y_2 + d_2 Z_2 > 0, \\ a_2 = -cp(\alpha)\hat{w}J_{34} + d_2 Z_2 d_1 Y_2 + \beta_2 Z_2 Y_2 > 0, \\ a_3 = cp(\alpha) - J_{34}d_1 \hat{w}Y_2 > 0, \end{cases}$$

and

$$a_1 a_2 - a_3 = -cp(\alpha)J_{34}d_2 \hat{w}Z_2 + d_1^2 d_2 Y_2^2 Z_2 + d_1 d_2^2 Y_2 Z_2^2 + \beta_2 d_1 Y_2^2 Z_2 + \beta_2 d_2 Y_2 Z_2^2 > 0.$$

Therefore, by the Routh-Hurwitz criterion, the sub-matrix A only has negative eigenvalues. Thus, E_{234} is asymptotically stable if and only if

$$1 - \frac{cp(\alpha)k - m}{d_1cp(\alpha)} < 0.$$

3.3.3 Existence and stability of the positive equilibrium

By solving the system

$$\begin{cases} 1 - x - y = 0, \\ k - d_1y - z + \beta_1x = 0, \\ f(\alpha, w) - d_2z + \beta_2y - p(\alpha)w = 0, \\ -m + cp(\alpha)z = 0, \end{cases} \quad (3.20)$$

we can find the expression of the possible positive equilibrium solution $E^* = (x^*, y^*, z^*, w^*)$

where

$$\begin{cases} x^* = \frac{cp(\alpha)(d_1 - k) + m}{cp(\alpha)(\beta_1 + d_1)}, \\ y^* = \frac{cp(\alpha)(\beta_1 + k) - m}{cp(\alpha)(\beta_1 + d_1)}, \\ z^* = \frac{m}{cp(\alpha)}, \end{cases}$$

and w^* is given by the equation

$$f(\alpha, w^*) - d_2z^* + \beta_2y^* - p(\alpha)w^* = 0.$$

Therefore, there exists a unique positive equilibrium if and only if the following inequalities hold

$$\begin{cases} cp(\alpha)(d_1 - k) + m > 0 \\ cp(\alpha)(\beta_1 + k) - m > 0, \\ f_0 - \frac{d_2m}{cp(\alpha)} + \frac{cp(\alpha)\beta_2(\beta_1 + k) - \beta_2m}{cp(\alpha)(\beta_1 + d_1)} > 0, \end{cases} \quad (3.21)$$

The Jacobian of the positive equilibrium is given by

$$J(E^*) = \begin{pmatrix} -x^* & -x^* & 0 & 0 \\ \beta_1 y^* & -d_1 y^* & -y^* & 0 \\ 0 & \beta_2 z^* & -d_2 z^* & J_{34} \\ 0 & 0 & cp(\alpha)w^* & 0 \end{pmatrix},$$

The corresponding characteristic equation is

$$\lambda^4 + a_1 \lambda^3 + a_2 \lambda^2 + a_3 \lambda + a_4 = 0,$$

where

$$\begin{cases} a_1 = d_1 y^* + d_2 z^* + x^* > 0, \\ a_2 = -J_{34} cp(\alpha)w^* + d_1 d_2 y^* z^* + \beta_1 x^* y^* + \beta_2 y^* z^* + d_1 x^* y^* + d_2 x^* z^* > 0, \\ a_3 = -J_{34} cp(\alpha) d_1 w^* y^* - J_{34} cp(\alpha) w^* x^* + \beta_1 d_2 x^* y^* z^* + d_1 d_2 x^* y^* z^* + \beta_2 x^* y^* z^* > 0, \\ a_4 = -J_{34} \beta_1 cp(\alpha) w^* x^* y^* - J_{34} cp(\alpha) d_1 w^* x^* y^* > 0. \end{cases}$$

Calculation gives

$$\begin{aligned} & a_1 a_2 - a_3 \\ &= -J_{34} cp(\alpha) d_2 w^* z^* + d_1^2 d_2 (y^*)^2 z^* + d_1 d_2^2 y^* (z^*)^2 + \beta_1 d_1 x^* (y^*)^2 + \beta_2 d_1 (y^*)^2 z^* + \beta_2 d_2 y^* (z^*)^2 \\ &+ d_1^2 x^* (y^*)^2 + 2d_1 d_2 x^* y^* z^* + d_2^2 x^* (z^*)^2 + \beta_1 (x^*)^2 y^* + d_1 (x^*)^2 y^* + d_2 (x^*)^2 z^* > 0 \end{aligned}$$

and

$$\begin{aligned} & a_1 a_2 a_3 - a_1^2 a_4 - a_3^2 \\ &= d_2 x^* z^* (cp(\alpha)w^* J_{34} + \beta_1 x^* y^*)^2 + d_1 d_2 y^* z^* (\beta_1 x^* y^* + cp(\alpha)w^* J_{34})^2 + \text{positive terms} > 0. \end{aligned}$$

Therefore, by the Routh-Hurwitz criterion, the positive equilibrium is locally asymptotically stable.

For readers' convenience, we summarize the results obtained above about the existence and stability of all the equilibria in Table 3.2.

Table 3.2: Condition of existence and stability of the equilibria in model (3.14)

Equilibrium solution	Existence	Stability
E_0	Always	Unstable
E_1	Always	Unstable
E_2	Always	$1 - k/d_1 < 0$ and $f_0 < -\beta_2 k/d_1$
E_3	$f_0 > 0$	Unstable
E_{12}	$k < d_1$	$f_0 < \frac{\beta_2 k + \beta_2 \beta_1}{d_1 + \beta_1}$
E_{13}	$f_0 > 0$	$\frac{md_2}{cp(\alpha)} > f_0 > d_2(k + \beta_1)$
E_{23}	$d_2 k > f_0 > -\beta_2 k/d_1$	$f_0 > d_2 k - d_1 d_2 - \beta_2$ and $p(\alpha) < \frac{m(d_1 d_2 + \beta_2)}{c(k\beta_2 + d_1 f_0)}$
E_{34}	$f_0 > d_2 m/cp(\alpha)$	Unstable
E_{123}	$d_2(k + \beta_1) > f_0 > \max\left(d_2 k - d_1 d_2 - \beta_2, -\frac{\beta_2(k + \beta_1)}{d_1 + \beta_1}\right)$	$p(\alpha) < \frac{m(\beta_1 d_2 + d_1 d_2 + \beta_2)}{c(\beta_1 \beta_2 + \beta_1 f_0 + \beta_2 k + d_1 f_0)}$
E_{134}	$f_0 > d_2 m/cp(\alpha)$	$p(\alpha) < \frac{m}{c(k + \beta_1)}$
E_{234}	$cp(\alpha)k - m > 0$ and $f_0 > \frac{d_2 m}{cp(\alpha)} - \frac{\beta_2 cp(\alpha)k - \beta_2 m}{d_1 cp(\alpha)}$	$1 - \frac{cp(\alpha)k - m}{d_1 cp(\alpha)} < 0$
E^*	Condition (3.21)	Stable

As was done to rescaled model (3.5) in Section 2, we can also examine the relationship how the population size for each species at the stable positive equilibrium depends on the anti-predation level α . Indeed, we can calculate to obtain

$$\frac{dz^*}{d\alpha} = \frac{-m}{cp^2(\alpha)} \frac{dp}{d\alpha} > 0.$$

By using implicit differentiation on the system (3.20), we can also determine $\frac{dx^*}{d\alpha} > 0$ and $\frac{dy^*}{d\alpha} < 0$. However, we are not able to determine the sign of $\frac{dw^*}{d\alpha}$.

From the above discussion, we see that after incorporating the benefit obtained by the meso-predator's anti-predation response in reducing the predation by the large carnivores, the final population sizes of the meso-predator, its prey and its prey's prey are increasing, decreasing, and increasing respectively with respect to the response strength α . This alternating pattern is totally opposite to the one obtained in Section 2 on this context.

3.3.4 Numerical simulations

In this part, we present some numerical simulations to illustrate the analytical results obtained above. To this end, we choose

$$B(\alpha, N_4) = \frac{R_3}{1 + c_1 \alpha N_4} \quad \text{and} \quad a_{34}(\alpha) = \frac{1}{1 + c_2 \alpha}$$

in (3.5), leading to the following system

$$\begin{cases} \frac{dN_1}{d\tau} = N_1 (R_1 - a_{11}N_1 - a_{12}N_2), \\ \frac{dN_2}{d\tau} = N_2 (R_2 - a_{22}N_2 - a_{23}N_3 + a_{21}N_1), \\ \frac{dN_3}{d\tau} = N_3 \left(\frac{R_3}{1 + c_1 \alpha N_4} - D_3 - a_{33}N_3 + a_{32}N_2 - \frac{N_4}{1 + c_2 \alpha} \right), \\ \frac{dN_4}{d\tau} = N_4 \left(-D_4 + \frac{cN_3}{1 + c_2 \alpha} \right), \\ N_1(0) \geq 0, \quad N_2(0) \geq 0, \quad N_3(0) \geq 0, \quad N_4(0) \geq 0, \end{cases} \quad (3.22)$$

We fix the parameters

$$\begin{aligned} R_1 = 3, \quad a_{11} = 1, \quad a_{12} = 0.4, \quad R_2 = 1, \quad a_{22} = 0.2, \quad a_{23} = 0.5, \quad a_{21} = 0.5, \\ R_3 = 3, \quad D_3 = 1, \quad a_{33} = 0.5, \quad a_{32} = 0.05, \quad c_1 = 0.4, \quad D_4 = 0.1, \quad c = 0.5, \quad c_2 = 0.2, \end{aligned} \quad (3.23)$$

and illustrate how α impacts the population dynamics.

For the above set of parameter values, $k = 1/3 < d_1 = 1/2$, the bifurcation diagram with respect to α is given in Figure 3.5. There is a transcritical bifurcation between E^* and E_{123} where the critical value α^* is given by

$$f_0 - \frac{d_2 m}{c p(\alpha^*)} + \frac{c p(\alpha^*) \beta_2 (\beta_1 + k) - \beta_2 m}{c p(\alpha^*) (\beta_1 + d_1)} = 0.$$

Using the parameter values in (3.23), we can solve this equation to obtain $\alpha^* \approx 97.77777780$. We can observe a trophic cascade in Figure 3.5 inside the coexistence region with respect to increment of α . Contrary to the previous section, this cascade shows an increasing population in odd level and decreasing population in even level.

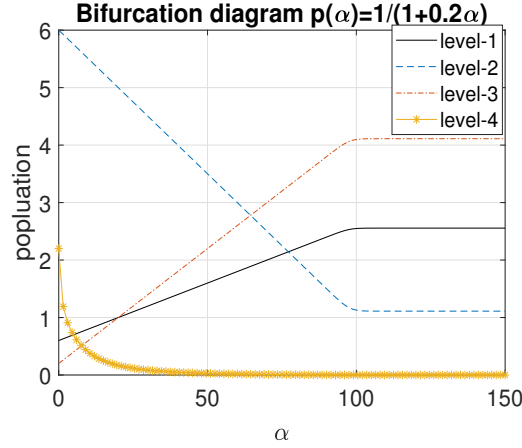


Figure 3.5: Bifurcation diagram of (3.22) when $k < d_1$.

Next, we change R_1 from $R_1 = 3$ to $R_1 = 1$ in (3.23) and keep the same values for other parameters. We then have $k = R_2/R_1 = 1$ and $d_1 = a_{22}/a_{12} = 1/2$ so that $k > d_1$. For this case, we observe more complicated dynamical behaviours: there are three critical values for α , denoted by $\bar{\alpha}_1$, $\bar{\alpha}_2$ and $\bar{\alpha}_3$, which are given by

$$\begin{cases} cp(\bar{\alpha}_1)(d_1 - k) + m = 0 \\ cp(\bar{\alpha}_2)(\beta_1 + k) - m = 0, \\ \frac{md_2}{cp(\bar{\alpha}_3)} = f_0. \end{cases}$$

Using the parameter values in (3.23), we obtain $\bar{\alpha}_1 = 20$, $\bar{\alpha}_2 = 70$ and $\bar{\alpha}_3 = 95$. In figure 3.6, when $0 < \alpha < \bar{\alpha}_1$, E_{234} is stable; when $\bar{\alpha}_1 < \alpha < \bar{\alpha}_2$, E^* is stable; when $\bar{\alpha}_2 < \alpha < \bar{\alpha}_3$, E_{134} is stable; when $\bar{\alpha}_3 < \alpha$, E_{13} is stable. We can also observe trophic cascade in this case as is shown in Figure 3.6.

In the last two cases, we can see that population size of large carnivores at the positive equilibrium is monotonically decreasing. We point out that this is dependent on the choice of the benefit reflecting term $p(\alpha) = a_{34}(\alpha)/a_0$. To see this, we change c_2 from 0.2 to 2 (corresponding to a more significant benefit to N_3 and disadvantage to N_4), then, as is shown in Figure 3.7-(a), we can see a transcritical bifurcation from E^* to E_{123} at threshold value $\tilde{\alpha} = 10.43750000$, and before this value, $w^*(\alpha)$ is not monotone: it increases first and then decreases. Figure 3.7-(b) is an enlargement of (a) in which, one can more clearly see that

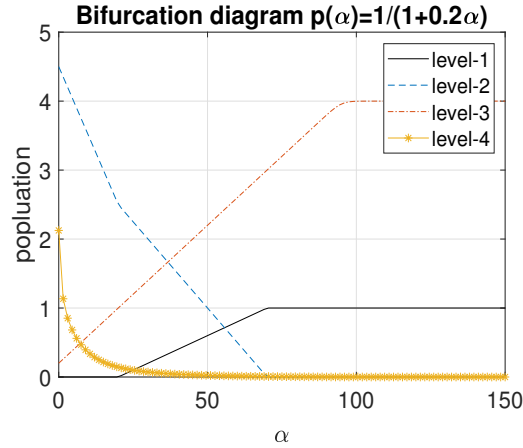


Figure 3.6: Bifurcation diagram of (3.22) when $k > d_1$.

while the lower trophic still follow the cascade, the top predator (w^*) increases first and then decreases with respect to the increment of α . Thus, the response function $p(\alpha)$ has an impact of the trophic cascade.

3.4 Conclusion and discussions

A recent experimental study [26] in fields observed a phenomenon of trophic cascade in a food chain population system consisting of three species, i.e., meso-carnivore on top, its prey in the middle and the prey's prey in the bottom, caused by the fear of virtual large carnivores which is implemented by playback of the large carnivores. This phenomenon, together with some recent works on fear effect in two species predator-prey models, has motivated us to theoretically explore the mechanisms for such trophic cascade in this chapter. To this end, we have proposed two models, (3.3) and (3.5), with (3.3) directly corresponding to the scenario of field study in [26], and (3.5) being an extension to include a benefit in the meso-carnivore from the anti-predation response, in addition to a cost, as in (3.3). In order to incorporate the benefit term into the model, we have to add the population of the large carnivores into the interplay, making (3.5) a 4-D system.

We have thoroughly analyzed the two models, using the approach of dynamical systems. For each of the two models, we have obtained complete structure of the equilibria, and established their stability/instability in terms of the model parameters, in the form of thresholds for

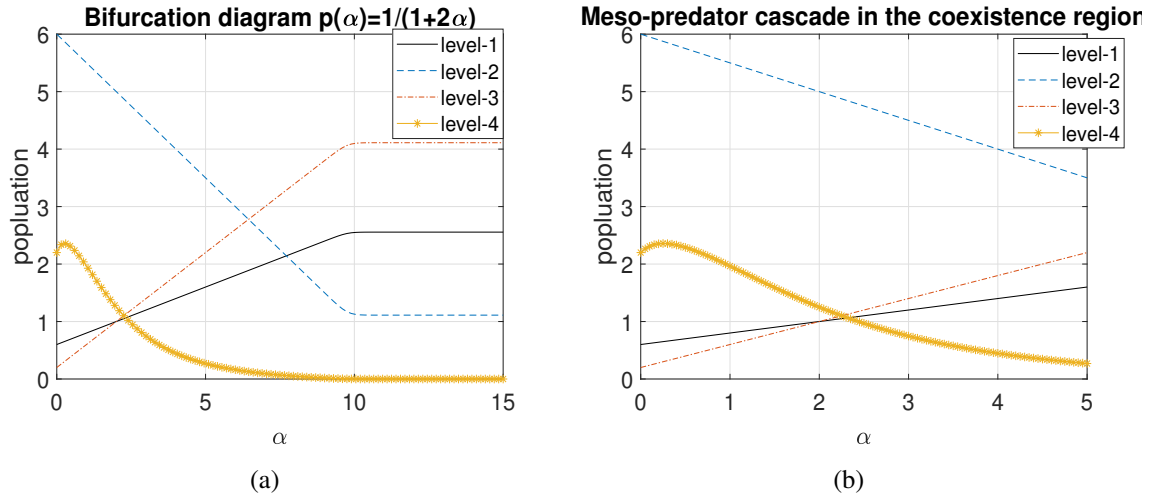


Figure 3.7: (a) Bifurcation diagram of (3.22) when $c_2 = 2$, (b) In the region when the coexistence equilibrium E^* is stable, we can observe a meso-predator cascade with non-monotonically change on top predator.

certain parameters. For model (3.3) our results show that an anti-predation response *at lower level* is *beneficial* to the top and bottom species (N_3 and N_1); while *at higher level*, it is *beneficial* to the middle species (N_2) but *disadvantageous* to N_3 and N_1 , confirming the phenomenon of trophic cascade reported in that experimental study. For model (3.5), our results show that there are now three threshold values for the response level α , distinguishing ranges for α accounting for various combinations of co-existence among the four species. Particularly, within certain range of parameters, the model also demonstrates the phenomenon of trophic cascade but with an opposite alternating pattern for the three species (the meso-carnivore, its prey and its prey's prey): increasing the response level α is *beneficial* to N_3 and N_1 but *disadvantageous* to N_2 . This change is attributed to the effect of the benefit of the anti-predation response in reducing the predation and its balance with cost of such a response.

Our results can have ecological implications as they may suggest practical strategies of management/control for maintaining biodiversity. For example, in some ecosystems, populations of some meso-predators have been observed to increase significantly due to the loss/extinction of larger carnivores, and this has in turn put some pressure on the meso-predators' preys for their survivals. Our results on model (3.3) suggest that by creating certain virtual situations (e.g, vocal) mimicking the large carnivore predators, one may expect to reduce the populations of the meso-predators, and consequently relax the pressure on the meso-predators' preys. On

the other hand, if the large (top) predators of the meso-predators are present, their predation on the meso-predators poses a major threat to the meso-predators. In such a case, by our results on model (3.5), creating the aforementioned virtual situations may stimulate the meso-predators to increase their anti-predation response level, which will then reduce the predation risk by the top predators. This way, the *benefit* of anti-predation response of the meso-predators in reducing the predation risk may outplay the *cost* in production, and thus, enhance the survival probability of the meso-predators. Such a net benefit in the meso-predators can then be passed on to the lower level species in an alternating fashion. Therefore, the risk events such as fear effect in some species in an ecosystem may actually offer a management tool in shifting the structure of ecosystem and help conserve the biodiversity.

Note that in our model, we have used the mass action or Holling Type I functional responses as the predation mechanism. For some species between which the predation involves foraging, this mechanism is not suitable and other types of functional responses should be adopted. It would be interesting and worthwhile to investigate the population dynamics in models like (3.3) and (3.8) with such replaced functional responses. We also point out that in our models, we have only considered fear effect of meso-carnivore species N_3 against the large carnivores N_4 . Such fear effect may also exist in N_2 against N_3 and in N_1 against N_2 . Modeling fear effect in those or in all levels would also be interesting but would be very challenging mathematically.

We remark that for predator-prey interactions between *two species only*, the recent works mentioned in the introduction may also suggest some possible extensions and expansions of the two models in this chapter. For example, one may also incorporate age structure, spatial structure, digestion delay, extra food, stochastic noise, as was done in [8, 18, 32, 33, 34]. Efforts on all these lines will greatly enhance our understanding of predator-prey interactions, and enrich the theory in this area.

Bibliography

- [1] Boonstra, R. et al., *The impact of predator-induced stress on the snowshoe hare cycle*. Ecol. Monogr. **68**(1998) , 371–394.
- [2] Castillo-Chavez, C., Thieme, H. R., *Asymptotically autonomous epidemic models*, In: O. Arino et al: *Mathematical Population Dynamics: Analysis of Heterogeneity, I. Theory of Epidemics* (pp. 33-50). Wuerz, Canada, 1995
- [3] Clinchy, M., L. Zanette, R. Boonstra, J. C. Wingfield, and J. N. M. Smith, *Balancing food and predator pressure induces chronic stress in songbirds*. Proceedings: Biological Sciences **271**(2004), 2473–2479.
- [4] Creel, S., J. Winnie, B. Maxwell, K. L. Hamlin, and M. Creel.,*Elk alter habitat selection as an antipredator response to wolves*. Ecology **86**(2005), 3387–3397.
- [5] Creel, S., D. Christianson, S. Liley, and J. A. Winnie, *Predation risk affects reproductive physiology and demography of elk*. Science **315**(2007), 960.
- [6] Creel, S., Christianson, D., *Relationships between direct predation and risk effects*, Trends Ecol Evolut **23**(2008), 194-201.
- [7] Cresswell, W., *Predation in bird populations*, J Ornithol **152**(2011), 251-263.
- [8] Das, A, Samanta G. P., *Modeling the fear effect on a stochastic prey-predator system with additional food for the predator*, J. Phys. A: Math. Theor. **51** (2018) 465601 (26pp).
- [9] Freedman, H., Waltman, P., *Persistence in models of three interacting predator-prey populations*, Math. Biosci. **68** (1984), 213–231.

- [10] Gauze, G. F., *The Struggle for Existence*, The Williams and Wilkins company, 1934.
- [11] Hastings, A., Powell, T., *Chaos in a three-species food chain*, Ecology, **72**(3) (1991), 896-903.
- [12] Hsu, S., Ruan, S., Yang, T., *Analysis of three species Lotka-Volterra food web models with omnivory*, J. Math. Anal. Appl. **426** (2015), 659–687.
- [13] Krikorian, N., *The Volterra model for three species predator–prey systems: boundedness and stability*, J. Math. Biol. **7** (2) (1979), 117–132.
- [14] Lima, S. L., *Nonlethal effects in the ecology of predator-prey interactions*, Bioscience **48**(1998), 25-34.
- [15] Lima, S. L., *Predators and the breeding bird: behavioural and reproductive flexibility under the risk of predation*, Biol Rev **84**(2009), 85-513.
- [16] Lotka, A. J., *Analytical Note on Certain Rhythmic Relations in Organic Systems*, Proc. Natl. Acad. Sci. U.S.A. **6**(1920), 410-415 .
- [17] Lotka, A. J., *Elements of Physical Biology*, Williams and Wilkins (1925).
- [18] Mondal, S., Maiti, A. Samanta, G. P., *Effects of Fear and Additional Food in a Delayed Predator-Prey Model*, Biophysical Reviews and Letters, **13** (2018), 157-177.
- [19] Panday, P., Pal, N., Samanta, S., Chattopadhyay, J., *Stability and bifurcation analysis of a three-species food chain model with fear*, Int. J. Bifurc. Chaos **28** (2018), 1850009.
- [20] Panday, P., Pal, N., Samanta, S., Chattopadhyay, J., *A Three Species Food Chain Model with Fear Induced Trophic Cascade*, Int. J. Appl. Comput. Math **5** (2019), 100.
- [21] Peckarsky, B.L. et al., *Sublethal consequences of streamdwelling predatory stoneflies on mayfly growth and fecundity*. Ecology **74**(1993), 1836–1846.
- [22] Perko, L., *Differential equations and dynamical systems*, Springer, New York(1996)
- [23] Schmitz, O. J., A. P. Beckerman, and K. M. O’Brien. *Behaviorally mediated trophic cascades: effects of predation risk on food web interactions*. Ecology **78**(1997), 1388–1399.

- [24] Schmitz, O. J., V. Krivan, and O. Ovadia. *Trophic cascades: the primacy of trait-mediated indirect interactions*. Ecology Letters, **7**(2004), 153–163.
- [25] Smith, H., *Monotone Dynamical Systems: An Introduction to the Theory of Competitive and Cooperative Systems*, Amer. Math. Soc. Math. Surveys and Monographs **Vol. 41**, 1995.
- [26] Suraci, J. P., Clinchy, M., Dill, L. M., Roberts, D., Zanette, L. Y., *Fear of large carnivores causes a trophic cascade*, Nat Commun. **7**(2016), 10698.
- [27] Tollrian, R. and Harvell, C.D., *The evolution of inducible defenses: current ideas*. In The Ecology and Evolution of Inducible Defenses (Tollrian, R. and Harvell, C.D., eds), Princeton University Press, (1999), 306–321.
- [28] Valeix, M., A. J. Loveridge, S. Chamaille-Jammes, Z. Davidson, F. Murindagomo, H. Fritz, and D. W. Macdonald, *Behavioral adjustments of African herbivores to predation risk by lions: spatiotemporal variations influence habitat use*. Ecology **90**(2009), 23–30.
- [29] Volterra, V., *Variazioni e fluttuazioni del numero d'individui in specie animali conviventi*, Mem. Acad. Lincei Roma. **2**(1926), 31-113.
- [30] Volterra, V., *Variations and fluctuations of the number of individuals in animal species living together*, In Chapman, R. N. Animal Ecology. McGraw-Hill, 1931.
- [31] Wang, X., Zanette, L. Y., Zou, X., *Modelling the fear effect in predator-prey interactions*, J Math Biol. **73**(2016), 1179-1204.
- [32] Wang, X., Zou, X., *Modeling the Fear Effect in Predator-Prey Interactions with Adaptive Avoidance of Predators*, Bull Math Biol **79**(2017), 1325-1359.
- [33] Wang, X., Zou, X., *Pattern formation of a predator-prey model with the cost of anti-predator behaviours*, Mathematical Biosciences and Engineering, **15**(2018), 775-805.
- [34] Wang, Y., Zou, X., *On a predator prey system with digestion delay and anti-predation strategy*, J. Nonlinear Sciences, **30**(2020), 1579-1605
- [35] Zanette, L., *Synergistic effects of food and predators on annual reproductive success in song sparrows*. Proceedings: Biological Sciences **270**(2003), 799-803.

- [36] Zanette, L. Y., White, A. F., Allen, M. C., Clinchy, M., *Perceived predation risk reduces the number of offspring songbirds produce per year*, *Science* **334** (6061)(2011), 1398-1401.

Chapter 4

Evolution of anti-predation response of prey in predator-prey interactions

4.1 Introduction

Predator-prey interaction is one of the most classic topics in ecology and evolutionary biology. However, more and more field experiments and observations have been reported in recent years, which provides evidences showing that the indirect effects due to a prey's fear of predator can be as important as that of direct predation [5, 6, 14, 19, 21, 27, 28]. Because of these reported results, indirect effects between predator and prey have received increasing attention. Particularly, mathematical modelling has been recognized as a useful tool for understanding the role that indirect effect can play in predator-prey interactions. In this regard, Wang et. al. [22] proposed an ODE model to incorporate indirect effect (fear effect) in the prey's production in a classic Lotka-Volterra model:

$$\begin{cases} \frac{du}{dt} = f(\alpha, v(t)) r_0 u(t) - d u(t) - a u^2(t) - p(u(t)) v(t), \\ \frac{dv}{dt} = c p(u(t)) v(t) - m v(t). \end{cases} \quad (4.1)$$

Here $u(t)$ is the population of the prey species, $v(t)$ is the population of the predator species, r_0 is the intrinsic growth rate of the prey, d is the natural (density independent) mortality rate of the prey and $a u(t)$ denotes the density dependent death rate from intra-species' competition,

c is the transfer rate of the biomass between predator and prey. The function $g(u)$ is the functional response governing the encounters of the predator and the prey. The function $f(\alpha, v)$ is incorporated into the model to account for the prey's anti-predation response with the positive parameter α measuring the level of the prey's anti-predation response, once the prey have perceived the risk from the predator. Therefore, it is natural to assume that $f(\alpha, v)$ is decreasing with respect to both α and v . By analyzing this model, Wang et al [22] revealed some new insights into the predator-prey interaction, compared to the classic models. Especially, the model predicted some similar results observed in the field experimental study [28] which claimed that, without the real predation, the fear effect itself can reduce the prey's reproduction by as much as 40%.

We noticed that in (4.1), the authors only considered the costs of anti-predation response which leads to a decrement in prey's reproduction. But in most cases, if not all, an anti-predation response of the prey will lead to higher level of vigilance which will make predation more difficult. In other words, in addition to the costs in the production, an anti-predation response should also have some benefits for the prey, for example, help avoiding the predation and hence, reducing the predation rate. This suggests a modification to the predation term $p(u)v$ by incorporating a dependence on the anti-predation level α in a decreasing way, that is, replacing $p(u)v$ by $p(\alpha, u)v$ with $p(\alpha, u)$ being decreasing in α .

Since Wang et. al. [22], there have occurred more models investigating various aspects of anti-predation strategy by considering either costs, or benefits or both. These studies covered a wild range of topics including the integrating effect of anti-predation strategy and time delay [23, 25], the spatial problems on fear effect [24], food chain models with anti-predation strategy [17, 18, 26], among others. These researches have compared the predator-prey systems with and without indirect effects and as a result, showed indirect effects play an important role in predator-prey interaction and can not be ignored. However, all of above studies mostly focus on ecological aspects of anti-predation strategy.

Besides these ecological findings, there is also a natural evolutionary question: how an anti-predation strategy evolves? This chapter intends to address this question. We will use the method of adaptive dynamics to study the evolutionary stability of anti-predation strategy.

To this end, we use (4.1) as the starting point but incorporate a benefit of the anti-predation response for the resident prey to obtain a basic ODE system for the interactions of a resident prey and the predator

$$\begin{cases} \frac{du_r}{dt} = f(\alpha_r, v(t)) r_0 u_r(t) - d u(t) - a u_r^2(t) - g(\alpha_r) \beta u_r(t) v(t), \\ \frac{dv}{dt} = c g(\alpha_r) \beta u_r(t) v(t) + b(v(t)). \end{cases} \quad (4.2)$$

where we have added an subscript r to the unknown $u(t)$ and parameter α to indicate that $u_r(t)$ is the population of the *resident* prey playing an anti-predation strategy α_r . Here, for simplicity, we adopt the Holling Type I functional response $p(\alpha, u) = g(\alpha)\beta u$ where β denotes the natural encounter rate between predator and prey without anti-predation response; however, in the equation for the predator growth, we use a general growth function $b(v)$ to allow the model to accommodate both specialist predator (e.g., when $b(v) = -mv$) and generalist predator (e.g., when $b(v) = rv(1 - v/K)$). By their meanings of costs and benefits, the functions $f(\alpha, v)$ and $g(\alpha)$ are assumed to satisfy the following conditions:

$$\left\{ \begin{array}{l} f \text{ and } g \text{ are continuous differentiable,} \\ f(0, v) = 1, f(\alpha, 0) = 1, \frac{\partial f}{\partial \alpha} < 0, \frac{\partial f}{\partial v} < 0, \\ \lim_{\alpha \rightarrow \infty} f(\alpha, v) = 0, \lim_{v \rightarrow \infty} f(\alpha, v) = 0; \\ g(0) = 1, \frac{dg}{d\alpha} < 0, \\ \lim_{\alpha \rightarrow \infty} g(k) = 0. \end{array} \right. \quad (4.3)$$

Now, assume there is a mutant prey with its population denoted by $u_m(t)$ and a different anti-predation response level α_m . Then, combining the competition between the two prey strains and predations of the predator on the two prey strains, (4.2) is naturally expanded to the following

three dimensional ODE system

$$\begin{cases} \frac{du_r}{dt} = f(\alpha_r, v(t)) r_0 u_r(t) - d u_r(t) - a u_r(t) (u_r(t) + u_m(t)) - g(\alpha_r) \beta u_r(t) v(t), \\ \frac{du_m}{dt} = f(\alpha_m, v(t)) r_0 u_m(t) - d u_m(t) - a u_m(t) (u_r(t) + u_m(t)) - g(\alpha_m) \beta u_m(t) v(t), \\ \frac{dv}{dt} = c g(\alpha_r) \beta u_r(t) v(t) + c g(\alpha_m) \beta u_m(t) v(t) + b(v(t)), \end{cases} \quad (4.4)$$

With this model, we will use method of adaptive dynamics to answer how the anti-predation strategy evolves. We first explore the dynamics of (4.2) by which we obtain conditions to confirm a positive steady state for the resident prey and the predator. Then we assume a mutant strain of prey species merges with small population, and perform an invasion analysis to find out whether the mutant can successfully invade the resident. In the case of successful invasion, we are also interested in the population dynamics for both prey strains, by investigating whether the mutants will replace the residents and become new residents such that the environment reach to a new steady state, or the mutant prey can coexist with the resident prey. A central notion in evolutionary game theory, called *evolutionarily stable strategy (ESS)* (see, e.g., Maynard Smith and Price[16]) will be examined. A strategy is called evolutionarily stable if a resident species playing this strategy can not be invaded by small amount of mutants with any other strategy. A related concept is *convergence stable strategies*. Roughly speaking, a convergence stable strategies is such a singular strategy that when two species (strains) are playing different strategies, whichever playing a strategy closer to the convergence stable strategies will outcompete the other. A strategy which is both evolutionarily stable and convergence stable is recognized as a *continuously stable strategy (CSS)*. To get rid of the confusion between CSS and convergence stable strategy (which also has the abbreviation CSS in some literature [13]), we follow the notation in [10] and use *evolutionary attracting strategy (EAS)* to denote convergence stable strategy. The theoretical way to find an ESS is to compute the invasion exponent and the corresponding selection gradient. An alternative graphic way to find the evolutionary stable of a singular strategy is called pairwise invasibility plot which is visual and convenient in demonstrating results. In this chapter, we will use the abbreviation "PIP" to denote pairwise invasibility plot.

There are also other studies on evolution related problems in predator-prey interactions. For

example, the evolution of predator strategy in capture rate are studied [1, 2, 4], where possible cyclic behaviour of population and optimal capture rate are explored. The evolution of prey strategy(anti-predation strategy) is also studied in [2, 3, 12]. A recent work [29] define the evolutionary stability for one type of predator-prey model and also discuss the possible occurrence of evolutionary branching. Last but not the least, [8, 9, 11, 15] consider co-evolution between predator and prey species. In this chapter, motivated by [22] for the anti-predation strategy, we study the evolution of prey's anti-predation strategy as an response to the fear of predator. Comparing to the references mentioned above, there are two main differences between our study and previous studies. First, we consider *both specialist and generalist predators*, while the previous studies focus on specialist predators. Secondly, the cost for the prey is *density dependent* whereas in the previous studies, and the costs (benefits) are purely strategy driven.

The remainder of this chapter is organized as follows. In Section 2, we set up our starting point of invasion analysis, including address the well-posedness of the model (4.5) and apply stability analysis to find the feasible region of the anti-predation strategy such that a globally asymptotically stable coexistence equilibrium occurs. In Section 3, we start from the steady state in Section 2. Assuming there is a rare mutant prey with different anti-predation strategy, we apply invasion analysis to show the conditions of whether it can successfully invade or not. We first use this analysis tool on general model (4.4). Then we use two examples with specialist predator and generalist predator respectively. We compare the results of these model theoretically and numerically and point out the main difference in the results of different types of predator. In Section 4, we summarize the results obtained from previous sections and discuss their biological implications. We also suggest some possible directions for future study on evolutionary stability of anti-predation strategies.

4.2 Preliminaries

We begin with analyzing the basic model (4.2). To simplify notations, we temporarily drop the subscript r in (4.2) to consider

$$\begin{cases} \frac{du}{dt} = f(\alpha, v(t)) r_0 u(t) - d u(t) - a u^2(t) - g(\alpha) \beta u(t) v(t), \\ \frac{dv}{dt} = c g(\alpha) \beta u(t) v(t) + b(v(t)). \end{cases} \quad (4.5)$$

The functions $f(\alpha, v)$, $g(\alpha)$, $b(v)$, as well as all parameters in (4.5) are explained after(4.2).

4.2.1 Well-posedness of (4.5)

By the fundamental theory of ODEs, we know that the for any given initial values (u_0, v_0) for u and v , the initial value problem associate with (4.5) has a unique solution. Moreover, if u_0 and v_0 are non-negative (positive), the solution $(u(t), v(t))$ remains nonnegative (positive) for all $t \geq 0$.

If $r_0 < d$, one can easily show that the prey species goes extinct even without the predator. Therefore, we only need to consider the case of $r_0 > d$ which is assumed in the rest of the chapter.

Next, we show the solution is bounded. In the first equation of system (4.5),by the non-negativity of $v(t)$ and the assumption (4.3), we have

$$\frac{du}{dt} \leq u(r_0 - d - au).$$

By the comparison theorem, we can obtain $\lim_{t \rightarrow \infty} \sup u(t) \leq \frac{r_0 - d}{a}$.

For the boundedness of $v(t)$, we distinguish the two cases for $b(v)$ representing specialist and generalist predator scenarios respectively. When $b(v(t)) = -m v(t)$, we consider $P = cu + v$. Then we have

$$\frac{dP}{dt} = cu(r_0 f(\alpha, v) - d - au) - mv.$$

For any $\mu \in (0, m)$, the equation can be rewritten as

$$\frac{dP}{dt} + \mu P = cu(r_0 f(\alpha, v) - d + \mu - au) - (m - \mu)v.$$

By non-negativity of $v(t)$ and the assumption (4.3), we have

$$\frac{dP}{dt} + \mu P \leq cu(r_0 - d + \mu - au) \leq \frac{c(r_0 - d + \mu)^2}{4a}.$$

By the comparison theorem, we have

$$P \leq P_0 e^{-\mu t} + (1 - e^{-\mu t}) \frac{c(r_0 - d + \mu)^2}{4a\mu},$$

which implies

$$\limsup_{t \rightarrow \infty} P(t) \leq \frac{c(r_0 - d + \mu)^2}{4a\mu}.$$

The boundedness of $P(t)$ and $u(t)$ together implies that $v(t)$ is also bounded.

If $b(v(t)) = r v(t) \left(1 - \frac{v(t)}{K}\right)$, then

$$\frac{dv}{dt} \leq \frac{c g(\alpha) \beta (r_0 - d)}{a} v(t) + r v(t) \left(1 - \frac{v(t)}{K}\right),$$

which implies

$$\limsup_{t \rightarrow \infty} v(t) \leq \frac{(c g(\alpha) \beta (r_0 - d) + a r) K}{a r}.$$

So we can also conclude the system is bounded.

The existence, uniqueness, non-negativity and boundedness of solutions to (4.5) with non-negative initial values obtained above established the well-posedness of basic model (4.5).

4.2.2 Dynamics of (4.5)

Now we discuss all possible equilibria of system (4.5) and investigate their stability.

Case I for specialist predator: $b(v(t)) = -m v(t)$. In this case, there are in total three possible equilibrium solutions: the trivial solution $E_0 = (0, 0)$, the predator free equilibrium

$E_1 = \left(\frac{r_0-d}{a}, 0\right)$ and the coexistence equilibrium $E^* = (u^*, v^*)$ given by

$$\begin{cases} r_0 f(\alpha, v^*) - d - au^* - g(\alpha)\beta v^* = 0, \\ c g(\alpha)\beta u^* - m = 0. \end{cases} \quad (4.6)$$

The trivial equilibrium always exists; the predator free equilibrium exists when $r_0 > d$; and the coexistence equilibrium exists *if and only if*

$$r_0 - d - \frac{am}{c g(\alpha)\beta} > 0. \quad (4.7)$$

To determine the stability of the equilibria, we compute the Jacobian matrix of (4.5), which is

$$J(u, v) = \begin{pmatrix} r_0 f(\alpha, v) - d - 2au - g(\alpha)\beta v & r_0 u \frac{\partial f(\alpha, v)}{\partial v} - g(\alpha)\beta u \\ c g(\alpha)\beta v & c g(\alpha)\beta u - m \end{pmatrix}. \quad (4.8)$$

By substituting the respective the equilibrium into (4.8) and analyzing the eigenvalues of the resulting matrices, we obtain the following conclusions:

- (i) when $r_0 < d$, the trivial solution E_0 is the only equilibrium and it is locally asymptotically stable;
- (ii) when $r_0 > d$, the trivial equilibrium loses its stability and the predator free equilibrium and E_1 comes into existence; moreover
 - (ii-1) if $r_0 < d + \frac{am}{c g(\alpha)\beta}$ (i.e., (4.7) is reversed), E_1 is locally asymptotically stable;
 - (ii-2) if $r_0 > d + \frac{am}{c g(\alpha)\beta}$ (i.e., (4.7) holds), E_1 becomes unstable and E^* comes into existence and is locally asymptotically stable;

The above results are directly obtained from the conditions for the corresponding Jacobian matrices to be stable or unstable. We can also present the results in (ii)-(iii) above in terms of the anti-predator strategy parameter α . Note that under (4.3), $d + am/c g(\alpha)\beta$ increases from $d + am/c\beta$ to ∞ . Thus, if

$$d + \frac{am}{c\beta} < r_0 \quad (4.9)$$

then there exists a unique $\hat{\alpha} > 0$ such that

$$d + \frac{am}{cg(\alpha)\beta} = \begin{cases} < r_0, & \text{for } \alpha \in (0, \hat{\alpha}); \\ = r_0, & \text{for } \alpha = \hat{\alpha}; \\ > r_0, & \text{for } \alpha \in (\hat{\alpha}, \infty). \end{cases}$$

Therefore, assuming (4.9), there is an equilibrium bifurcation at $\hat{\alpha}$ for the parameter α in the following sense:

- (ii-1)* if $\alpha > \hat{\alpha}$, then the predator free equilibrium $\left(\frac{r_0-d}{a}, 0\right)$ is locally asymptotically stable;
- (ii-2)* if $\alpha < \hat{\alpha}$, then the predator free equilibrium $\left(\frac{r_0-d}{a}, 0\right)$ becomes unstable and there occurs the coexistence equilibrium (u^*, v^*) which is locally asymptotically stable.

Rewrite (4.7) and (4.9) as $cg(\alpha)\beta\frac{r_0-d}{a} > m$ and $c\beta\frac{r_0-d}{a} > m$ respectively. The left hand sides of these two inequalities measure the predating capability of the predator when the prey plays anti-predator strategy α or plays no anti-predator strategy. Thus, the results in (ii-1) and (ii-2) means that if the predator is not capable enough such that $c\beta\frac{r_0-d}{a} < m$, the prey does not need to play an anti-predator strategy and it can maintain its population to the level $(r_0 - d)/a$; but if the predator is a sufficient capable such that $c\beta\frac{r_0-d}{a} > m$, then the prey's anti-predator strategy will make difference: sufficient large response level $\alpha > \hat{\alpha}$ can still help the prey to maintain its population at the level $(r_0 - d)/a$; while insufficient response level can only maintain its population at a lower level $u^*(\alpha) < (r_0 - d)/a$. Note that $u^*(\alpha)$ is increasing in α , and $u^* = u^*(\alpha) \rightarrow (r_0 - d)/a$ as $\alpha \rightarrow \hat{\alpha}$.

For this case of specialist predator, consumption of prey is the sole source for the predator's growth. With this in mind, we relate conditions (4.7) in (ii-1)-(ii-2) the basic reproduction number of the predator:

$$R_{v_0}(\alpha) = \frac{cg(\alpha)\beta}{m} \cdot \frac{(r_0 - d)}{a}.$$

The condition in (ii-1) corresponds to $R_{v_0}(\alpha) < 1$, whereas the condition in (ii-2) corresponds to $R_{v_0}(\alpha) > 1$. Note that $R_{v_0}(\alpha)$ is decreasing in α .

Case II for generalist predator: $b(v(t)) = rv(t)(1 - v(t)/K)$. For this case, there are *four* possible equilibrium solutions and they are: the trivial solution $E_0 = (0, 0)$; the predator

free equilibrium $E_1 = \left(\frac{r_0-d}{a}, 0\right)$ (if $r_0 > d$); the predator only equilibrium $E_2 = (0, K)$ (since this is a generalist predator scenario); and the coexistence equilibrium $E^* = (u^*, v^*)$ which is determined by

$$\begin{cases} r_0 f(\alpha, v^*) - d - a u^* - g(\alpha) \beta v^* = 0, \\ c g(\alpha) \beta u^* + r \left(1 - \frac{v^*}{K}\right) = 0. \end{cases} \quad (4.10)$$

Simple analysis of (4.10) shows that the coexistence equilibrium exists *if and only if*

$$r_0 f(\alpha, K) - d - g(\alpha) \beta K > 0. \quad (4.11)$$

Note that (4.11) implies $r_0 > d$.

In order to discuss the stability of these equilibria, We calculate the Jacobian matrix of model (4.5) for this $b(v)$ as below:

$$J(u, v) = \begin{pmatrix} r_0 f(\alpha, v) - d - 2 a u - g(\alpha) \beta v & r_0 u \frac{\partial f(\alpha, v)}{\partial v} - g(\alpha) \beta u \\ c g(\alpha) \beta v & c g(\alpha) \beta u + r - \frac{2 r v}{K} \end{pmatrix}. \quad (4.12)$$

By substituting the respective equilibria into (4.12), and analyzing the eigenvalues of the resulting matrices, we conclude the following.

- (i) E_0 is always unstable.
- (ii) E_1 exists if and only if $r_0 > d$, but it is unstable when it exists.
- (iii) E_2 always exists and it is locally asymptotically stable if and only if

$$r_0 f(\alpha, K) - d - g(\alpha) \beta K < 0. \quad (4.13)$$

- (iii) When (4.13) is reversed (e.g. (4.11) holds), E_2 becomes unstable and the coexistence equilibrium $E^* = (u^*, v^*)$ comes into existence and it is locally asymptotically stable.

Unlike condition (4.7) for Case I, conditions (4.11) and its reverse (4.13) contains both $f(\alpha, K)$ and $g(\alpha)$ and hence, their dependence on the anti-predation strategy α is more com-

plicated and hence, the equilibrium bifurcation from E_2 leading to the occurrence of the stable coexistence equilibrium E^* cannot be that conveniently expressed in terms of the strategy parameter α , as for Case I. To see this, we let $G(\alpha) = r_0 f(\alpha, K) - d - g(\alpha)\beta K$. From the stability analysis of equilibrium E_2 and E^* , $G(\alpha)$ is an survival index for the prey, determining whether or not the prey will survive: if $G(\alpha) < 0$, then the prey will go to extinction; if $G(\alpha) > 0$, then the prey will persist with $u(t) \rightarrow u^* = u^*(\alpha)$ as $t \rightarrow \infty$. Now $G(0) = (r_0 - d) - \beta K$ and $G(\infty) = -d < 0$. Thus, if

$$(r_0 - d) - \beta K > 0, \quad (4.14)$$

meaning that the generalist predator is not that good at predateding the prey (βK is small), then $G(\alpha) > 0$ for small $\alpha \geq 0$, suggesting that $\alpha = 0$ should be favoured by the prey. But if

$$(r_0 - d) - \beta K < 0, \quad (4.15)$$

meaning the predator is good at predateding the prey, then $G(0) < 0$ and hence, the prey will go extinct when doing nothing. It is hoped that $G(\alpha)$ has a *positive maximum* at some value of $\alpha > 0$, implying that appropriate response level will help the prey survive. This of course depends on the choices of f and g , there are actually many choices for f and g that can achieve this expectation, and in Section 3, we will choose a particular pair to move forward to obtain more detailed results.

Condition (4.11) can also be rewritten in terms of the basic reproduction number of the prey:

$$R_{u0} = R_{u0}(\alpha) := \frac{r_0 f(\alpha, K)}{d + g(\alpha)\beta K} > 1.$$

Similar to the above analysis on the effect of α on the survival index $G(\alpha)$ about the threshold value 0, analysis on the impact of α on $R_{u0}(\alpha)$ about the threshold value 1 can also lead to similar conclusions to those in the above paragraph.

Remark The local asymptotic stability for the equilibria stated above for both Cases I and II can actually be shown to be global as well. This can be achieved by applying the Dulac-Bendixson theorem [20]. Indeed, just as in Theorem 3.2 in [22], we can consider the Dulac function $B(u, v) = 1/(uv)$ to rule out periodic solutions, and consequently conclude global

stability for all those cases of local stability.

4.3 Invasion analysis

In this section, we study the corresponding evolutionary problem to find out how the anti-predation strategy α evolves. We first assume the predator and the resident prey have reached the coexistence steady state. According to the results on (4.5) with u and α replaced by u_r and α_r , as stated in (ii-2) for Case I and in (iv) for Case II, such an assumption is ensured by (4.5) for Case I and by (4.11) for Case II. Then, the model system (4.4) has the mutant free equilibrium $E^0 = (u_r^*, 0, v^*)$. Note that u_r^* and v^* depends on the resident prey's strategy α_r , and thus, whenever there is a need of emphasis on this fact, we will write $u_r^* = u_r^*(\alpha_r)$ and $v^* = v^*(\alpha_r)$.

Now we assume there is a rare mutant, meaning that $u_m(0)$ is very small. To determine whether the mutant can invade or not, we need to explore if the $u_m(t)$ component in the solution of (4.4) will grow or decay near E^0 . For this purpose, we linearize (4.4) at E^0 and obtain the Jacobian matrix of (4.4) at E^0 as

$$J(u_r^*, 0, v^*) = \begin{pmatrix} J_{11} & J_{12} \\ 0 & h(\alpha_r, \alpha_m) \end{pmatrix}. \quad (4.16)$$

where $J_{11} = J(u_r^*, v^*)$ is the Jacobian matrix of (4.5) with α replaced by α_r and u replaced by u_r , and

$$h(\alpha_r, \alpha_m) = r_0 f(\alpha_m, v^*(\alpha_r)) - d - a u_r^*(\alpha_r) - g(\alpha_m) \beta v^*(\alpha_r).$$

By the assumption in the beginning of this section, J_{11} is a stable 2×2 matrix and hence stability of E^0 is fully determined by the sign of $h(\alpha_r, \alpha_m)$: E^0 is asymptotically stable if $h(\alpha_r, \alpha_m) < 0$; E^0 is unstable if $h(\alpha_r, \alpha_m) > 0$. The former corresponds to the case that $u_m(t)$ will decay near E^0 , while the latter corresponds to the case that $u_m(t)$ will grow near E^0 . We call $h(\alpha_r, \alpha_m)$ the invasion exponent, and its sign measures whether the mutant can invade or not.

The direction of evolution from the current anti-predation level α_r is defined as the selection

gradient of $h(\alpha_r, \alpha_m)$ with respect to α_m at $\alpha_m = \alpha_r$:

$$s(\alpha_r) = \left[\frac{\partial}{\partial \alpha_m} h(\alpha_r, \alpha_m) \right]_{\alpha_m = \alpha_r} = r_0 \frac{\partial f(\alpha_m, v^*)}{\partial \alpha_m} \Big|_{\alpha_m = \alpha_r} - g'(\alpha_r) \beta v^*. \quad (4.17)$$

It tells which direction the anti-predation level will evolve from the current level α_r . A strategy α_r^* where $s(\alpha_r^*) = 0$ is known as an evolutionarily singular strategy, which vanishes the selection gradient. To proceed further, we need the following definitions.

Definition 4.3.1 Let α_r^* be a singular strategy, that is, $s(\alpha_r^*) = 0$.

- (i) α_r^* is said to be an evolutionary stable strategy (ESS) if it cannot be invaded by any nearby strategy $\alpha_m \neq \alpha_r^*$.
- (ii) α_r^* is said to be an evolutionary attracting strategy (EAS), also called a convergence stable strategy by some people) if a resident strategy α_r what is near α_r^* but $\alpha_r \neq \alpha_r^*$ can be invaded by a mutant strategy α_m if and only if α_m is closer to α_r^* .
- (iii) We say mutual invasibility occurs near α_r^* if there are pairs of strategies α_r and α_m such that $h(\alpha_r, \alpha_m) > 0$ and $h(\alpha_m, \alpha_r) > 0$ both hold, implying that both prey strains can co-exist.

By [10], a singular strategy α_r^* is an ESS if

$$C_{22} := r_0 \frac{\partial^2 f(\alpha_m, v^*)}{\partial \alpha_m^2} \Big|_{\alpha_m = \alpha_r = \alpha_r^*} - g''(\alpha_r^*) \beta v^* < 0. \quad (4.18)$$

Define

$$\begin{aligned} C_{11} &:= \frac{\partial^2 h(\alpha_r, \alpha_m)}{\partial \alpha_r^2} \\ &= \left[r_0 \left(\frac{\partial^2 f}{\partial v^{*2}} \left(\frac{dv^*}{d\alpha_r} \right)^2 + \frac{\partial f}{\partial v^*} \frac{d^2 v^*}{d\alpha_r^2} \right) - a \frac{d^2 u^*}{d\alpha_r^2} - g(\alpha_m) \beta \frac{d^2 v^*}{d\alpha_r^2} \right] \Big|_{\alpha_m = \alpha_r = \alpha_r^*}. \end{aligned} \quad (4.19)$$

Then, by [10], a singular strategy α_r^* is an EAS if $C_{11} > C_{22}$; and there occurs mutual invasibility near α_r^* if $C_{11} > -C_{22}$.

In the rest of this section, to be more mathematical tractable, we choose the following particular forms for the two fear effect functions

$$f(\alpha, v) = \frac{1}{1 + c_2 \alpha v}, \quad g(\alpha) = \frac{1}{1 + c_1 \alpha}. \quad (4.20)$$

Here c_1, c_2 are positive constants and they represent efficiencies of the anti-predation responses in reducing production and avoiding predation respectively. With the above adoption, we will be able show, in more details, the steps of invasion analysis for specialist and generalist predators defined by Case I and Case II respectively. We will also present some numerical simulations to demonstrate our theoretical results.

To begin, we do some further reparation with the above chosen f and g . Firstly, the equation $s(\alpha_r^*) = 0$ is now simplified to

$$\frac{\sqrt{\beta c_1}}{1 + c_1 \alpha_r^*} = \frac{\sqrt{r_0 c_2}}{1 + c_2 \alpha_r^* v^*(\alpha_r^*)}. \quad (4.21)$$

Furthermore, the composed parameter C_{22} can also be given more explicitly expressed as

$$C_{22} = r_0 \left. \frac{\partial^2 f(\alpha_m, v^*)}{\partial \alpha_m^2} \right|_{\alpha_m = \alpha_r = \alpha_r^*} - g''(\alpha_r^*) \beta v^* = \frac{2 r_0 c_2^2 (v^*)^2}{(1 + c_2 \alpha_r^* v^*)^3} - \frac{2 \beta c_1^2 v^*}{(1 + c_1 \alpha_r^*)^3}. \quad (4.22)$$

By substituting equation (4.21) into (4.22), we conclude that $C_{22} < 0$ (α_r^* is ESS) if

$$v^*(\alpha_r^*) < \frac{c_1}{c_2}. \quad (4.23)$$

Also from the equation (4.21), we know that $v^*(\alpha_r^*)$ can be represented as

$$v^*(\alpha_r^*) = \frac{c_1}{c_2} \sqrt{\frac{r_0 c_2}{\beta c_1}} + \frac{\sqrt{\frac{r_0 c_2}{\beta c_1}} - 1}{c_2 \alpha_r^*}. \quad (4.24)$$

Therefore, when $\frac{r_0 c_2}{\beta c_1} < 1$, then $v^*(\alpha_r^*) < \frac{c_1}{c_2}$, implying that the strategy α_r^* is an (locally) ESS when it exists in the feasible region of α_r ; when $\frac{r_0 c_2}{\beta c_1} > 1$, then $v^*(\alpha_r^*) > \frac{c_1}{c_2}$, implying that even if a singular strategy α_r^* exists, it may not be an ESS. For the latter case, there may not exist a singular strategy at all, as will be demonstrated in the numerical examples in the follow two

subsections.

4.3.1 With specialist predator

In this subsection, we consider (4.4) with $b(v) = -mv$, leading to

$$\begin{cases} \frac{du_r}{dt} = f(\alpha_r, v(t)) r_0 u_r(t) - d u_r(t) - a u_r(t) (u_r(t) + u_m(t)) - g(\alpha_r) \beta u_r(t) v(t), \\ \frac{du_m}{dt} = f(\alpha_m, v(t)) r_0 u_m(t) - d u_m(t) - a u_m(t) (u_r(t) + u_m(t)) - g(\alpha_m) \beta u_m(t) v(t), \\ \frac{dv}{dt} = c g(\alpha_r) \beta u_r(t) v(t) + c g(\alpha_m) \beta u_m(t) v(t) - m v(t), \end{cases} \quad (4.25)$$

where the two fear effect functions f and g are as in (4.20). Since we are only interested in whether the mutant can invade when it is rare, we focus on the boundary equilibrium solution $E^0 = (u_r^*, 0, v^*)$ where

$$\begin{cases} u_r^* = \frac{m (1 + c_1 \alpha_r)}{c \beta}, \\ \left[\frac{\beta c_2 \alpha_r}{1 + c_1 \alpha_r} v^{*2} + \left[c_2 \alpha_r d + \frac{c_2 \alpha_r a m (1 + c_1 \alpha_r)}{c \beta} + \frac{\beta}{1 + c_1 \alpha_r} \right] v^* - H = 0. \end{cases} \quad (4.26)$$

where $H = r_0 - d - \frac{am(1+c_1\alpha_r)}{c\beta}$. By (4.7), there is a unique positive $v^* = v^*(\alpha_r^*)$ satisfying (4.26) if and only if

$$r_0 - d - \frac{am(1+c_1\alpha_r)}{c\beta} > 0.$$

Thus, we can conclude that in order for E^0 to exist, the resident's strategy α_r needs to be in the feasible region

$$0 < \alpha_r < \frac{(r_0 - d) c \beta - a m}{c_1 a m} =: \hat{\alpha}_r.$$

Next, we use some numerical examples to demonstrate the theoretical results obtained above. To this end, we set

$$r_0 = 0.03, \quad d = 0.01, \quad a = 0.01, \quad m = 0.05, \quad c = 0.4, \quad c_1 = c_2 = 1, \quad \beta = 1. \quad (4.27)$$

With these values, (4.26) can be explicitly solved for to obtain

$$\begin{cases} u_r^* = u_r^*(\alpha_r) = 0.125 + 0.125 \alpha_r, \\ v^* = v^*(\alpha_r) = \frac{0.000625 (-\alpha_r^3 - 10 \alpha_r^2 - 9 \alpha_r - 800 + J)}{\alpha_r}. \end{cases} \quad (4.28)$$

where

$$J = \sqrt{\alpha_r^6 + 20 \alpha_r^5 + 118 \alpha_r^4 - 1420 \alpha_r^3 + 60881 \alpha_r^2 + 62400 \alpha_r + 640000}.$$

The upper bound for the feasible region for α_r is also calculated as

$$\hat{\alpha}_r = \frac{(r_0 - d) c \beta - a m}{c_1 a m} = 15.$$

Plugging the second equation in (4.28) into (4.21) and solving the resulting equation numerically, we then obtain an evolutionarily singular strategy α_r^* as

$$\alpha_r^* = 6.130616080,$$

which in term leads to

$$v^*(\alpha_r^*) = 0.03834181285 < 1 = \frac{c_1}{c_2}.$$

Therefore, α_r^* is actually a (locally) evolutionarily stable strategy. We can also numerically calculate C_{22} and C_{11} as

$$C_{22} = -0.0001646851833, \quad \text{and} \quad C_{11} = 0.0002364439905.$$

Thus, $C_{11} > C_{22}$ and $C_{11} > -C_{22}$ both hold, implying that α_r^* is also evolutionarily attracting, and near α_r^* mutual invasibility may occur meaning that coexistence is possible.

By applying numerical simulations using the parameter values given in (4.27), we present pairwise invasibility plots (PIP) for system (4.25) in Figure 4.1. From the PIP, we can find the region of successful invasion by mutant and find a unique intermediate ESS in the feasible region of anti-predation strategy. The plot also confirms that the singular strategy α_r^* is not only an ESS and but also an EAS. This implies that when the mutant strategy and the resident

strategy are on the same side of the α_r^* , then the mutant strategy cannot invade if it is further away than the resident strategy is from the α_r^* (i.e., either $\alpha_r^* < \alpha_r < \alpha_m$ or $\alpha_m > \alpha_r > \alpha_r^*$); however, when the mutant strategy and the resident strategy are on the opposite sides of the ESS α_r^* , successful invasion by the mutant strategy is *still possible* even if it is further away from α_r^* than the resident strategy is. Right pane in Figure 1 is the mutual invasibility obtained by reflect the curve in the left pane about the diagonal line. The region with double plus signs (i.e., + +) correspond to the strategies for the resident and mutant strains by which mutual invasibility occurs. This presents the scenario that the invasion is mild and hence will not replace the other strain, leading to co-existence of the two strains.

In Figure 4.2, we use three strategy pairs of values for the resident strategy and the mutant strategy (α_r, α_m) to illustrate the eventual results of the three-dimensional predator-prey system (4.25) with initial condition at (u_r^*, ϵ, v^*) with ϵ small, which accounts for the scenario of a rare mutant initially appearing when the resident prey and the predator settles at the positive equilibrium. These three pairs of values are chosen respectively from the three types of regions in the right pane in Figure 4.1. These simulations, clearly demonstrate the three possible outcomes: (i) the mutant prey can successfully invade and replace the original resident prey to become the new resident prey, as is shown in Figure 4.2-(a); (ii) the mutant prey cannot invade at all, reflected by the fact that the corresponding solution approaches $(u_r^*, 0, v^*)$ as is shown Figure 4.2-(b); (iii) the mutant prey can invade but mildly, without wiping out the original resident, reflected by the fact that the corresponding solution approaches a new steady state with all three component positive, accounting for coexistence of all three species/strains, as is shown in Figure 4.2-(c).

At this point, we would like to make a remark on the biological implication of the condition $\frac{r_0 c_2}{\beta c_1} < 1$ that guarantees the existence of an ESS α_r^* . Note that (i) β accounts for the predator's capability in predating the prey and $c_1 = |g'(0)|$ measures the efficiency of the prey's anti-predation response in avoiding predation; (ii) r_0 stands for the prey's capability in reproduction and $c_2 = \left| \frac{\partial f(\alpha, v)}{\partial(\alpha v)} \right|_{\alpha=0}$ measures the efficiency of the prey's anti-predation response in reducing its reproduction. Therefore, the quantity $\frac{r_0 c_2}{\beta c_1}$ plays a role of comparing the cost and the benefit of anti-predation response at low level (α equal or near 0) with the given efficiencies c_1 and c_2 . Accordingly, the condition $\frac{r_0 c_2}{\beta c_1} < 1$ (equivalent to $\beta c_1 - r_0 c_2 > 0$) corresponds to the scenario

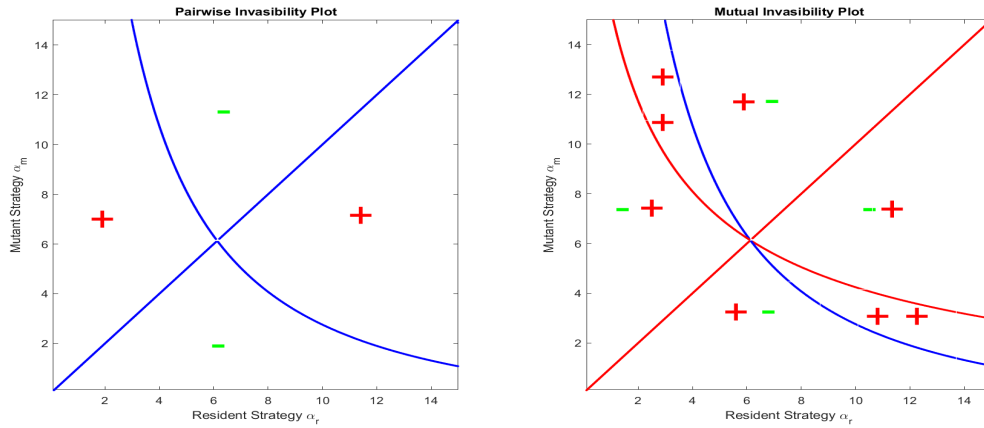
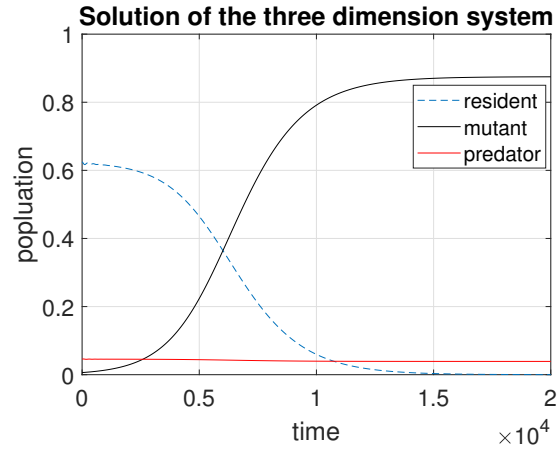


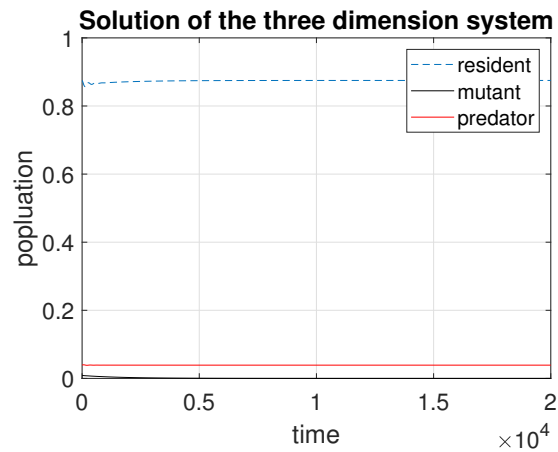
Figure 4.1: Pairwise invasibility plot (PIP) for the mutant and for both the resident and the mutant. Left: plot for invasibility of the mutant prey where the two regions carrying “+” (“-”) symbols denote strategy ranges for the mutant prey to be able (unable) to invade the resident prey. Right: plot for mutual invasibility where the two regions with double +’s stand for the strategy ranges for both resident and mutant preys to be able to mildly invade each other leading to co-persistence.

that benefit is larger than the cost, and thus, justifies the need of an anti-predation response; and if $\frac{r_0 c_2}{\beta c_1} < 1$, such a need is not justified and there may be no need for such a response.

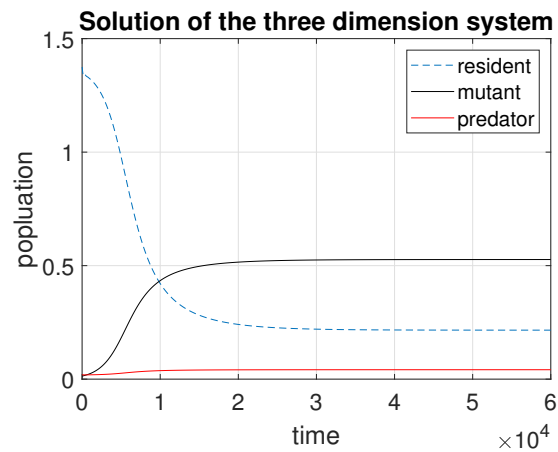
To demonstrate the latter case above, we keep all parameter values in (4.27) except for changing r_0 to 1.5, leading to $\frac{r_0 c_2}{\beta c_1} = 1.5 > 1$. Then, we find that there is no positive root for the equation (4.21). In fact, the selection gradient now remains negative for all strategies in the feasible range of anti-predation strategy (see Figure 4.3), and thus, there is no singular strategy and no or lower response level is favoured. This is confirmed/supported by the numerical simulations on the population dynamics of the model system (4.25) presented in Figure 4.4. In Figure 4.4(a), $\alpha_r = 6 > \alpha_m = 4$, we can see the mutant invades prey and replaces the resident prey to become the new resident prey. In Figure 4.4(b), $\alpha_r = 6 < \alpha_m = 10$, we can see the rare mutant is immediately wiped and the system recovers to its steady state before the rare mutant appears. Therefore, the prey strain with lower anti-predation response level is favoured and no co-existence is possible.



(a)



(b)



(c)

Figure 4.2: Numerical solutions to (4.25) with parameters given in (4.27) and the initial condition is set to be (u_r^*, ϵ, v^*) where ϵ is small. The strategy pair (α_r, α_m) is chosen respectively from the three types of regions in the right pane in Figure 4.2: (a) when $(\alpha_r, \alpha_m) = (4, 6)$ which is in the $(-, +)$ region, the mutant can grow when rare and eventually replace the resident to become the new resident; (b) when $(\alpha_r, \alpha_m) = (6, 4)$ which is in the $(+, -)$ region, the mutant can not invade when rare, and after a small fluctuation, the solution converge to the equilibrium $(u_r^*, 0, v^*)$; (c) when $(\alpha_r, \alpha_m) = (10, 4)$ which is in it is in the $(+, +)$ region — the mutual invasibility region, the mutant can invade when rare, without replacing the resident, resulting in the co-existence of both the mutant and the resident preys.

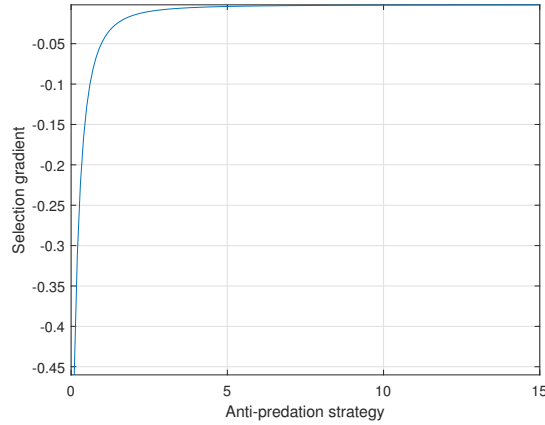


Figure 4.3: With parameter values given in (4.27) except that r_0 is changed to $r_0 = 1.5$, the selection gradient $s(\alpha)$ remains negative.

4.3.2 With generalist predator

In this subsection, we consider the scenario of a generalist predator for (4.4) with $b(v) = rv(1 - v/K)$, leading to

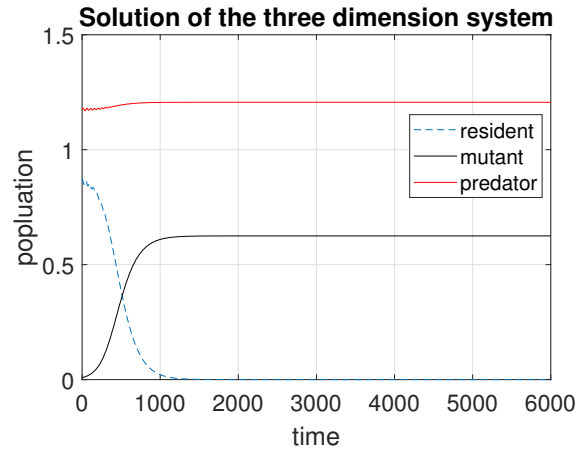
$$\begin{cases} \frac{du_r}{dt} = f(\alpha_r, v(t)) r_0 u_r(t) - d u_r(t) - a u_r(t) (u_r(t) + u_m(t)) - g(\alpha_r) \beta u_r(t) v(t), \\ \frac{du_m}{dt} = f(\alpha_m, v(t)) r_0 u_m(t) - d u_m(t) - a u_m(t) (u_r(t) + u_m(t)) - g(\alpha_m) \beta u_m(t) v(t), \\ \frac{dv}{dt} = c g(\alpha_r) \beta u_r(t) v(t) + c g(\alpha_m) \beta u_m(t) v(t) + r v(t) \left(1 - \frac{v(t)}{K}\right). \end{cases} \quad (4.29)$$

Again, we are only interested in whether the mutant prey can invade when it is rare, and if it can, will it replace the resident prey (strong invasion) or co-exist with the resident prey (mild invasion). With f and g given by (4.20), u_r^* and v^* in $E_0 = (u_r^*, 0, v^*)$ are given by

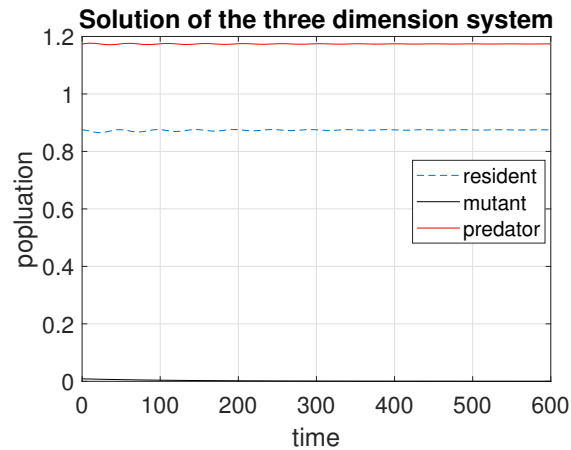
$$\begin{cases} \frac{r_0}{1 + c_2 \alpha_r v^*} - d - a u_r^* - \frac{\beta v^*}{1 + c_1 \alpha_r} = 0, \\ \frac{c \beta u_r^*}{1 + c_1 \alpha_r} + r \left(1 - \frac{v^*}{K}\right) = 0. \end{cases} \quad (4.30)$$

From equation(4.11), (4.30) has unique positive solution (u^*, v^*) if and only if

$$F(\alpha_r) = d c_1 c_2 K \alpha_r^2 + [d(c_1 + c_2 K) + c_2 \beta K^2 - c_1 r_0] \alpha_r + (\beta K + d - r_0) < 0. \quad (4.31)$$



(a)



(b)

Figure 4.4: Numerical simulations of the population dynamics of (4.25). Parameter values are as in (4.27) except that r_0 is changed to $r_0 = 1.5$. The initial condition is set to the form (u_r^*, ϵ, v^*) where ϵ is small. (a) For $\alpha_r = 6$ and $\alpha_m = 4$ (scenario of $\alpha_m < \alpha_r$), the mutant can grow and invade even when it is rare, and it eventually replaces the resident and become the new resident. (b) For $\alpha_r = 6$ and $\alpha_m = 10$ (scenario of $\alpha_m > \alpha_r$), the mutants die out and can not invade when rare; after a small fluctuation, the populations are back to the equilibrium $(u_r^*, 0, v^*)$.

Since $F(\alpha_r)$ is a quadratic function of α_r , we can discuss the feasible region

$$\Omega = \{\alpha_r \mid F(\alpha_r) < 0 \text{ and } \alpha_r > 0\},$$

in terms of the coefficients of $F(\alpha_r)$ as below:

(p1) When $F(0) = \beta K + d - r_0 < 0$, then $F(\alpha_r) = 0$ has a unique positive root α_r^+ and $\Omega = (0, \alpha_r^+)$.

(p2) When $F(0) = \beta K + d - r_0 > 0$, and $F'(0) = d(c_1 + c_2 K) + c_2 \beta K^2 - c_1 r_0 \geq 0$, then Ω is empty.

(p3) When $F(0) = \beta K + d - r_0 > 0$, and $F'(0) = d(c_1 + c_2 K) + c_2 \beta K^2 - c_1 r_0 < 0$, then $F(\alpha_r)$ has a minimum F_{\min} attained at the positive value of $\alpha_r = \tilde{\alpha}_r$ where

$$\tilde{\alpha}_r = \frac{c_1 r_0 - d(c_1 + c_2 K) - c_2 \beta K^2}{2dc_1 c_2 K},$$

and thus,

(p3-1) if $F_{\min} = F(\tilde{\alpha}_r) \geq 0$, then Ω is empty;

(p3-2) if $F_{\min} = F(\tilde{\alpha}_r) < 0$, then $F(\alpha_r) = 0$ has two positive roots $\alpha_r^{1+} < \alpha_r^{2+}$, and $\Omega = (\alpha_r^{1+}, \alpha_r^{2+})$.

As for the specialist predator case in Subsection 3.1, next we use some numerical examples to illustrate our theoretical results for the generalist predator case. To this end, in addition to keeping the values of those parameters given in (4.27), we also specify the values for the parameters r and K in the demography term of the predator in (4.29), as below

$$\begin{cases} r_0 = 0.03, & d = 0.01, & a = 0.01, & m = 0.05, \\ c = 0.4, & c_1 = c_2 = 1, & \beta = 1, & r = 0.01, & K = 0.01. \end{cases} \quad (4.32)$$

Following the calculations above, we can find the boundary equilibrium $(u_r^*, 0, v^*)$ to be given

by the following formulas:

$$\begin{cases} u_r^* = \frac{\alpha_r^3 - 138\alpha_r^2 - 239\alpha_r - 4100 + Q}{80(\alpha_r + 1)(\alpha_r^2 + 2\alpha_r + 41)} - \frac{\alpha_r + 1}{40}, \\ v_r^* = \frac{\alpha_r^3 - 138\alpha_r^2 - 239\alpha_r - 4100 + Q}{200\alpha_r(\alpha_r^2 + 2\alpha_r + 41)}. \end{cases} \quad (4.33)$$

where

$$Q = \sqrt{\alpha_r^6 + 124\alpha_r^5 + 52166\alpha_r^4 + 172164\alpha_r^3 + 2598321\alpha_r^2 + 3288200\alpha_r + 16810000}.$$

In this case, we have $d + \beta K - r_0 = -0.01 < 0$. The feasible region of α_r is given by $\Omega = (0, \alpha_r^+)$ where $\alpha_r^+ = 199.5012500$. By solving equation (4.21) and the second equation in (4.28), we obtain an evolutionarily singular strategy α_r^* as $\alpha_r^* = 6.522176963$ and the corresponding $v_r^*(\alpha_r^*)$ as

$$v^*(\alpha_r^*) = 0.04643837017 < \frac{c_1}{c_2} = 1.$$

That is, α_r^* is (locally) evolutionarily stable. To explore the evolutionary attracting property and the mutual invasibility of this singular strategy, we can calculate $C_{22} = -0.0001597058850$ and $C_{11} = 0.0001940213681$. Thus, we have both $C_{11} > C_{22}$ and $C_{11} > -C_{22}$ implying that α_r^* is indeed also (locally) an EAS and mutual invasibility may occur near this α_r^* leading to coexistence of both the resident and mutant prey species.

In Figure 4.5, we present pairwise invasibility plots (PIP) for system (4.29), using the parameter values given in (4.32). The left plane is the plot for the invasibility of the mutant prey, in which there are four regions: the two regions with “+” (“-”) symbols represent the strategy range for the mutant prey to be able (unable) to invade the resident prey. The right pane is the plot for mutual invasibility in which there are six regions. The paired symbols in each region tell which prey strain can invade: regions with (+, -) represent the range of (α_r, α_m) in which the mutant prey cannot invade; regions with (-, +) stand for the range of (α_r, α_m) in which the mutant can invade and replace the resident; while regions with (+, +) account for the range of (α_r, α_m) in which the both mutant and resident preys will both co-exist.

From the plots in Figure 4.5, we can see that there is a singular strategy which is determined

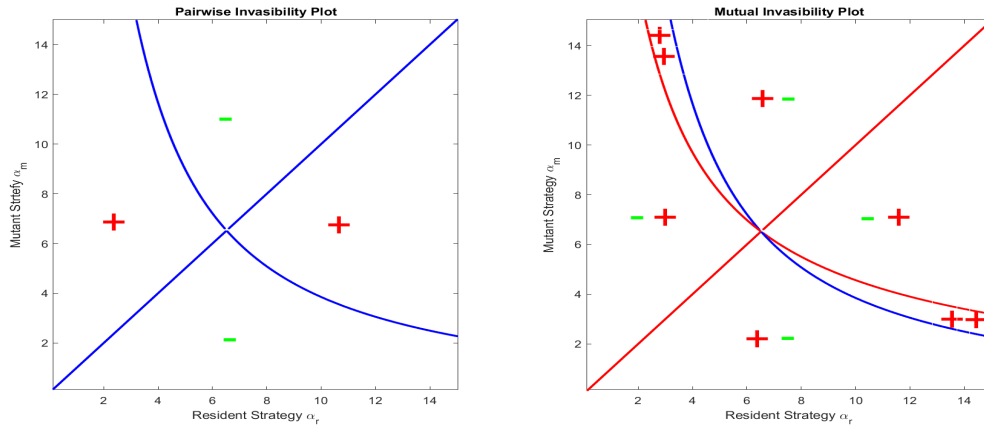
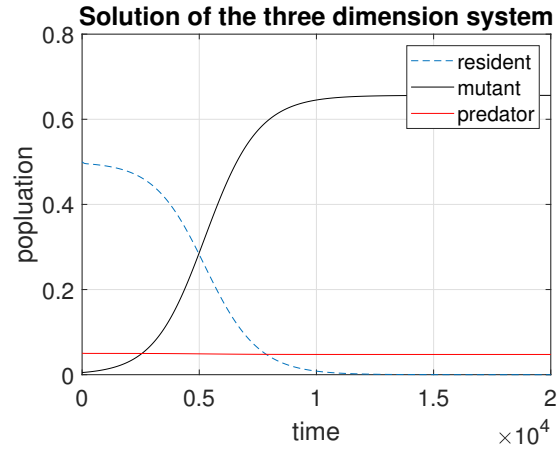


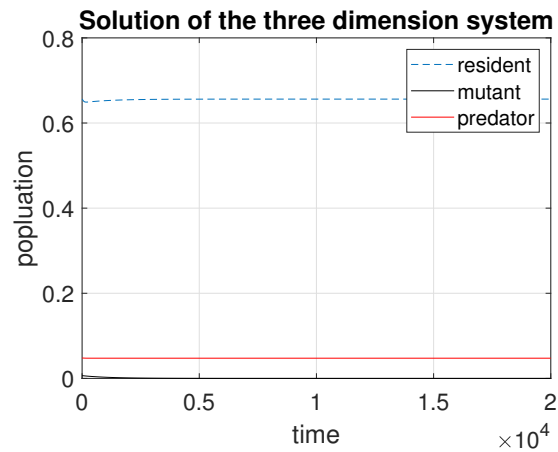
Figure 4.5: Pairwise invasibility plot(PIP) and mutual invasibility plot. In the PIP, ”+” region denotes where mutants can invade the residents while in ”-” region mutants fail to invade residents. In the mutual invasibility plot, ”++” region notes where mutants and residents are mutually invasive and thus may cause coexistence of both species.

by the intersection of the diagonal line and the curve. The plots also confirms that this singular strategy is both (locally) evolutionarily stable and evolutionarily attracting (hence continuously stable). We particularly point out that, just as in the specialist predator case, for the generalist predator case, coexistence of both the resident and mutant preys is still possible when they play different anti-predation strategies (see the two regions with two “+’s” symbols in right pane in Figure 4.5. In Figure 4.6, we use three pairs of values for (α_r, α_m) , respectively located in the three different types of the regions in the right pane in Figure 4.5, to illustrate three different outcomes. These simulations clearly show that the mutant prey can (i) either successfully invade and replace the original resident prey to become the new resident (Figure 4.6-(a)); (ii) or go extinct and the system bringing the populations of the three species back to $(u_r^*, 0, v^*)$ (Figure 4.6-(b)); (iii) or grow but without wiping the resident prey, leading to a new steady state with coexistence of all three subpopulations (Figure 4.6-(c)).

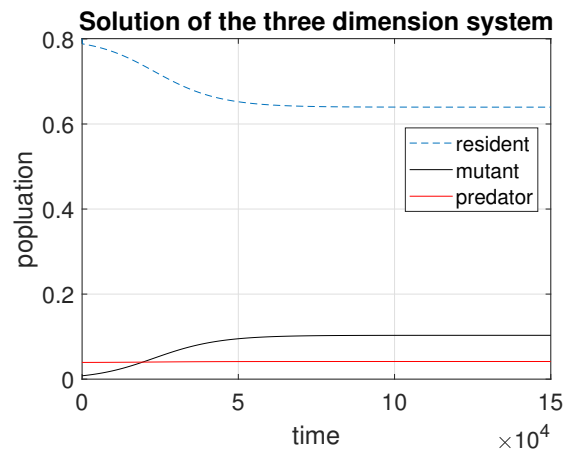
Similar to Subsection 3.1, we can also numerically examine the impact of the condition $\frac{r_0 c_2}{\beta c_1} < 1$. Keeping all parameter values given in (4.32) except for changing r_0 to 1.5. We now have $\frac{r_0 c_2}{\beta c_1} = 1.5 > 1$. In this case, after some computations, we find there is no positive equation (4.21). In fact, the selection gradient $s(\alpha_r)$ is always less than 0 for feasible anti-predation strategy(see Figure 4.7). Thus, there is no singular strategy, and this suggesting a weaker strategy is favoured. This conclusion is numerically confirmed by numerical simulations of



(a)



(b)



(c)

Figure 4.6: Numerical solutions to (4.29) with parameters given in (4.32) and the initial condition is set to be (u_r^*, ϵ, v^*) where ϵ is small. The strategy pair (α_r, α_m) is chosen respectively from the three types of regions in the right pane in Figure 4.2: (a) when $(\alpha_r, \alpha_m) = (4, 6)$ which is in the $(-, +)$ region, the mutant can grow when rare and eventually replace the resident to become the new resident; (b) when $(\alpha_r, \alpha_m) = (6, 4)$ which is in the $(+, -)$ region, the mutant can not invade when rare, and after a small fluctuation, the solution converge to the equilibrium $(u_r^*, 0, v^*)$; (c) when $(\alpha_r, \alpha_m) = (10, 4)$ which is in it is in the $(+, +)$ region — the mutual invasibility region, the mutant can invade when rare, without replacing the resident, resulting in the co-existence of both the mutant and the resident preys.

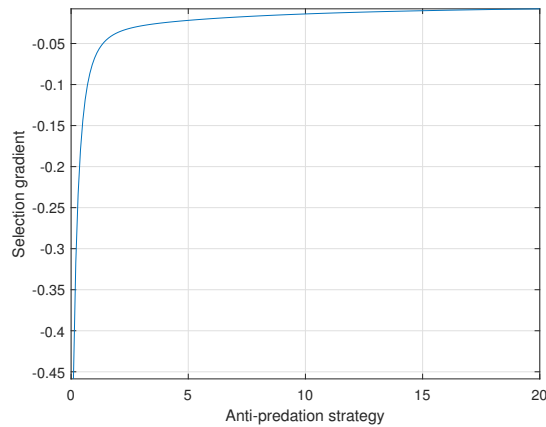


Figure 4.7: With parameter values given in (4.32) except that r_0 is changed to $r_0 = 1.5$, the selection gradient $s(\alpha)$ remains negative.

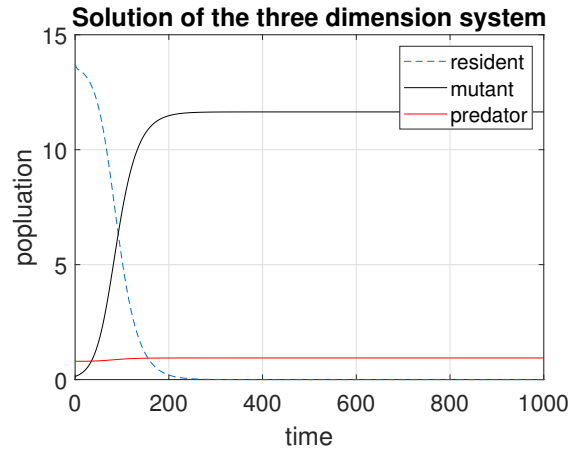
solutions to (4.29), presented in in Figure 4.8, where we use $(\alpha_r, \alpha_m) = (6, 4)$ for Figure 4.8-(a) and $(\alpha_r, \alpha_m) = (6, 10)$ for Figure 4.8-(b).

The numerical results above show that, as in the case of specialist predator, for the generalist predator case, the quantity $\frac{r_0 c_2}{\beta c_1}$ affected by the efficiencies of the prey's anti-predation response in reducing the production (cost) and in avoiding the predation (benefit) still plays an important role. When the cost of anti-predation strategy is relatively large, there is no intermediate ESS and weaker strategy is always more favoured; when the cost of anti-predation strategy is relatively small, if there exists an evolutionarily singular strategy inside the feasible region of residents' strategy, then it is an ESS, meaning that the prey strain that plays this anti-predation strategy can not be invaded by the other prey strain playing a different strategy.

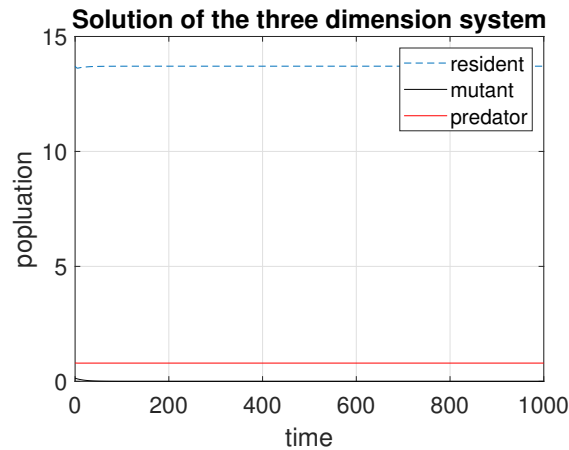
4.3.3 Difference between specialist and generalist predator

In the last section, we have shown that model (4.25) and model (4.29) have some similar dynamical behaviors with respect to evolutionary stability. However, because of the different types of the predator, there are also some differences between two systems that are worth mentioned.

First, the feasible regions of the anti-predation strategy for the residents are different. In model (4.25), the feasible region always has the form as $\alpha_r \in \left(0, \frac{(r_0-d)c\beta-am}{c_1 am}\right)$, that is, in order to



(a)



(b)

Figure 4.8: Numerical simulations of the population dynamics of (4.29). Parameter values are as in (4.32) except that r_0 is changed to $r_0 = 1.5$. The initial condition is set to the form (u_r^*, ϵ, v^*) where ϵ is small. (a) For $\alpha_r = 6$ and $\alpha_m = 4$ (scenario of $\alpha_m < \alpha_r$), the mutant can grow and invade even when it is rare, and it eventually replaces the resident and become the new resident. (b) For $\alpha_r = 6$ and $\alpha_m = 10$ (scenario of $\alpha_m > \alpha_r$), the mutants die out and can not invade when rare; after a small fluctuation, the populations are back to the equilibrium $(u_r^*, 0, v^*)$.

observe the coexistence between predator and prey, the anti-predation strategy must be maintained under certain level. Otherwise, the predator species will go extinct. But in model (4.29), since the predator can persist with absence of prey. The feasible region of the anti-predation strategy changes to two possibilities. When $F(0) = \beta K + d - r_0 < 0$ the feasible region is $(0, \alpha_r^+)$ where α_r^+ denotes the positive root of $F(\alpha_r) = 0$ from inequality (4.31). That is, if the carrying capacity of the generalist predator is small, the prey can apply anti-predation strategy from 0 to certain level. When the strategy exceeds this level, the prey can not survive due to its huge cost on reproduction but not as huge benefit from defense of predator. When $F(0) = \beta K + d - r_0 > 0$, we need to further check $F'(0)$ and F_{\min} . When $F'(0)$ and F_{\min} are both negative, then the feasible region of α_r is given by $(\alpha_r^{1+}, \alpha_r^{2+})$, where $\alpha_r^{1+} < \alpha_r^{2+}$ are the two distinct positive roots of $F(\alpha_r) = 0$ from inequality (4.31). This means when the carrying capacity of the generalist predator is increasing. The prey, in order to survive, can not apply weak anti-predation strategy anymore. A weak strategy will cause a huge predation rate such that the prey population is suffered severely by direct predation and thus goes extinct. Of course, if the carry capacity of the predator keeps increasing, then the prey can not survive no matter what strategy they apply due to abundance of predator.

The difference on feasible region of the anti-predation strategy directly leads to the second main difference on the dynamics between model (4.25) and model (4.29). That is, whether the mutants can invade with an anti-predation strategy outside of the feasible region.

We first show that in model (4.29), a mutant with anti-predation strategy α_m can never invade when rare if α_m does not belong to the feasible region of residents strategy α_r . Consider the invasion exponent

$$h(\alpha_r, \alpha_m) = r_0 f(\alpha_m, v^*) - d - au^* - g(\alpha_m)\beta v^*.$$

We know a successful invasion requiring a positive invasion exponent. Since α_m is not in the feasible region. We have $r_0 f(\alpha_m, K) - d - g(\alpha_m)K < 0$. From equation (4.30), we also have $u^* > 0$ and $v^* > K$. Using the monotonicity of function $f(\alpha, v)$ with respect to v , we can

conclude

$$\begin{aligned} h(\alpha_r, \alpha_m) &= r_0 f(\alpha_m, v^*) - d - a u^* - g(\alpha_m) \beta v^* \\ &< r_0 f(\alpha_m, K) - d - g(\alpha_m) \beta K < 0. \end{aligned}$$

Therefore, the mutant can not successfully invade the resident when rare. In another word, for model (4.29), we can conclude that a singular strategy α^* , if exists, must appears in the feasible region of α_r . Moreover, whether it is an ESS is determined by $\frac{r_0 c_2}{\beta c_1}$.

However, it is not true for the case of specialist predator. In fact, we can easily find a example for model (4.25) that a singular strategy is not in the feasible region. Let $r_0 = 0.03$, $d = 0.01$, $a = 0.05$, $m = 0.05$, $c = 0.4$, $c_1 = c_2 = 1$ and $\beta = 1$. The feasible region of α_r is give by $(0, 2.2)$. But by solving equation (4.21), we find a singular strategy $\alpha_r^* = 4.003614398 > 2.2$. In Figure 4.9, we show that in this example, a mutant with anti-predation strategy $\alpha_m = 2.4$, which does not belong to the feasible region, can still successfully invade. Before the mutants replacing the residents, the predator species goes extinct first. That leads to the coexistence of two strains of prey species with absence of predator. In conclusion, for model (4.25), a mutant with a strategy outside of the feasible region can still invade. Remember the feasible region in model (4.25) is always in the form of $\left(0, \frac{(r_0-d)c\beta-am}{c_1 am}\right)$, which means the mutants must apply a strong strategy. With the growing of the mutants population, the predator will be eliminated by such a strong strategy and only prey species can persist.

4.4 Conclusion and discussions

Recent field studies and mathematical modelings suggest importance to incorporate indirect effect when considering a predator-prey interaction. Wang et al [22] proposed an ODE model included the fear effect which leads to a cost in reproduction. Further modification in [23, 24, 25, 26] suggests the benefit of anti-predation strategy which is, obviously, reducing the risk of predation should also be taken into account. In this chapter, based on the ecological facts from these previous work, we propose a model to answer the corresponding evolutionary problem. We look for an optimal anti-predation strategy that can avoid invasion by a mutant and we also

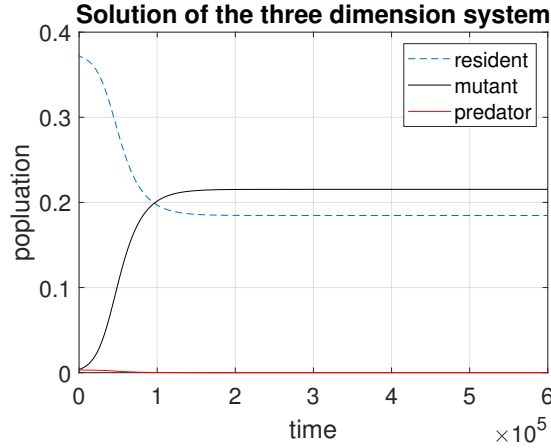


Figure 4.9: $\alpha_r = 2$, $\alpha_m = 2.4 > 2.2$ is outside of the feasible region. We can find the mutants can still invade and start replace the residents. However, the predator population tends to 0 first and since the absence of predator, the two strains of prey coexist.

find the direction of evolving of the trait.

We start from a general system (4.4) that we use general cost and benefit functionals satisfied condition (4.3) and demographic functional of the predator so it can be either specialist and generalist. We find condition for the singular strategy to be an ESS is

$$C_{22} = r_0 \left. \frac{\partial^2 f(\alpha_m, v^*)}{\partial \alpha_m^2} \right|_{\alpha_m = \alpha_r = \alpha_r^*} - g''(\alpha_r^*) \beta v^* < 0,$$

which shows the curvature of cost and benefit functional play an important role to determine the evolutionary stability of the singular strategy.

In order to make our result more clear, we then use a detailed expression of f and g as $f(\alpha, v) = 1/(1 + c_2 \alpha v(t))$ and $g(\alpha) = 1/(1 + c_1 \alpha)$ where c_1, c_2 are positive coefficients. By using this pair of simple form of f and g , we analyze the model (4.25) and model (4.29) to compare the qualitative results of evolutionary stability between different type of predator, namely, specialist predator and generalist predator.

We first stated some similar behavior in both model. Regardless of the type of predator, the evolutionary stability of the singular strategy always determined by the anti-predation efficiency indicator $I = \frac{r_0 c_2}{\beta c_1}$. If $I < 1$, the singular strategy in the feasible region of α_r is a locally ESS. If $I > 1$, the singular either does not exist and a weaker strategy is always more favored. The biological implication is that when I is large, it means either r_0 is large or β is

small. In both case, it shows reducing the predator risk is not as worthwhile as maintained the reproduction size. That is, the cost in reproduction exceeds much than the benefit from reducing the predation risk. Therefore, a weaker anti-predation strategy has more evolutionary advantages than a stronger strategy. In contrary, when I is small, it means the benefits of reducing predation risk can somehow make up the cost from reproduction and therefore a stronger anti-predation strategy is preferred in certain region. That is, an intermediate optimal strategy is possible.

We also point out an important difference between the models with different type of predators, that is, the feasible region of resident preys' strategy α_r . If the predator is specialist, a weak anti-predation strategy is enough to confirm the persistence of prey species. This is because the predator will go extinct with the absence of prey and therefore the size of prey's population restrict the size of predator's population. Also, a extremely strong strategy will decrease the predation risk such that the predator can not reproduce themselves and become extinct. But this feature changed dramatically if the predator is generalist. The population of the predator is not limited by the prey anymore but mainly by its own demographic dynamics. Now, the carrying capacity of predator plays an important role. When the carrying capacity is small, satisfying $r_0 - d - \beta K > 0$, a weak strategy can still confirm the persistence of the prey. But since the predator can survive with the absence of the prey, any strong strategy can not help prey to wipe the predator like in the specialist case. Then an extremely strong strategy will only suffer the prey species with its heavy cost on prey's reproduction. As a result, prey will go extinct due to its over reaction on anti-predation response. However, when the carrying capacity of predator becomes large, we can find not only extremely strong strategies will eliminate prey species but also weak strategies will do so. This is because the abundant of predators can consume more preys if the anti-predator response is low. In this case, both under estimation of the predation and over reaction on defense can lead prey to extinction. Only intermediate anti-predation strategy can help prey survive.

The difference in the feasible region of resident preys' strategy α_r directly affects the evolution process. We find in model (4.29) with generalist predator, a mutant with strategy outside of the feasible region can never invade the resident population. This also tells us that a singular

strategy, once exists, must be located inside the feasible region and its evolutionary stability is totally determined by the efficiency indicator I . If $I < 1$, then it is an ESS. But in model (4.25) with specialist predator, a singular strategy can be found outside the feasible region which will lead to the fact that the selection gradient in the feasible region is always positive and a stronger strategy is favored. As a result, the anti-predation strategy will evolve along the direction of stronger strategies and eventually make the predator go extinct. On the invasion point of view, Figure 4.9 shows a mutant with strategy outside the feasible region, can still invade, break the balance between predator and prey, and wipe the predator.

In conclusion, we find the condition of evolutionary stability in general model (4.4) and use two examples to show the qualitative results in more explicit way including define the anti-predation efficiency indicator, show the relationship between the efficiency indicator and evolutionary stability of the anti-predation strategy and compare these results with different types of predator.

We modified the ODE model in [22] as the basic model and added the benefit from the anti-predation strategy by considering the effect of reducing the predation risk. In this chapter, we use a simple form of f and g functions which give us mathematical convenience to illustrate the qualitative behavior of the model. One future direction is to apply more realistic functional response of the cost and benefit functions. In [7], the author mentioned there has not been a general theory to measure the relative magnitude of the impact between direct predation and anti-predation response. Although there have been some experiments [19, 28] using manipulate predator who can deliver only risk effects to measure the significant impact of indirect effect alone. These measurements still leave spaces to understand how the results generalize to more natural environment with coexistence of direct and indirect effects. A pair of more complicated and realistic cost and benefit functionals f and g may provide richer and more precise prediction of the optimal anti-predation strategy in the sense of evolution. Another direction is in our model, we use mass action as our functional response of predation which can lead to a globally asymptotically stable steady state as our starting point. But in reality, mechanism of interaction between predator and prey can be different. So we can apply Holling Type II, Holling Type III or other type of functions as our functional response. But now the original

two dimensional resident-predator system can have more complicated dynamical behavior like periodic solutions. Then the invasion exponent is time varying which will lead to some interesting questions. Last and not the least, since in our model, under certain condition, the mutants can coexist with the resident and the predator. Then a natural question is after a new steady state is reached of this mutant-resident-predator system, how will the anti-predation strategy further evolve by considering whether a new mutant can invade this three species steady state. These are some future direction beyond the scope of this chapter and may interest us to do some future work on this topic.

Bibliography

- [1] Abrams, PA., *Foraging time optimization and interactions in food webs*. Am. Nat. **124**(1984), 80-96.
- [2] Abrams, PA., *Adaptive responses of predators to prey and prey to predators: the failure of the arms race analogy*. Evolution **40**(1986), 1229-1247.
- [3] Abrams, PA., *The evolution of antipredator traits in prey in response to evolutionary change in predators.*, Oikos **59**(1990), 147-56.
- [4] Abrams, PA., *Adaptive foraging by predators as a cause of predator-prey cycles*. Evol. Ecol. **6**(1992), 56-72.
- [5] Boonstra, R. et al., *The impact of predator-induced stress on the snowshoe hare cycle*. Ecol. Monogr. **68**(1998) , 371–394.
- [6] Creel, S., D. Christianson, S. Liley, and J. A. Winnie, *Predation risk affects reproductive physiology and demography of elk*, Science **315**(2007), 960.
- [7] Creel, S., Christianson, D., *Relationships between direct predation and risk effects*, Trends Ecol Evolut **23**(2008), 194-201.
- [8] Diekmann, U., Marrow, P., Law, R., *Evolutionary cycling in predator-prey interactions: population dynamics and the Red Queen.*, J. Theor. Biol. **176**(1995), 91-102.
- [9] Diekmann, U., Law, R., *The dynamical theory of coevolution: a derivation from stochastic ecological processes.*, J. Math. Biol. **34**(1996), 579-612.

- [10] Diekmann, O., *Beginner's Guide to Adaptive Dynamics*, Banach Center Publications, **63** (2004), 47-86.
- [11] Gavrillets, S., *Coevolutionary chase in exploiter-victim systems with polygenic characters.*, J. Theor. Biol. **186**(1997), 527-534.
- [12] Ives, AR., Dobson, AP. *Antipredator behavior and the population dynamics of simple predator-prey systems.*, Am. Nat. **130**(1987), 431-437.
- [13] Lam, K. Y., Lou, Y., *Evolutionarily stable and convergent stable strategies in reaction-diffusion models for conditional dispersal.* Bull Math Biol **76**(2) (2014), 261–291.
- [14] Lima, S. L., *Nonlethal effects in the ecology of predator-prey interactions*, Bioscience **48**(1998), 25-34.
- [15] Marrow, P., Cannings, C., *Evolutionary instability in predator-prey systems.*, J. Theor. Biol. **160**, 135-150.
- [16] Maynard Smith, J., Price, G., *The logic of animal conflict*, Nature, **246**(1973), 15–18.
- [17] Panday, P., Pal, N., Samanta, S., Chattopadhyay, J., *Stability and bifurcation analysis of a three-species food chain model with fear*, Int. J. Bifurc. Chaos **28** (2018), 1850009.
- [18] Panday, P., Pal, N., Samanta, S., Chattopadhyay, J., *A Three Species Food Chain Model with Fear Induced Trophic Cascade*, Int. J. Appl. Comput. Math **5** (2019), 100.
- [19] Peckarsky, B.L. et al., *Sublethal consequences of streamdwelling predatory stoneflies on mayfly growth and fecundity.* Ecology **74**(1993), 1836–1846.
- [20] Perko, L., *Differential equations and dynamical systems*, Springer, New York(1996)
- [21] Tollrian, R. and Harvell, C.D., *The evolution of inducible defenses: current ideas.* In The Ecology and Evolution of Inducible Defenses (Tollrian, R. and Harvell, C.D., eds), Princeton University Press, (1999), 306–321.
- [22] Wang, X., Zanette, L. Y., Zou, X., *Modelling the fear effect in predator-prey interactions*, J Math Biol. **73**(2016), 1179-1204.

- [23] Wang, X., Zou, X., *Modeling the Fear Effect in Predator-Prey Interactions with Adaptive Avoidance of Predators*, Bull Math Biol **79**(2017), 1325-1359.
- [24] Wang, X., Zou, X., *Pattern formation of a predator-prey model with the cost of anti-predator behaviours*, Mathematical Biosciences and Engineering, **15**(2018), 775-805.
- [25] Wang, Y., Zou, X., *On a predator prey system with digestion delay and anti-predation strategy*, J Nonlinear Sciences, **30**(2020), 1579-1605
- [26] Wang, Y., Zou, X., *On mechanisms of trophic cascade caused by anti-predation response in food chain systems*, Mathematics in Applied Sciences and Engineering, **1**(2)(2020), 181-206
- [27] Zanette, L., *Synergistic effects of food and predators on annual reproductive success in song sparrows*. Proceedings: Biological Sciences, **270**(2003), 799-803.
- [28] Zanette, L. Y., White, A. F., Allen, M. C., Clinchy, M., *Perceived predation risk reduces the number of offspring songbirds produce per year*, Science **334** (6061)(2011), 1398-1401.
- [29] Zu, J., Takeuchi, Y., *Adaptive evolution of anti-predator ability promotes the diversity of prey species: critical function analysis.*, BioSystems, **109**(2012), 192–202.

Chapter 5

Conclusions and discussions

Throughout this thesis, we proposed differential equation models to study the ecological and evolutionary features of anti-predation strategies. We have considered three different aspects of such strategies to better understand predator-prey interactions and more complicated ecosystems. These works are mainly motivated by empirical studies [7, 8, 13, 14, 18] which all suggest that the indirect effect in predator-prey interaction is as important as and sometimes even more stronger than direct predation. We developed theories and used numerical simulations to visually demonstrate the role anti-predation response plays in the systems and how it evolves.

We started from considering two-species predator-prey interaction to explore the integrated impact of anti-predation response and digestion delay. Motivated by the model from [17], we considered not only the cost of anti-predation response in reproduction of prey, but also took the benefit of avoiding direct predation into account in our modified model. In addition, we compared two types of functional responses: Holling Type I and Holling Type II [1, 5, 12]. We found in both models that a high level of anti-predation response can inhibit periodic solutions and stabilize the system. In the model with Holling Type I functional response, an intermediated anti-predation response level confirms the stability of the coexistence between predator and prey. A relatively low level of anti-predation response incorporated with large digestion delay can cause Hopf bifurcation leading to the occurrence of limit cycles. So in our model, even with Holling Type I functional response, periodic oscillation of predator and prey

population is possible while it is impossible in previous modeling in [17]. With Holling Type II functional response, Hopf bifurcation can be generated by both delay effect and functional response itself, so there are richer possibility for existence of periodic solutions when anti-predation response is in a relatively low level.

In Chapter 3, we explored the impact of anti-predation response in a food chain motivated by the field study [14]. The anti-predation response of top prey not only has a great impact on its own population but also affects the species in lower trophic levels. This top-down process forms so-called trophic cascade phenomenon [16]. We first considered the same situation as in the field study [14] that large carnivore does not exist and only its playback is released as a source for spreading predation risk. We proposed a three dimensional food chain model and successfully exhibited the phenomenon of trophic cascade in the same direction with field study [14]. We also argued this is because of the manipulating of the perceived fear. In this case anti-predation response can not gain any benefits and therefore is purely harmful. Then, we proposed a four dimensional food chain model with restoring the large carnivore as the apex predator so that the top prey can have some benefits from their anti-predation strategies. Although in both models, the population of top prey decreases after introducing playback from predator and restoring predator respectively, we predicted that anti-predation response plays different roles in two situations and establishes trophic cascade in opposite direction. This result is meaningful for ecosystem management since empirical studies have reported abundance of herbivore or mesopredator because of the loss of top predator (large carnivore) due to human activities [2, 6, 11]. We compared two control methods in reducing the number of overgrowth population and provided a complete theoretical analysis to show the difference between manipulating fear and restoring apex predator. These methods can help shifting the balance of complicated ecosystems and conserving the biodiversity [16].

In Chapter 4, we examined the evolution aspect of anti-predation strategy by using adaptive dynamics method [4]. We identified a quantity for the efficiency of anti-predation response. That is, if the costs on reproduction are relatively larger than the benefits from defending or the predator is inefficient in catching and eating prey even without anti-predation response, then the anti-predation response wastes energy and a weaker strategy is favored. Otherwise,

the trade-off between costs and benefits can increase the fitness of prey in certain range and an intermediate evolutionarily stable strategy may exist. If the evolutionarily stable strategy is also convergence stable, then it can be a possible endpoint of evolution. In addition, we compared the evolution under different predation types: generalist predator and specialist predator. If the predator is a specialist, an extremely high level anti-predation strategy has evolutionary advantage since it can limit the size of predator population, and it will end up with breaking the balance of the ecosystem and rule out the predator species. However, if the predator is a generalist, the prey species can not regulate the size of predator by any strategy they apply. In this case, the carrying capacity of the predator becomes an important parameter. When the carrying capacity is small, weak anti-predation response from prey can still help them survive. When the carrying capacity is large enough, both under and over response of anti-predation behavior will lead the prey to extinction. Only intermediate anti-predation response can help the prey survive and the evolution force drives the strategy to a positive level. In both cases, we showed that a stable dimorphism is possible when there is an intermediate evolutionarily stable anti-predation strategy.

So far, we have studied three areas of anti-predation strategy in both ecological and evolutionary aspects. We have used dynamical system theory [10] and adaptive dynamics [4] to reveal qualitative behavior of anti-predation strategy. So naturally, in the next step, along these frameworks, quantitative analysis can be done to predict the population dynamics more precisely. The central problem for quantitative analysis is how to measure more realistic functional response of the cost and benefit functions. In [3], the author mentioned there has not been a general theory to measure the relative magnitude of the impact between direct predation and anti-predation response. We also discussed in Chapter 1 that for the costs, most field studies focus on estimating allocation costs[15] which are observable. But other types of costs, such as opportunity cost, are really hard to measure. Another problem is that indirect effect and direct effect are correlated. Although some field studies [9, 18] used manipulated predation risk to measure the impact of indirect effect alone, these measurements still leave plenty spaces to understand what is the real magnitude of the impact from anti-predation response when it coexists with direct predation. A pair of more complicated and realistic cost and benefit functionals can give us more precise prediction of population dynamics. Besides, in our models, we assumed

all the costs reflecting a decrement in reproduction and the benefits reflecting a decrement in predation risk. However, as we discussed in Chapter 1, costs can come from different aspects and impact not only the reproduction mechanism of the prey. For example, anti-predation strategies can change the choice of habitat and foraging strategy of the prey species [14], reduce the ability of intra-species' competition and even develop self-damage behavior which will increase death rate. Therefore, there are really plenty of topics that can be included in models considering anti-predation response depending on different species. We leave these as our future directions of work on fear effect in predator-prey interactions.

Bibliography

- [1] Arditi, R., Ginzburg, L. R., *Coupling in predator-prey dynamics: ratio dependence.*, Journal of Theoretical Biology **139**(1989), 311-326.
- [2] Alverson, W.S., Waller, D.M., Solheim, S.L., *Forests too deer: edge effects in northern Wisconsin.*, Conserv. Biol. **2**(1988), 348–358.
- [3] Creel, S., Christianson, D., *Relationships between direct predation and risk effects.*, Trends Ecol Evolut **23**(2008), 194-201.
- [4] Diekmann, O., *Beginner's Guide to Adaptive Dynamics*, Banach Center Publications, **63** (2004), 47-86.
- [5] Holling, C. S., *The functional response of predator to prey density and its role in mimicry and population regulation.*, Mem. Ent. Sec. Can. **45**(1965), 1-60.
- [6] McShea, W. J., Underwood, H. B., Rappole, J. H., *The Science of Overabundance: Deer Ecology and Population Management*. Washington, DC: Smithsonian Inst. Press (1997).
- [7] Nelson, E. H. et al., *Predators reduce prey population growth by inducing changes in prey behavior.* Ecology **85**(2004), 1853–1858.
- [8] Pangle, K. L. et al., *Large nonlethal effects of an invasive invertebrate predator on zooplankton population growth rate.* Ecology **88**(2007), 402–412.
- [9] Peckarsky, B. L. et al., *Sublethal consequences of streamdwelling predatory stoneflies on mayfly growth and fecundity.* Ecology **74**(1993), 1836–1846.
- [10] Perko, L., *Differential equations and dynamical systems*, Springer, New York(1996).

- [11] Rooney, T. P., Waller D. M., *Direct and indirect effects of deer in forest ecosystems.* For.Ecol. Manag. **181**(2003), 165–176.
- [12] Rosenzweig, M. L., MacArthur, R. H., *Graphical representation and stability conditions of predator-prey interactions.*, American Naturalist **97** (1963), 209-223.
- [13] Schmitz, O. J., A. P. Beckerman, and K. M. O'Brien. *Behaviorally mediated trophic cascades: effects of predation risk on food web interactions.* Ecology **78**(1997), 1388–1399.
- [14] Suraci, J. P., Clinchy, M., Dill, L. M., Roberts, D., Zанette, L. Y., *Fear of large carnivores causes a trophic cascade.*, Nat Commun. **7**(2016), 10698.
- [15] Tollrian, R., Harvell, C. D., *The Ecology and Evolution of Inducible Defenses.*, Princeton University Press (1999).
- [16] Terborgh, J., Estes, J. A., *Trophic Cascades: Predators, Prey, and the Changing Dynamics of Nature.*, Island Press (2010).
- [17] Wang, X., Zанette, L. Y., Zou, X., *Modelling the fear effect in predator-prey interactions.*, J Math Biol. **73**(2016), 1179-1204.
- [18] Zанette, L. Y., White, A. F., Allen, M. C., Clinchy, M., *Perceived predation risk reduces the number of offspring songbirds produce per year.*, Science **334** (6061)(2011), 1398-1401.

Curriculum Vitae

Name: Yang Wang

Post-Secondary Education and Degrees: University of Western Ontario
London, ON
2014 - 2021 Ph.D. Candidate

University of Western Ontario
London, ON
2013 - 2014 M.Sc.

Shanghai Jiaotong University
Shanghai, China
2009 - 2013 B.Sc.

Honours and Awards: Graduate Student Teaching Award (2019)
Western Graduate Research Scholarships (2014-2021)
Excellent Undergraduate Student Scholarship (2009-2012)

Related Work Experience: Teaching Assistant, University of Western Ontario (2014-2021)
Research Assistant, University of Western Ontario (2014-2021)

Publications:

Wang, Y., Zou, X., *On a predator prey system with digestion delay and anti-predation strategy*, J. Nonlinear Sci., **30**(2020), 1579-1605.

Wang, Y., Zou, X., *On mechanisms of trophic cascade caused by anti-predation response in food chain systems*, Mathematics in Applied Sciences and Engineering, **1**(2)(2020), 181-206.

Wu C., Wang Y., Zou X., *Spatial-temporal dynamics of a Lotka-Volterra competition model with nonlocal dispersal under shifting environment*, J. Differential Equations, **267**(2019), 4890-4921.

Yuan Y., Wang Y., Zou X., *Spatial–temporal dynamics of a Lotka–Volterra competition model with a shifting habitat* Discrete Contin. Dyn. Syst. Ser. B, **24**(2019), 5633-5671.